The Role of Nuclear Receptor Signaling in Vertebrate Liver Development

A dissertation presented

by

Maija Kristine Garnaas

to

The Division of Medical Sciences

in partial fulfillment of the requirements

for the degree of

Doctor of Philosophy

in the subject of

Genetics

Harvard University

Cambridge, Massachusetts

February 2014

ABSTRACT

Dissertation Advisor: Dr. Wolfram Goessling Maija Kristine Garnaas

The Role of Nuclear Receptor Signaling in Vertebrate Liver Development

Proper embryonic development requires precise genetic regulation of cell growth and differentiation. Organogenesis, the origin and formation of internal organs, must be exquisitely choreographed to ensure correct temporal and spatial patterning of functional organs within the developing organism. The liver is a vital organ responsible for hundreds of essential metabolic functions, but the intricate pathways controlling organ specification, differentiation, and positioning have not been fully elucidated. Uncovering the molecular mechanisms involved in hepatogenesis will enhance our understanding of normal liver development as well as inform the design of therapeutics to combat liver disease. Nuclear receptors are evolutionarily recent signal transducers that occupy a special niche in gene regulation, acting as direct connections between a ligand and its downstream transcriptional target. Nuclear receptor signaling governs many physiological processes, however its impact on liver development is not well understood.

In this dissertation, I explore the functions of two nuclear receptor signaling pathways in embryonic zebrafish liver development. First, I define the role of retinoic acid signaling during liver specification. Retinoic acid positively impacts liver development, and individual retinoic acid receptors (RARs) exert distinct effects on hepatic specification. One receptor, Rargb, is uniquely responsible for positioning the liver along the left-right axis and functions upstream of BMP signaling to regulate organ sidedness. Loss of Rargb results in an embryonic phenotype reminiscent of the human heterotaxic condition right atrial isomerism, or Ivemark Syndrome.

Second, I delineate the impact of physiological and environmental estrogens on hepatic differentiation. Estrogenic compounds negatively regulate liver development and exert their effect through estrogen receptor 2 (ESR2) isoforms. In particular, estrogen exposure prevents hepatic differentiation, and embryonic estrogen production and response are carefully orchestrated to enable timely liver maturation. This effect is conserved across vertebrate species.

Together, these studies provide novel insight into the function of nuclear receptor signaling during embryonic liver development. Continued investigation into transcriptional regulation of hepatic specification and differentiation will expand our understanding of and engender new therapies for liver dysfunction.

TABLE OF CONTENTS

LIST OF FIGURES AND TABLES

Chapter 1: Introduction

Chapter 2: *Rargb regulates organ laterality in a zebrafish model of right atrial isomerism*

Chapter 3: *Estrogen inhibits hepatoblast differentiation in an Esr2-dependent manner*

Chapter 4: Ongoing and Future Work

Appendix: *Genome-wide association and functional follow-up reveals new loci for kidney function*

LIST OF ABBREVIATIONS

Adh	Alcohol dehydrogenase
AFP	Alpha-fetoprotein
ALT	Alanine aminotransferase
Amhc	Atrial myosin heavy chain
AP	Alkaline phosphatase
APC	Adenomatous polyposis coli
AR	Androgen receptor
ATRA	All-trans retinoic acid
BMP	Bone morphogenetic protein
BPA	Bisphenol A
BrdU	Bromodeoxyuridine
BRE	BMP response element
Casp	Caspase
ChIP-seq	Chromatin immunoprecipitation sequencing
Ck	Cytokeratin
CKD	Chronic kidney disease
Cmlc	Cardiac myosin light chain
Crabp	Cellular retinoic acid binding protein
Cyp	Cytochrome P450
DAB	3,3'-Diaminobenzidine
DAPI	4',6-Diamidino-2-phenylindole
DDT	Dichlorodiphenyltricloroethane
DEAB	4-diethylaminobenzaldehyde
DMBA	Dimethylbenzanthracene
DMSO	Dimethyl sulfoxide
DNA	Deoxyribonucleic acid
Dpf	Days post-fertilization
DPN	Diarylpropionitrile
E1	Estrone
E2	Estradiol
E3	Estriol
EE	17 alpha-ethynylestradiol
eGFR	Estimated glomerular filtration rate
EIA	Enzyme immunoassay
ER	Estrogen receptor (mammalian nomenclature)
ERE	Estrogen response element
ESR	Estrogen receptor (zebrafish nomenclature)
FACS	Fluorescence-activated cell sorting
FGF	Fibroblast growth factor
FITC	Fluorescein isothiocyanate
FoxA	Forkhead box A
Gata	GATA-binding factor
GFP	Green fluorescent protein
GPER	G-protein coupled estrogen receptor
GR	Glucocorticoid receptor
GWAS	Genome-wide association study
Hand	Heart and neural crest derivatives expressed
HCC	Hepatocellular carcinoma

H&E	Hematoxylin and eosin
Hhex	Hematopoietically-expressed homeobox protein
HNF	Hepatic nuclear factor
Hpf	Hours post-fertilization
Hsp	Heat shock protein
IGF	Insulin-like growth factor
IgG	Immunoglobulin G
IHC	Immunohistochemistry
Lfabp	Liver fatty acid binding protein
LPM	Lateral plate mesoderm
MO	Morpholino
MPP	1,3-*Bis*(4-hydroxyphenyl)-4-methyl-5 -[4-(2-piperidinylethoxy)phenol]-1*H*-pyrazole dihydrochloride
MR	Mineralocorticoid receptor
NCoR	Nuclear co-repressor
NR	Nuclear receptor
PBS	Phosphate buffered saline
PCNA	Proliferating cell nuclear antigen
PFA	Paraformaldehyde
PHTPP	4-[2-Phenyl-5,7-*bis*(trifluoromethyl)pyrazolo[1,5-*a*]pyrimidin-3-yl]phenol
Pitx	Paired-like homeodomain transcription factor
PPAR	Peroxisome proliferator-activated receptor
PPT	4,4',4''-(4-Propyl-[1*H*]-pyrazole-1,3,5 -triyl)*tris*phenol
PR	Progesterone receptor
Prox	Prospero homeobox protein
qPCR	Quantitative polymerase chain reaction
RA	Retinoic acid
Raldh	Retinaldehyde dehydrogenase
RAR	Retinoic acid receptor
RARE	Retinoic acid reponse element
Rbp	Retinol-binding protein
Rdh	Retinol dehydrogenase
RNA-seq	RNA sequencing
RXR	Retinoid X receptor
Shh	Sonic hedgehog
Smad	Sma/mothers against decapentaplegic homolog
SMRT	Silencing mediator for retinoic acid and thyroid hormone receptors
SNP	Single nucleotide polymorphism
Spaw	Southpaw
Srd	Steroid 5-alpha reductase
STM	Septum transversum mesenchyme
TR	Thyroid receptor
TUNEL	Terminal deoxynucleotidyl transferase dUTP nick end labeling
VDR	Vitamin D receptor
Vmhc	Ventricular myosin heavy chain
Wnt	Wingless-type MMTV integration site family member

ACKNOWLEDGMENTS

Thank you, Wolfram. You have been a wonderful mentor, and I have learned a great deal from you about science and, perhaps more importantly, about life. Thank you for encouraging my ideas, pushing me to be innovative in thought and action, and always being available as a sounding board. In the face of hardship, your optimism, thoughtfulness, and humility have remained constant, and that has been inspiring. Thank you also for supporting my endeavors outside of the lab, understanding that science isn't everything, and life's too short. You are remarkable.

Thank you to all members of the Goessling Lab, past and present. The lab has been a happy home for me, due in large part to the people in it. I have learned so much from every one of my colleagues; their scientific expertise, insight, and support have been instrumental to my development as a graduate student. Special thanks to Claire Cutting, my first lab mate, loyal friend, and comedic foil, and Kristen Alexa, whose generosity, kindness, and scientific know-how have kept me afloat.

Thank you to Dr. Trista North and the members of her laboratory with whom the exchange of ideas in lab meetings, practice talks, and manuscript reviews were integral to my scientific growth.

Thank you to Dr. Ramani Ramchandran for his mentorship at the NIH Post-baccalaureate Fellowship Program and the Children's Research Institute at The Medical College of Wisconsin. Ramani was and continues to be an outstanding teacher and scientist. His enthusiasm for science is infectious, and being a member of his lab was an invaluable learning experience.

Thank you to David Keener, my high school biology teacher and one of the best teachers I've ever had. His class was interesting, rigorous, and thoroughly enjoyable. He set the wheels in motion…

Thank you to my dissertation advisory committee, Drs. Clifford Tabin, Ramesh Shivdasani, and Calum MacCrae, for their guidance over the years. Thanks also to Drs. Clifford Tabin, Richard Maas, Caroline Burns, and Michael Pack for agreeing to serve on my dissertation defense committee.

Thank you to the Garnaas and Sedor families for always expressing interest in my latest pursuits and being my biggest advocates – it means so much to me to have such a caring and involved extended family.

Thank you to my friends. To my graduate school classmates Amanda Lee Edwards and Amy Shyer – your friendships have truly enriched my life in Boston, and I am so thankful to have met you in the first few weeks of class. To my Boston Graduate School League teammates – I am so lucky to have had the opportunity to continue to play the sport that I love with a group of fun, interesting, and accomplished graduate students. To my Princeton soccer girls, Emily Behncke, Megan Bernard, Maura Gallagher, Madeleine Jackson, and Romy Trigg-Smith, and dorm mates, Keala Carter and Nike Lawrence – the best part of college was meeting such an amazing group of women. Thank you for being the sisters I never had.

Lastly, and most importantly, thank you Mom and Dad for your unwavering love and support. Thank you for instilling in me the confidence to do anything, providing perspective when necessary, demonstrating what hard work looks like, feigning interest in my experiments, making me laugh, and teaching me life's basics – how to write, draw, appreciate music, throw a ball better than the boys, and do my taxes. I am so grateful for your sacrifices and selflessness. This thesis would not exist without you. I love you.

CHAPTER 1

Introduction

DEVELOPMENTAL BIOLOGY PROVIDES INSIGHT INTO HUMAN DISEASE

Developmental biology is defined as the study of the mechanisms by which organisms grow and develop. The process of converting a single cell to tissues, organs, and ultimately a viable organism consists of a sequence of remarkable and complex events. In the words of developmental biologist Scott Gilbert, "…forming an embryo is the hardest thing you will ever do… One of the critical differences between you and a machine is that a machine is never required to function until after it is built. Every animal has to function as it builds itself" (Gilbert, 2008). Development is intricately controlled by a series of transcriptional cascades. Strict temporal and spatial control of gene expression drives cell specification, differentiation, and proliferation, all of which are imperative for proper development.

Investigating how individual organs develop (organogenesis) is extraordinarily useful for understanding human biology and pathology. Uncovering the mechanisms by which development unfolds and homeostasis is achieved not only provides us with an encyclopedia of knowledge of the requisite elements but also provides the foundation for understanding aberrations that contribute to a variety of disease states. Identifying the molecular players involved in development most obviously impacts our understanding of developmental abnormalities such as congenital organ defects, however its utility goes beyond the embryo. In many adult disease states, cells or entire organs improperly reactivate genetic pathways used during development to their detriment. Cells' improper activation of and failure to turn off proliferative signals is a hallmark of many cancers. Our ability to recognize these signals as repurposed from the developmental setting is integral to the production of successful therapies.

Similarly, understanding developmental signaling will also allow us to harness its advantageous aspects for use as medical treatment. For example, a number of genes are normally only expressed during embryonic or fetal life in progenitor cells, which are

responsible for populating organ primordia and setting in motion differentiation cascades that ultimately lead to the generation of multiple cell types and a complex organ. If recycled in a highly controlled manner in the adult, these cellular signals may aid in regenerating damaged tissues that may otherwise be incapable of naturally repairing themselves. Indeed, investigations of developmental genes are often couched within the development-cancer-regeneration trilogy and for good reason. Development is driven by hundreds of elaborate signaling pathways that work in concert to create a fully functional embryo. Understanding these processes in the complicated developmental milieu can only further our comprehension of their effect in the adult, whether they reappear during disease or are intentionally applied for therapeutic purposes.

THE ZEBRAFISH MODEL

Model organisms, non-human species used to study biological phenomena, are the workhorses of developmental biology. Where human research is not feasible or considered unethical, *in vivo* animal models provide a useful proxy for understanding early developmental events. There are a number of model organisms in use today – prokaryotes, fungi, invertebrates, and vertebrates – and each offers particular advantages. Vertebrate animals, closest evolutionarily to humans, are well suited for studies on organ development. The zebrafish (*Danio rerio*) has emerged as one of the most powerful models to investigate early development, and it is the backbone of this thesis.

The zebrafish emerged as a house pet cum highly tractable genetic organism in the 1980s when George Streisinger, considered the founding father of zebrafish genetics, published a study in which he described the generation of homozygous diploid zebrafish to facilitate mutant isolation and analysis (Streisinger et al., 1981). The following decade, Christiane Nüsslein-Volhard and Wolfgang Driever pioneered a number of

genome-wide mutagenesis screens, uncovering a slew of genes responsible for a range of embryonic phenotypes as well as mutations resulting in organ defects reminiscent of human pathologies (Driever et al., 1996; Haffter et al., 1996; Kane et al., 1996). Importantly, these studies demonstrated that effective large-scale genetic screens could be conducted in vertebrates, not just flies and worms. As a model, the advantages of the zebrafish are many. 71.4% of human genes have a zebrafish ortholog, and 82% of human genes associated with human morbidity have a zebrafish ortholog (Howe et al., 2013). As such, the zebrafish has been used successfully to elucidate the mechanism of a number of human diseases (Lieschke and Currie, 2007). Zebrafish embryos are externally fertilized and optically transparent, allowing for direct observation, and they exhibit high fecundity (a single mating pair can produce 300 embryos a week) and develop rapidly (the heart starts to beat at 1 day post-fertilization). Furthermore, zebrafish are highly amenable to chemical and genetic manipulation (Kari et al., 2007; Zon and Peterson, 2005). As a case in point, our laboratory conducted a chemical genetic screen using zebrafish embryos, testing roughly 2,600 bioactive compounds for their effects on organogenesis, and two hits from this screen are the bases for Chapters 2 and 3 of this thesis.

THE LIVER

Human liver

The liver is an essential organ responsible for a number of metabolic, endocrine, and exocrine functions. It plays vital roles in nutrient processing, including glycogen storage and cholesterol synthesis and transport, blood detoxification, and secretion of serum proteins and bile. The liver is primarily composed of hepatoctyes – they make up three-quarters of its volume – which function in concert with a number of other cell types including biliary epithelial cells (cholangiocytes), endothelial cells, Kupffer cells

(macrophages), and hepatic stellate cells. The liver lobule is the basic architectural unit of the liver and consists of hexagonal plates of hepatocytes (Figure 1-1). Portal triads, each containing a hepatic artery, portal vein, and bile duct, border each of the six corners of the lobule. Blood enters the lobule via the hepatic artery and portal vein, supplying oxygen and nutrients to the organ, and then flows through a network of sinusoidal capillaries before it leaves through the central vein located at the lobule's middle. Bile generated by hepatocytes is collected first into bile caniculi then drained into bile ducts where it is either secreted into the small intestine or stored in the gall bladder.

Altered liver function resulting from developmental defects, inflammation, cirrhosis, or cancer leads to significant morbidity and mortality, however treatment options for these conditions remain extremely limited. It is estimated that one in every ten Americans suffers from liver disease, and liver disease in one of the top ten causes of death in the United States. Liver transplant is the only long-term option for treating advanced liver failure, however there is a great disparity between the number of patients requiring transplant and the number of available organs. In the United States, 6,000 liver transplants are performed annually while nearly 17,000 patients remain on the waiting list (American Liver Foundation, 2013). Continued investigations into the molecular mechanisms responsible for hepatic specification will engender new and better therapies to combat liver dysfunction.

Liver development in terrestrial vertebrates

Endoderm, one of the three primary germ layers, is established during gastrulation, and the liver arises from the anterior portion of the primitive gut tube, or foregut endoderm (Le Douarin, 1975) (Figure 1-2A). Cell fate-mapping studies have

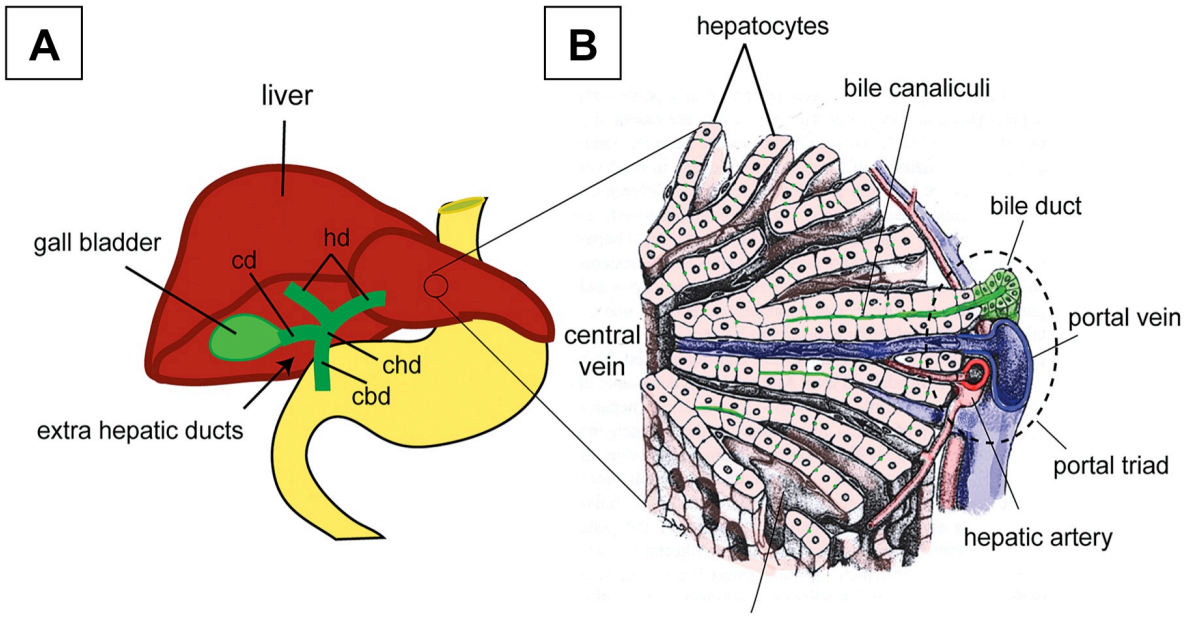

Figure 1-1. Human liver architecture.

(A) Schematic depicting the arrangement of the liver (red), gall bladder (green), and stomach and intestine (yellow) in the adult. Bile secreted by the liver is collected by a network of intrahepatic ducts (hd) and drained from the liver into the common hepatic duct (chd). From there, bile enters the gall bladder via the cystic duct (cd) or the duodenum via the common bile duct (cbd), where it facilitates digestion.

(B) Schematic illustrating the cellular architecture of the liver. The primary functional unit of the liver comprises a hexagonal sheet of hepatocytes containing a central vein and portal triad consisting of a bile duct, portal vein, and hepatic artery. Taken from Zorn, 2008.

Figure 1-2 (next page). Vertebrate liver development.

(A) In the mouse, the liver (red) is derived from the foregut endoderm (fg, yellow), and hepatic progenitors are first identifiable by gene expression at e8. Specified hepatoblasts bud into the surrounding mesencyme forming the liver diverticulum (ld), and as the liver continues to grow outwardly, it ultimately forms a distinct liver bud (lb). By e15, hepatoblasts have begun differentiating into hepatocyte and biliary lineages, and the liver continues to mature after birth.

(B-F) Zebrafish liver development. Hepatic progenitors are specified in the gut tube by 24 hpf (B), and the liver bud emerges to the left of the midline between 24-28 hpf (arrowhead, C). The newly formed liver bud continues to expand outwardly from 48 hpf onward (D, E), and a furrow forms to separate the liver from the intestinal bulb (black arrow). The pancreas also emerges from the foregut endoderm at this time (asterisks in C, D). By 5 dpf, the liver (red) lies ventral and anterior to the swim bladder (sb) and notochord (n), with one lobe sitting atop the head of the pancreas (green). At this point in development, the liver has formed bilateral (left and right) lobes. Images in (B-D) are dorsal views of *foxA3:GFP* transgenic reporter fish. (E) depicts expression of the hepatocyte marker *lfabp*. Adapted from Field et al., 2003; Zorn, 2008; Tao and Peng, 2009; Chu and Sadler, 2009.

Figure 1-2 (continued)

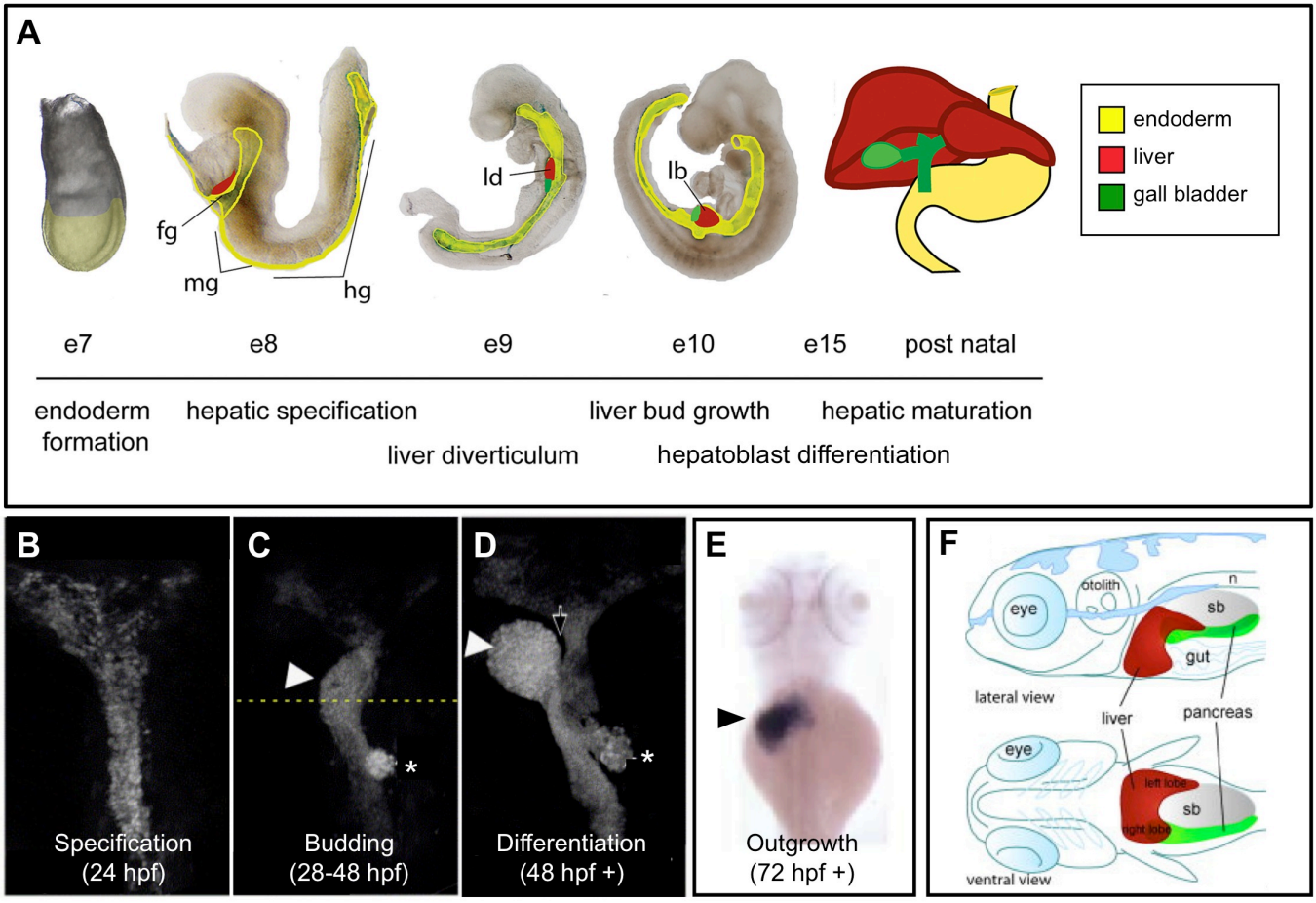

established that liver progenitors originate in three separate domains within the developing foregut (Tremblay and Zaret, 2005). Upon foregut closure, the bilateral and medial domains merge, and the hepatic endoderm is specified. The first morphological indicator of liver specification is an out-pocketing of foregut epithelium known as the liver diverticulum. The anterior region of the diverticulum ultimately generates the liver and intrahepatic bileducts, whereas the posterior portion forms the gall bladder and extrahpatic bile ducts (Zorn, 2008; Si-Tayeb et al., 2010).

As hepatic progenitor cells bud into the surrounding stroma, they receive instructive signals from neighboring tissues (Le Douarin, 1975; Cascio and Zaret, 1991). Fibroblast growth factor (Fgf) and bone morphogenetic protein (Bmp) signals generated by adjacent pre-cardiac mesoderm and septum transversum mesenchyme (STM), respectively, induce hepatic progenitors (hepatoblasts) and promote outgrowth of the liver primordium (Jung et al., 1999; Rossi et al., 2001). Secreted Fgfs also suppress the default pancreatic fate of the ventral endoderm (Deutsch et al., 2001). Following specification of the hepatic endoderm, the earliest known marker of the developing liver is hematopoietically-expressed homeobox protein (Hhex), a homeodomain transcription factor. Loss of *Hhex* results in failed liver bud outgrowth, however expression of liver-specific genes and a slight swelling of the endoderm are still detectable (Keng et al., 2000; Martinez Barbera et al., 2000), suggesting that specification of the hepatic lineage still occurs in *Hhex* null mice. Hhex and another homeodomain transcription factor, Prospero homeobox protein 1 (Prox1), also regulate hepatic differentiation and proliferation (Sosa-Pineda et al., 2000). Members of the hepatic nuclear factor (Hnf), GATA-binding factor (Gata), and forkhead box A (FoxA) families of transcription factors direct hepatic specification and coordinate subsequent differentiation of hepatoblasts into mature hepatocyte and bile-duct lineages (Zaret, 2002), while wingless-type MMTV integration site family member (Wnt) signaling modulates expansion of the hepatocyte

population (Thompson and Monga, 2007).

Liver development in zebrafish

The zebrafish (*Danio rerio*) is an excellent model for the study of vertebrate organogenesis. Embryos develop *ex utero*, are optically clear, and hundreds of embryos can be produced weekly for large-scale genetic manipulations or chemical screens. In addition, the zebrafish is uniquely suited for studying liver development because the liver is not a site of hematopoiesis as it is in mice (Davidson and Zon, 2004), allowing for investigation of liver defects without complications from anemia or early lethality.

In the fish, hepatic progenitors are first identifiable by *hhex* expression at 18 hours post fertilization (hpf) in the anterior endoderm. Between 24 and 28 hpf, hepatoblasts aggregate and emerge as a bud to the left of the midline (Figure 1-2, B-C) (Field et al., 2003). By 48 hpf, the liver begins to function, and specified hepatocytes express mature markers such as *liver fatty acid binding protein* (*lfabp*) (Figure 1-2, D-E) (Her et al., 2003). At this stage, a furrow also forms to separate the liver bud from the intestine, and the remaining cells connecting these organs form the hepatic duct. As in mice, this initial budding phase is characterized by expression of a number of *foxA* and *gata* factors, as well as *hhex*, *prox1*, and *hnf4* in the liver primordium (Field et al., 2003). Subsequent outgrowth of the liver bud is driven by accelerated hepatocyte proliferation. The mature liver is bi-lobed and consists of a larger left lobe that lies adjacent to the anterior gut and a smaller right lobe that abuts the head of the pancreas (Figure 1-2F) (Chu and Sadler, 2009).

Importantly, the molecular programs governing liver development are conserved among vertebrates (Stainier, 2002; Zorn and Wells, 2007). Expression of dominant negative forms of Fgf and Bmp receptors following heat shock induction revealed that Bmp and Fgf signals are required during hepatoblast specification (18-22 hpf), but are

largely dispensable for maintenance of specified liver progenitors (Shin et al., 2007). Furthermore, expression of Fgf and Bmp signals in the surrounding mesoderm prevents specification of pancreatic lineages (Chung et al., 2008; Dong et al., 2007). Hepatic specification is defective in *prometheus/wnt2bb* and *adenomatous polyposis coli* (*APC*) mutants (Goessling et al., 2008; Ober et al., 2006), also demonstrating a conserved requirement for Wnt signaling during hepatogenesis.

Given that precursors of many endodermal organs derive along the anterior-posterior axis of the digestive tract, it is not surprising that multiple signaling inputs are required to specify the liver primordium. What makes one endodermal domain competent to interpret and translate these signals into the hepatic fate remains one of the outstanding questions in the field of liver development. Identifying additional liver-specific signals and elucidating their regulation in space and time will advance our understanding of hepatic development and homeostasis.

NUCLEAR RECEPTOR SIGNALING

Nuclear receptors (NRs) are defined as ligand-activated transcription factors that bind to and thereby regulate downstream gene targets. NRs are organized in a modular fashion, containing five to six functional domains that are designated A-E/F (Figure 1-3A) (Renaud and Moras, 2000). Each domain is relatively autonomous such that exchanging the same domain among related NRs does not significantly impact NR function (Aranda and Pascual, 2001). The two most highly conserved domains are the DNA-binding domain (DBD) (C) and ligand-binding domain (LBD) (E), which mediate NR's ability to activate transcription. The DBD is located nearer the N-terminus and contains two zinc-finger motifs, whereas the LBD is located closer to the C-terminus and is composed of a series of alpha helices. The A and F domains flanking these regions are highly variable and often contain an autonomous (ligand-independent) transcriptional

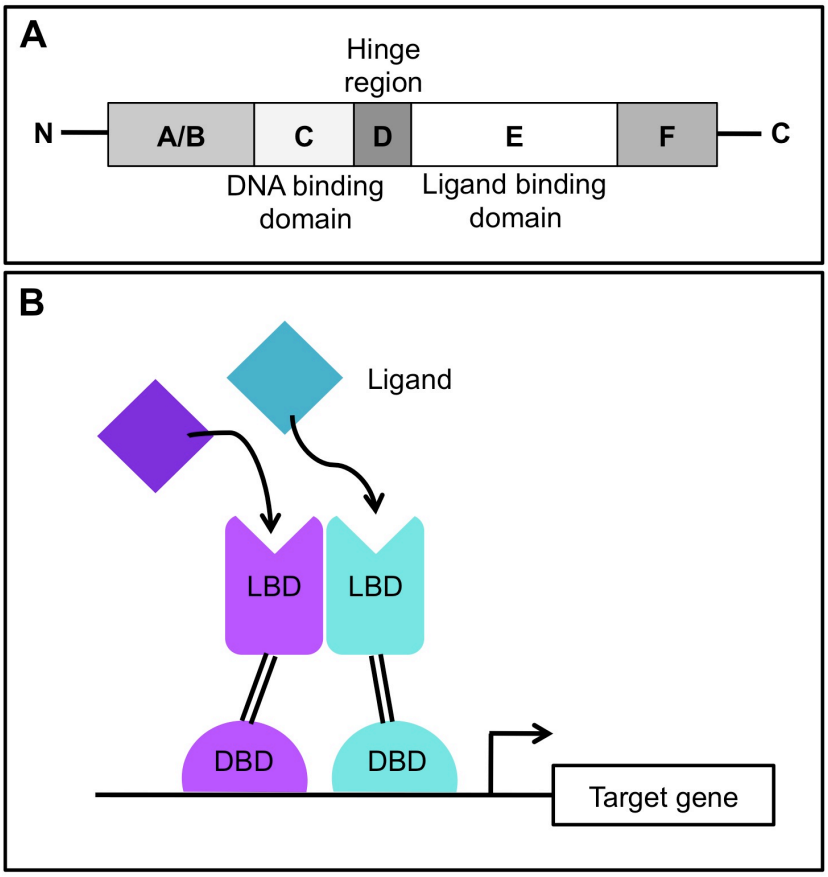

Figure 1-3. Nuclear receptor structure and signaling.

(A) Nuclear receptors typically consist of five to six functional domains: a variable N-terminal domain A/B, a DNA binding domain C, a hinge domain D, a ligand binding domain E, and a variable C-terminal domain F.

(B) Nuclear receptor signal transduction is initiated when ligands such as retinoids or steroid hormones bind to the ligand binding domain (LBD) of their associated nuclear receptors. Receptors may either homo- or heterodimerize and bind to downstream transcriptional targets via their DNA binding domain (DBD). In the case of retinoic acid receptors (RARs), receptors are situated on the promoter of the target gene, and ligand binding causes release of a corepressor complex allowing for transcription to proceed. Estrogen receptors (ERs) are normally localized to the cytoplasm but translocate to the nucleus following ligand activation. Adapted from Handschin and Meyer, 2003.

activation function termed AF-1. A second transcriptional activation domain is found in the LBD/E domain, however it is strictly ligand-dependent. NRs are primarily activated by lipophilic molecules such as steroid hormones, vitamin derivatives, and fatty acids; the alpha helices in the LBD create a hydrophobic pocket that has high affinity for these lipophilic ligands.

The NR superfamily is subdivided into three classes – the steroid, thyroid/retinoid, and orphan receptor families (Cheskis, 2004; Robinson-Rechavi et al., 2003; Tata, 2002). Steroid receptors include the estrogen receptor (ER), androgen receptor (AR), progesterone receptor (PR), glucocorticoid receptor (GR), and mineralocorticoid receptor (MR). Typically, inactive steroid receptors are bound to heat shock proteins (Hsp) in the cytoplasm. Following ligand binding, steroid receptors are released from the Hsp complex, homodimerize, and translocate to the nucleus to bind to NR response elements on target gene promoters (Figure 1-3B). Thyroid/retinoid receptors include the vitamin D receptor (VDR), retinoic acid receptor (RAR), thyroid receptor (TR), and peroxisome proliferator-activated receptor (PPAR). In contrast to the steroid receptor subclass, thyroid/retinoid receptors generally function as heterodimers in complex with retinoid X receptors (RXR). Moreover, these receptor heterodimers function as gene silencers in the absence of ligand via recruitment of co-repressors such as the nuclear co-repressor (NCoR) and silencing mediator for retinoic acid and thyroid hormone receptors (SMRT) (Collingwood et al., 1999; Smirnov, 2002). Ligand binding alleviates this repression, allowing for target activation.

To date, 48 members have been identified in the NR superfamily in humans (Imai et al., 2013). There are more NR paralogs in zebrafish than mammals due to a genome duplication event during teleost evolution (Postlethwait et al., 1998). Phylogenetically, all NRs share a common ancestor, and it is hypothesized that NRs originated as orphan receptors. Lines of evidence supporting this theory include the fact that orthologs of

classically liganded receptors have not been identified in non-bilaterian animals (suggesting a more recent evolution of the liganded NRs), and NRs can elicit cellular responses independent of ligand activation, for example by conformational changes mediated by phosphorylation (Markov and Laudet, 2011). It is widely believed that ancestral NRs originally acted as environment and nutrient sensors since their existence well preceded the development of any endocrine system. There is remarkable similarity between the xenobiotic response and steroid metabolism pathways, as both make use of the cytochrome P450 (Cyp) hydroxylating enzymes. This suggests that dietary metabolites such as steroids derived from cholesterol or retinoids derived from β-carotene may have at one point acted as endogenous hormones (Khersonsky et al., 2006). By using NRs to sense environmental toxins or internal nutrient levels, an organism may have thereby appropriately regulated production of necessary detoxification enzymes. Certainly, the evolution of animals and NR signaling occurred in parallel, as the development of additional and more complex NR-ligand pairs allowed for regulation between organ systems in more complex organisms. In fact, there is strong correlation between the number and kinds of cell types in an animal and the number of NR genes (Escriva et al., 2004; Escriva et al., 2000).

Continued investigation of the impact of NRs on embryonic development will undoubtedly aid in the creation of effective human therapies. NRs are attractive drug targets not only because they play integral roles in a host of development processes but because their activity is ligand-dependent, and many of the most effective clinical treatments consist of small hydrophobic compounds that can easily traverse a cell's plasma membrane to exert their effect.

Retinoic acid signaling

Retinoic acid (RA) is the active form of vitamin A (retinol). Vitamin A is an

essential nutrient that requires strict regulation during embryonic development, as vitamin A deficiency results in congenital malformations in heart, eye, circulatory, urogenital, and respiratory systems, and excessive vitamin A is teratogenic (Zile, 1998). RA exerts its effects on embryogenesis by regulating gene expression. However, unlike protein factors such as Fgf or Wnt that bind to cell surface receptors, RA acts directly on target genes in the nucleus via its receptors. Retinol, transported in the serum by retinol-binding protein 4 (Rbp4) to RA-generating tissue, is first converted to retinaldehyde by alcohol or retinol dehydrogenases (Adh or Rdh) then is further converted to RA by retinaldehyde dehydrogenases (Raldh). Adhs are widely expressed whereas Raldhs show tissue-specific expression (Duester, 2008; Liang et al., 2008). Spatial regulation of RA is further achieved by Cyp enzymes, which are responsible for degrading RA (White and Schilling, 2008), and cellular RA-binding proteins (Crabp), which facilitate RA uptake (Sessler and Noy, 2005). Once RA enters its target cell, it can bind to two types of retinoid receptors – the RA receptors (RARs) and retinoid X receptors (RXRs) – both of which are part of the NR superfamily (Pfahl and Chytil, 1996). In mammals, there are three orthologs of both RARs and RXRs (α, β, γ), and multiple isoforms of each RAR perform varied functions (Bastien and Rochette-Egly, 2004). Zebrafish possess all RXR subtypes but only RARα and γ orthologs. RARs bind all-*trans*-RA (ATRA), and RXRs bind its less common isomer 9-*cis*-RA. RXRs are known to heterodimerize with RARs, however ligand binding to the RAR component of heterodimers is sufficient for signal transduction in mice (Mic et al., 2003). Coupling of the ligand-receptor complex with a RA reponse element (RARE) on a target gene's promoter mediates transcription.

Estrogen signaling

Estrogen is a steroid hormone that plays a critical role in many aspects of human

physiology. Estrogen signaling is known to impact reproductive development and function, tissue growth, bone maintenance, and the cardiovascular, nervous, and immune systems. Not surprisingly, estrogen excess or deficiency has been linked to a number of diseases, including breast and prostate cancer, osteoporosis, and infertility (Heldring et al., 2007). Estrogen is a cholesterol derivative that is sequentially converted from progestagens to androgens and finally estrogens through a series of enzymatic reactions. The final rate-limiting step in estrogen biosynthesis is catalyzed by the Cyp enzyme aromatase (Cyp19a1). There are three naturally occurring estrogens – estriol, estradiol, and estrone – which bind to estrogen receptors (ERs) with differing affinities. Estradiol is the most potent circulating estrogen. To initiate signal transduction, estrogens pass through a cell's phospholipid membrane and bind to their cognate receptors in the cytoplasm. Following ligand binding, ERs are released from an inhibitory Hsp complex, homodimerize, and translocate to the nucleus to regulate downstream transcriptional programs. Ligand-bound ERs typically interact directly with estrogen response elements (EREs) in the target gene's promoter region, however they have also been shown to associate with other transcription factor complexes with AP-1 or SP-1 responsive elements (Kushner et al., 2000; Saville et al., 2000). Mammalian species possess two estrogen receptors, ERα and ERβ, which are products of two genes found on distinct chromosomes (Enmark et al., 1997; Gosden et al., 1986). Many fish species including zebrafish have three receptors, Esr1, Esr2a, and Esr2b; the Esr2 subtypes resulted from genome duplication during teleost evolution (Postlethwait et al., 1998). Estradiol exhibits similar binding affinities to each ER isoform in fish and mammals (Menuet et al., 2002). In all species, ERs show overlapping but distinct expression patterns in a number of organ systems, including the gonads, bone, muscle, liver, nervous system, vasculature, and adipose tissue (Chandrasekar et al., 2010; Matthews and Gustafsson, 2003). Recently, an additional estrogen target has been

identified, G-protein coupled estrogen receptor 1 (GPER), that is believed to transduce the estrogen signal non-genomically via phosphorylation of downstream kinases (Liu et al., 2009). Interestingly, whereas many NRs including the thyroid and RA receptors contain a ligand-binding cavity well tailored to their corresponding ligands, ERs possess a large ligand pocket relative to the size of estradiol (Brzozowski et al., 1997). This feature allows ERs to bind compounds with a range of structures, permitting a number of environmental pollutants (xenoestrogens) and plant-derived compounds (phytoestrogens) to elicit transcriptional responses similar to physiological estrogens.

Nuclear receptor signaling and the liver

A number of studies have implicated roles for several NRs in liver development and homeostasis, however the extent of NR signaling's effects on hepatogenesis has not been fully elucidated. Several components of the thyroid/retinoid NR signaling pathways are localized to the liver. Vitamin A is stored in hepatic stellate cells (Zou et al., 1998), and the RA synthesizing enzyme Raldh4 is uniquely expressed in the mammalian liver (Lin et al., 2003). The active form of vitamin D, $1\alpha,25(OH)_2D_3$, is synthesized in the liver, the liver expresses VDR, and ligand binding to VDR has been demonstrated in the livers of some fish species (Craig et al., 2008; Sundell et al., 1992). Additionally, steroid NRs such as ERs are highly expressed in both the embryonic and adult liver (Chandrasekar et al., 2010; Matthews and Gustafsson, 2003). The fact that many NR signaling components are found in the liver suggests they play an important role in the organ's development and regulation, however their effect on and interaction with other developmental signaling pathways during liver development has not been well characterized.

To date, the most well described NR in liver development is hepatic nuclear factor 4α (Hnf4α), which until recently was considered an orphan NR but is now known

to bind linoleic acid (Yuan et al., 2009). Hnf4α is expressed in hepatic progenitors as well as mature hepatocytes, and it binds roughly half of all genes expressed in the mouse liver (Odom et al., 2004). Loss of Hnf4α results in aberrant hepatocyte morphology and loss of hepatic enzymes (Li et al., 2000; Parviz et al., 2003; Watt et al., 2003). Aside from Hnf4α, however, the role of individual NRs in liver development and homeostasis has not been fully illuminated, and this fact was the driver of the research presented in this dissertation.

THESIS SUMMARY

In this dissertation, I examine the role of two NR signaling pathways in liver development. In Chapter 2, I demonstrate that retinoic acid signaling is a positive regulator of hepatogenesis and identify distinct roles for RA-synthesizing enzymes and receptors during hepatic specification in zebrafish. One RAR, Rargb, is uniquely responsible for conferring left-right positional information in the embryo. Loss of *rargb* results in bilateral livers, midline hearts, and asplenia – defects associated with the human pathology right atrial isomerism, or Ivemark Syndrome. I illustrate that Rargb functions upstream of Bmp to exert its effects on left-right patterning, uncovering a novel molecular mechanism by which organ asymmetry is regulated.

In Chapter 3, I describe the importance of estrogen signaling for proper hepatic differentiation. In zebrafish, estrogen signaling negatively regulates embryonic liver development, and its effect is primarily mediated via the Esr2 receptor subtype. Exposure to estradiol prevents hepatocyte differentiation, and in mice, embryos exposed to excess estrogen similarly display an undifferentiated phenotype characterized by surfeit hepatoblasts. In human embryonic stem cells, loss of activating epigenetic modifications at the ERβ locus, resulting in its downregulated expression, marks the

transition from definitive endoderm to differentiated liver cells. These results indicate that estrogen acts across to species to regulate liver differentiation.

In my final chapter, I highlight ongoing and future work that will augment our understanding of the impact of RA and estrogen signaling on liver development and homeostasis. I discuss a notable finding that estrogen acts in a biphasic manner during embryonic and larval liver development and describe ongoing studies intended to uncover the mechanism by which this occurs. I also detail experiments that will be performed to elucidate the impact of NR signaling on adult liver homeostasis and disease. Together, these completed and future investigations will expand our knowledge of NR signaling in liver development and promote the creation of novel and effective therapies for a number of diseases including developmental defects, hepatic dysfunction, and cancer.

REFERENCES

American Liver Foundation. (2013). Liver wellness: Increasing public awareness of liver health. http://www.liverfoundation.org/downloads/alf_download_29.pdf.

Aranda, A. and Pascual, A. (2001). Nuclear hormone receptors and gene expression. Physiol Rev 81, 1269-304.

Bastien, J. and Rochette-Egly, C. (2004). Nuclear retinoid receptors and the transcription of retinoid-target genes. Gene 328, 1-16.

Brzozowski, A. M., Pike, A. C., Dauter, Z., Hubbard, R. E., Bonn, T., Engstrom, O., Ohman, L., Greene, G. L., Gustafsson, J. A. and Carlquist, M. (1997). Molecular basis of agonism and antagonism in the oestrogen receptor. Nature 389, 753-8.

Cascio, S. and Zaret, K. S. (1991). Hepatocyte differentiation initiates during endodermal-mesenchymal interactions prior to liver formation. Development 113, 217-25.

Chandrasekar, G., Archer, A., Gustafsson, J. A. and Andersson Lendahl, M. (2010). Levels of 17beta-estradiol receptors expressed in embryonic and adult zebrafish following in vivo treatment of natural or synthetic ligands. PLoS One 5, e9678.

Cheskis, B. J. (2004). Regulation of cell signalling cascades by steroid hormones. J Cell Biochem 93, 20-7.

Chu, J. and Sadler, K. C. (2009). New school in liver development: lessons from zebrafish. Hepatology 50, 1656-63.

Chung, W. S., Shin, C. H. and Stainier, D. Y. (2008). Bmp2 signaling regulates the hepatic versus pancreatic fate decision. Dev Cell 15, 738-48.

Collingwood, T. N., Urnov, F. D. and Wolffe, A. P. (1999). Nuclear receptors: coactivators, corepressors and chromatin remodeling in the control of transcription. J Mol Endocrinol 23, 255-75.

Craig, T. A., Sommer, S., Sussman, C. R., Grande, J. P. and Kumar, R. (2008). Expression and regulation of the vitamin D receptor in the zebrafish, Danio rerio. J Bone Miner Res 23, 1486-96.

Davidson, A. J. and Zon, L. I. (2004). The 'definitive' (and 'primitive') guide to zebrafish hematopoiesis. Oncogene 23, 7233-46.

Deutsch, G., Jung, J., Zheng, M., Lora, J. and Zaret, K. S. (2001). A bipotential precursor population for pancreas and liver within the embryonic endoderm. Development 128, 871-81.

Dong, P. D., Munson, C. A., Norton, W., Crosnier, C., Pan, X., Gong, Z., Neumann, C. J. and Stainier, D. Y. (2007). Fgf10 regulates hepatopancreatic ductal system patterning and differentiation. Nat Genet 39, 397-402.

Driever, W., Solnica-Krezel, L., Schier, A. F., Neuhauss, S. C., Malicki, J., Stemple, D. L., Stainier, D. Y., Zwartkruis, F., Abdelilah, S., Rangini, Z. et al. (1996). A genetic screen for mutations affecting embryogenesis in zebrafish. Development 123, 37-46.
Duester, G. (2008). Retinoic acid synthesis and signaling during early organogenesis. Cell 134, 921-31.

Enmark, E., Pelto-Huikko, M., Grandien, K., Lagercrantz, S., Lagercrantz, J., Fried, G., Nordenskjold, M. and Gustafsson, J. A. (1997). Human estrogen receptor beta-gene structure, chromosomal localization, and expression pattern. J Clin Endocrinol Metab 82, 4258-65.

Escriva, H., Bertrand, S. and Laudet, V. (2004). The evolution of the nuclear receptor superfamily. Essays Biochem 40, 11-26.

Escriva, H., Delaunay, F. and Laudet, V. (2000). Ligand binding and nuclear receptor evolution. Bioessays 22, 717-27.

Field, H. A., Ober, E. A., Roeser, T. and Stainier, D. Y. (2003). Formation of the digestive system in zebrafish. I. Liver morphogenesis. Dev Biol 253, 279-90.

Goessling, W., North, T. E., Lord, A. M., Ceol, C., Lee, S., Weidinger, G., Bourque, C., Strijbosch, R., Haramis, A. P., Puder, M. et al. (2008). APC mutant zebrafish uncover a changing temporal requirement for wnt signaling in liver development. Dev Biol 320, 161-74.

Gosden, J. R., Middleton, P. G. and Rout, D. (1986). Localization of the human oestrogen receptor gene to chromosome 6q24----q27 by in situ hybridization. Cytogenet Cell Genet 43, 218-20.

Haffter, P., Granato, M., Brand, M., Mullins, M. C., Hammerschmidt, M., Kane, D. A., Odenthal, J., van Eeden, F. J., Jiang, Y. J., Heisenberg, C. P. et al. (1996). The identification of genes with unique and essential functions in the development of the zebrafish, Danio rerio. Development 123, 1-36.

Handschin, C. and Meyer, U. A. (2003). Induction of drug metabolism: the role of nuclear receptors. Pharmacol Rev 55, 649-73.

Heldring, N., Pike, A., Andersson, S., Matthews, J., Cheng, G., Hartman, J., Tujague, M., Strom, A., Treuter, E., Warner, M. et al. (2007). Estrogen receptors: how do they signal and what are their targets. Physiol Rev 87, 905-31.

Her, G. M., Yeh, Y. H. and Wu, J. L. (2003). 435-bp liver regulatory sequence in the liver fatty acid binding protein (L-FABP) gene is sufficient to modulate liver regional expression in transgenic zebrafish. Dev Dyn 227, 347-56.

Howe, K. Clark, M. D. Torroja, C. F. Torrance, J. Berthelot, C. Muffato, M. Collins, J. E. Humphray, S. McLaren, K. Matthews, L. et al. (2013). The zebrafish reference genome sequence and its relationship to the human genome. Nature 496, 498-503.

Imai, Y., Youn, M. Y., Inoue, K., Takada, I., Kouzmenko, A. and Kato, S. (2013). Nuclear receptors in bone physiology and diseases. Physiol Rev 93, 481-523.

Jung, J., Zheng, M., Goldfarb, M. and Zaret, K. S. (1999). Initiation of mammalian liver development from endoderm by fibroblast growth factors. Science 284, 1998-2003.

Kane, D. A., Hammerschmidt, M., Mullins, M. C., Maischein, H. M., Brand, M., van Eeden, F. J., Furutani-Seiki, M., Granato, M., Haffter, P., Heisenberg, C. P. et al. (1996). The zebrafish epiboly mutants. Development 123, 47-55.

Kari, G., Rodeck, U. and Dicker, A. P. (2007). Zebrafish: an emerging model system for human disease and drug discovery. Clin Pharmacol Ther 82, 70-80.

Keng, V. W., Yagi, H., Ikawa, M., Nagano, T., Myint, Z., Yamada, K., Tanaka, T., Sato, A., Muramatsu, I., Okabe, M. et al. (2000). Homeobox gene Hex is essential for onset of mouse embryonic liver development and differentiation of the monocyte lineage. Biochem Biophys Res Commun 276, 1155-61.

Khersonsky, O., Roodveldt, C. and Tawfik, D. S. (2006). Enzyme promiscuity: evolutionary and mechanistic aspects. Curr Opin Chem Biol 10, 498-508.

Kushner, P. J., Agard, D. A., Greene, G. L., Scanlan, T. S., Shiau, A. K., Uht, R. M. and Webb, P. (2000). Estrogen receptor pathways to AP-1. J Steroid Biochem Mol Biol 74, 311-7.

Li, J., Ning, G. and Duncan, S. A. (2000). Mammalian hepatocyte differentiation requires the transcription factor HNF-4alpha. Genes Dev 14, 464-74.

Liang, D., Zhang, M., Bao, J., Zhang, L., Xu, X., Gao, X. and Zhao, Q. (2008). Expressions of Raldh3 and Raldh4 during zebrafish early development. Gene Expr Patterns 8, 248-53.

Lieschke, G. J. and Currie, P. D. (2007). Animal models of human disease: zebrafish swim into view. Nat Rev Genet 8, 353-67.

Liu, S., Le May, C., Wong, W. P., Ward, R. D., Clegg, D. J., Marcelli, M., Korach, K. S. and Mauvais-Jarvis, F. (2009). Importance of extranuclear estrogen receptor-alpha and membrane G protein-coupled estrogen receptor in pancreatic islet survival. Diabetes 58, 2292-302.

Markov, G. V. and Laudet, V. (2011). Origin and evolution of the ligand-binding ability of nuclear receptors. Mol Cell Endocrinol 334, 21-30.

Martinez Barbera, J. P., Clements, M., Thomas, P., Rodriguez, T., Meloy, D., Kioussis, D. and Beddington, R. S. (2000). The homeobox gene Hex is required in definitive endodermal tissues for normal forebrain, liver and thyroid formation. Development 127, 2433-45.

Matthews, J. and Gustafsson, J. A. (2003). Estrogen signaling: a subtle balance between ER alpha and ER beta. Mol Interv 3, 281-92.

Menuet, A., Pellegrini, E., Anglade, I., Blaise, O., Laudet, V., Kah, O. and Pakdel, F. (2002). Molecular characterization of three estrogen receptor forms in zebrafish: binding

characteristics, transactivation properties, and tissue distributions. Biol Reprod 66, 1881-92.

Mic, F. A., Molotkov, A., Benbrook, D. M. and Duester, G. (2003). Retinoid activation of retinoic acid receptor but not retinoid X receptor is sufficient to rescue lethal defect in retinoic acid synthesis. Proc Natl Acad Sci U S A 100, 7135-40.

Ober, E. A., Verkade, H., Field, H. A. and Stainier, D. Y. (2006). Mesodermal Wnt2b signalling positively regulates liver specification. Nature 442, 688-91.

Odom, D. T., Zizlsperger, N., Gordon, D. B., Bell, G. W., Rinaldi, N. J., Murray, H. L., Volkert, T. L., Schreiber, J., Rolfe, P. A., Gifford, D. K. et al. (2004). Control of pancreas and liver gene expression by HNF transcription factors. Science 303, 1378-81.

Parviz, F., Matullo, C., Garrison, W. D., Savatski, L., Adamson, J. W., Ning, G., Kaestner, K. H., Rossi, J. M., Zaret, K. S. and Duncan, S. A. (2003). Hepatocyte nuclear factor 4alpha controls the development of a hepatic epithelium and liver morphogenesis. Nat Genet 34, 292-6.

Pfahl, M. and Chytil, F. (1996). Regulation of metabolism by retinoic acid and its nuclear receptors. Annu Rev Nutr 16, 257-83.

Postlethwait, J. H., Yan, Y. L., Gates, M. A., Horne, S., Amores, A., Brownlie, A., Donovan, A., Egan, E. S., Force, A., Gong, Z. et al. (1998). Vertebrate genome evolution and the zebrafish gene map. Nat Genet 18, 345-9.

Renaud, J. P. and Moras, D. (2000). Structural studies on nuclear receptors. Cell Mol Life Sci 57, 1748-69.

Robinson-Rechavi, M., Escriva Garcia, H. and Laudet, V. (2003). The nuclear receptor superfamily. J Cell Sci 116, 585-6.

Rossi, J. M., Dunn, N. R., Hogan, B. L. and Zaret, K. S. (2001). Distinct mesodermal signals, including BMPs from the septum transversum mesenchyme, are required in combination for hepatogenesis from the endoderm. Genes Dev 15, 1998-2009.

Saville, B., Wormke, M., Wang, F., Nguyen, T., Enmark, E., Kuiper, G., Gustafsson, J. A. and Safe, S. (2000). Ligand-, cell-, and estrogen receptor subtype (alpha/beta)-dependent activation at GC-rich (Sp1) promoter elements. J Biol Chem 275, 5379-87.

Sessler, R. J. and Noy, N. (2005). A ligand-activated nuclear localization signal in cellular retinoic acid binding protein-II. Mol Cell 18, 343-53.

Si-Tayeb, K., Lemaigre, F. P. and Duncan, S. A. (2010). Organogenesis and development of the liver. Dev Cell 18, 175-89.

Smirnov, A. N. (2002). Nuclear receptors: nomenclature, ligands, mechanisms of their effects on gene expression. Biochemistry (Mosc) 67, 957-77.

Sosa-Pineda, B., Wigle, J. T. and Oliver, G. (2000). Hepatocyte migration during liver development requires Prox1. Nat Genet 25, 254-5.

Stainier, D. Y. (2002). A glimpse into the molecular entrails of endoderm formation. Genes Dev 16, 893-907.

Streisinger, G., Walker, C., Dower, N., Knauber, D. and Singer, F. (1981). Production of clones of homozygous diploid zebra fish (Brachydanio rerio). Nature 291, 293-6.

Sundell, K., Bishop, J. E., Bjornsson, B. T. and Norman, A. W. (1992). 1,25-Dihydroxyvitamin D3 in the Atlantic cod: plasma levels, a plasma binding component, and organ distribution of a high affinity receptor. Endocrinology 131, 2279-86.

Tao, T. and Peng, J. (2009). Liver development in zebrafish (Danio rerio). J Genet Genomics 36, 325-34.

Tata, J. R. (2002). Signalling through nuclear receptors. Nat Rev Mol Cell Biol 3, 702-10.
Thompson, M. D. and Monga, S. P. (2007). WNT/beta-catenin signaling in liver health and disease. Hepatology 45, 1298-305.

Tremblay, K. D. and Zaret, K. S. (2005). Distinct populations of endoderm cells converge to generate the embryonic liver bud and ventral foregut tissues. Dev Biol 280, 87-99.

Watt, A. J., Garrison, W. D. and Duncan, S. A. (2003). HNF4: a central regulator of hepatocyte differentiation and function. Hepatology 37, 1249-53.

White, R. J. and Schilling, T. F. (2008). How degrading: Cyp26s in hindbrain development. Dev Dyn 237, 2775-90.

Yuan, X., Ta, T. C., Lin, M., Evans, J. R., Dong, Y., Bolotin, E., Sherman, M. A., Forman, B. M. and Sladek, F. M. (2009). Identification of an endogenous ligand bound to a native orphan nuclear receptor. PLoS One 4, e5609.

Zaret, K. S. (2002). Regulatory phases of early liver development: paradigms of organogenesis. Nat Rev Genet 3, 499-512.

Zile, M. H. (1998). Vitamin A and embryonic development: an overview. J Nutr 128, 455S-458S.

Zon, L. I. and Peterson, R. T. (2005). In vivo drug discovery in the zebrafish. Nat Rev Drug Discov 4, 35-44.

Zorn, A. M. (2008). Liver development, StemBook, ed. The Stem Cell Research Community, StemBook, doi/10.3824/stembook.1.25.1, http://www.stembook.org.

Zorn, A. M. and Wells, J. M. (2007). Molecular basis of vertebrate endoderm development. Int Rev Cytol 259, 49-111.

Zou, Z., Ekataksin, W. and Wake, K. (1998). Zonal and regional differences identified from precision mapping of vitamin A-storing lipid droplets of the hepatic stellate cells in pig liver: a novel concept of addressing the intralobular area of heterogeneity. Hepatology 27, 1098-108.

CHAPTER 2

Rargb regulates organ laterality in a zebrafish model of right atrial isomerism

Maija K. Garnaas[1,3], Claire C. Cutting[1], Alison Meyers[2], Peter B. Kelsey, Jr.[1], James M. Harris[2], Trista E. North[2,3], Wolfram Goessling[1,3]

[1]Genetics Division, Brigham and Women's Hospital, Harvard Medical School, Brigham and Women's Hospital, Boston, MA, USA. [2]Department of Pathology, Beth Israel Deaconess Medical Center, Harvard Medical School, Boston, MA, USA. [3]Harvard Stem Cell Institute, Cambridge, MA, USA.

This chapter contains the manuscript entitled "Rargb regulates organ laterality in a zebrafish model of right atrial isomerism", originally published in *Developmental Biology* on December 15, 2012 (372(2): 178-189). It has been modified to fit the style of this dissertation. Author attributions: MKG devised, executed, and analyzed experiments and wrote the manuscript. CCC, AM, PBK, and JMH performed and analyzed the chemical genetic screen. WG and TEN devised experiments and analyzed data.

ABSTRACT

Developmental signals determine organ morphology and position during embryogenesis. To discover novel modifiers of liver development, we performed a chemical genetic screen in zebrafish and identified retinoic acid as a positive regulator of hepatogenesis. Knockdown of the four RA receptors revealed that all receptors affect liver formation, however specific receptors exert differential effects. *Rargb* knockdown results in bilateral livers but does not impact organ size, revealing a unique role for Rargb in conferring left-right positional information. Bilateral populations of hepatoblasts are detectable in *rargb* morphants, indicating Rargb acts during hepatic specification to position the liver, and primitive endoderm is competent to form liver on both sides. Hearts remain at the midline and gut looping is perturbed in *rargb* morphants, suggesting Rargb affects lateral plate mesoderm migration. Overexpression of Bmp during somitogenesis similarly results in bilateral livers and midline hearts, and inhibition of Bmp signaling rescues the *rargb* morphant phenotype, indicating Rargb functions upstream of Bmp to regulate organ sidedness. Loss of *rargb* causes biliary and organ laterality defects as well as asplenia, paralleling symptoms of the human condition right atrial isomerism. Our findings uncover a novel role for RA in regulating organ laterality and provide an animal model of one form of human heterotaxia.

INTRODUCTION

During embryogenesis, the liver develops asymmetrically across the left-right axis. In human heterotaxic syndromes, misalignment of the visceral organs is often associated with cardiac defects and impaired bile duct formation and typically requires surgical intervention. Liver development originates in the endoderm where hepatic progenitors are specified from a multipotent precursor population. Expression of liver-specific transcription factors in a select population of endodermal cells is in part regulated by surrounding mesodermal tissues which provide inductive cues required for proper liver development and positioning. Many of these signaling pathways have been independently characterized, however the sequence and integration of genetic networks regulating liver development have not been well established.

In zebrafish, hepatoblasts are specified in the endodermal rod by 24 hours post-fertilization (hpf), and between 24-28 hpf, the gut begins to loop to the left, concordant with asymmetrical movements of the lateral plate mesoderm (LPM) (Field et al., 2003; Horne-Badovinac et al., 2003; Ober et al., 2003). Although the importance of mesoderm-endoderm signaling during liver development has been highlighted previously (Chung et al., 2008; Ober et al., 2006; Reiter et al., 1999; Reiter et al., 2001; Shin et al., 2007), it is not clear how many of these developmental signals intersect during hepatic specification and positioning.

Evidence that retinoic acid (RA) signaling is involved in endoderm formation first surfaced in a study of pancreatic specification in zebrafish (Stafford and Prince, 2002). Global inhibition of zebrafish RARs resulted in reduced or absent expression of endocrine and exocrine pancreas markers as well as *hhex*, a hepatic transcription factor. Analysis of zebrafish *raldh2* mutants (*neckless*, *aldh1a2*^{um22}, *aldh1a2*^{i26}) also revealed similar disruptions in endoderm development (Alexa et al., 2009; Stafford and Prince, 2002). Despite these studies, the function of a number of integral RA pathway

members, including *raldh3* and *raldh4*, and the impact of individual RARs on liver development remain unknown.

RA signaling has been further suggested to affect organ laterality. Early studies have demonstrated that inhibition of RA signaling or addition of excess RA leads to randomized heart looping in mice (Chazaud et al., 1999), and vitamin A deficient avian embryos develop reversed heart *situs* (Dersch and Zile, 1993), thereby suggesting a role for RA signaling in patterning organs across the left-right axis. The mechanism by which RA regulates organ positioning has not been elucidated. Lateral plate mesoderm (LPM) movements impact visceral organ positioning (Horne-Badovinac et al., 2001; Huang et al., 2008; Yin et al.), evoking the possibility that RA signaling exerts its effect on organ laterality via regulation of LPM migration.

In this study, we define the role of RA signaling during liver specification and positioning. In a large-scale chemical genetic screen, we identified RA as a regulator of normal liver development. We demonstrate that both RA synthesis and receptor-mediated signaling impact stages of hepatic specification, differentiation, and proliferation. We show for the first time that *raldh4* impacts liver development following hepatic specification. *Raraa, rarab*, and *rarga* knockdowns lead to smaller livers, whereas *rargb* knockdown results in bilateral livers, demonstrating receptor-specific effects on liver development. The heart and gut remain at the midline in *rargb* morphants, indicative of a left-right patterning defect, however Nodal signaling is unaffected in these embryos. We observe that transient upregulation of Bmp signaling also results in midline hearts and bilateral livers. Inhibition of Bmp signaling rescues the bilateral liver defect in *rargb* morphants, suggesting that RA normally inhibits Bmp signaling during organ laterality determination, and we indeed find that *rargb* knockdown results in elevated levels of phosphorylated Smads 1/5/8 in the developing embryo. *Rargb* morphants also develop bile duct defects and asplenia, and this phenotype

parallels the human heterotaxic syndrome right atrial isomerism, or Ivemark Syndrome (Ivemark, 1955) in which patients display a midline heart, midline or duplicated livers, biliary atresia, and asplenia, suggesting that proper RA signaling may be required for *situs solitus* of human organs.

RESULTS

A chemical genetic screen identifies retinoic acid signaling as a regulator of liver development

To identify novel regulators of liver development, we conducted a chemical genetic screen in zebrafish (Figure 2-1). We exposed wild type or *lfabp:GFP* fluorescent reporter embryos to a library of known bioactive compounds over the course of liver development (18-72 hpf) and scored embryonic liver size at 72 hpf by *in situ* hybridization or fluorescence microscopy, respectively. Compounds having an effect on liver development were grouped by mechanism of action. Out of 2640 compounds tested, 135 (5.1%) increased liver size, whereas 229 (8.7%) decreased liver size. We identified a number of molecular pathways that impact liver growth, including retinoic acid (RA) signaling. In particular, our screen uncovered eight hits corresponding to six compounds that affect RA signaling: vitamin A, all-trans retinoic acid (ATRA), isotretinoin, beta carotene, and the RA synthesis inhibitors diethylaminobenzaldehyde (DEAB) and disulfiram.

To corroborate our chemical screen findings and to determine the stage at which RA impacts liver development, we treated embryos with RA pathway compounds during specific time windows targeting hepatoblast specification (18-24 hpf), hepatoblast differentiation (24-48 hpf), and hepatocyte proliferation (48-72 hpf). At all time points, embryos treated with ATRA develop bigger livers, whereas embryos treated with DEAB

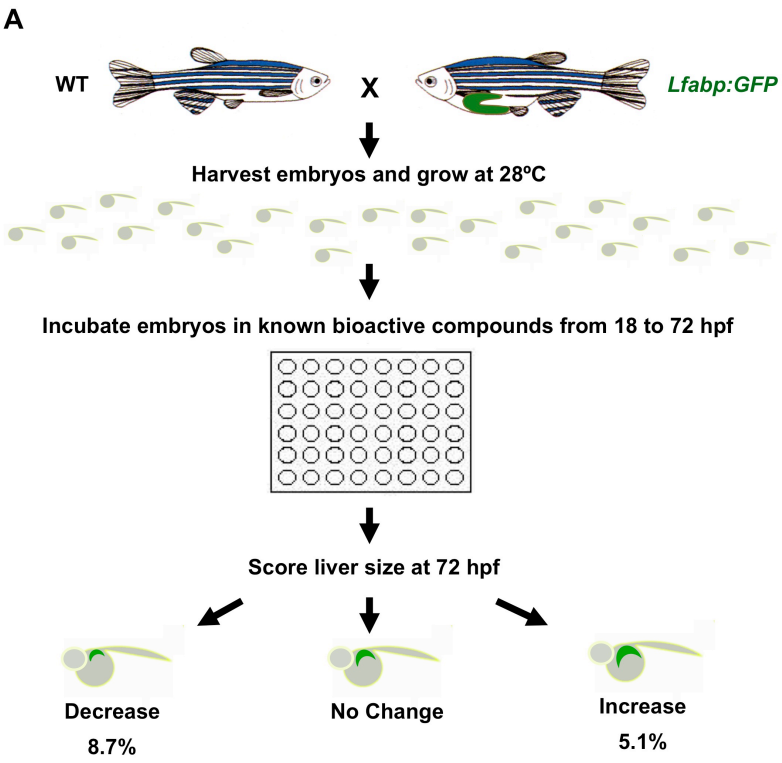

B

Compound	Effect on liver size
Retinoic acid	↑
Isotretinoin	↑
Retinol	↑
Beta-carotene	↑
DEAB	↓
Disulfiram	↓

Figure 2-1. A chemical genetic screen identifies retinoic acid as a regulator of embryonic zebrafish liver development.

(A) Chemical genetic screen workflow. Wild type (WT) or *lfabp:GFP* transgenic reporter fish were exposed to individual compounds from a library of 2640 known bioactives over the course of embryonic liver development (18-72 hpf). Alterations in liver size were detected by fluorescence microscopy and *in situ* hybridization for *lfabp*.

(B) Eight hits corresponding to six compounds were identified in the screen. Retinoic acid, isotretinoin, retinol, and beta-carotene increased liver size, whereas RA pathway inhibitors diethylaminobenzaldehyde (DEAB) and disulfiram decreased liver size.

or AGN193109, a pan-RAR inhibitor, develop smaller livers as determined by *lfabp in situ* hybridization (Figure 2-2, A-F; Figure 2-3, A-B) and GFP expression in live *lfabp:GFP* reporter embryos (Figure 2-2, G-I) at 72 hpf. These results suggest that RA signaling is important throughout all stages of hepatic specification, differentiation, and proliferation. RA pathway inhibitors DEAB and AGN193109 were most penetrant during the earliest treatment window (18-24 hpf), with ~50% of embryos developing smaller livers (DEAB: n=136; AGN193109: n=25). To confirm that our drug treatments impact RA signaling in the embryo, we treated *cyp26a1:eYFP* reporter fish with ATRA or DEAB at 18 hpf. Cyp26a1 promotes degradation of RA and is induced by RA in an auto-regulatory feedback loop (White et al., 1996; Abu-Abed et al., 2001; Sakai et al., 2001; Emoto et al., 2005). Treatment of *cyp26a1:eYFP* embryos with ATRA led to increased fluorescence throughout the embryo, with particularly increased intensity in the brain and liver, whereas DEAB treatment decreased fluorescence in these regions (Figure 2-2, J-L). These results demonstrate that RA signaling is active in the embryonic liver and is modulated by chemical exposure.

To determine whether changes in liver size in chemically treated embryos are related to changes in hepatic cell proliferation, we assessed BrdU incorporation at 24 hpf. We found that proliferation levels correspond to liver size: ATRA-treated embryos have more BrdU+ cells, and DEAB and AGN193109-treated embryos contain fewer BrdU+ cells (Figure 2-2, M-O). Quantification of BrdU+ cells in the area of the liver primordium (Figure 2-2O box, magnified in M'-O') revealed a significant decrease in proliferating hepatic cells in DEAB (n=5, t-test, p=0.001) (Figure 2-2P) and AGN193109-treated embryos (n=5, t-test, p=0.006) (Figure 2-3C) and an increase in BrdU+ cells in ATRA-treated embryos compared to DMSO controls. We verified these changes in hepatic cell proliferation by performing FACS at 72 hpf on *lfabp:GFP* embryos exposed to RA pathway compounds from 18-24 hpf. Quantification of GFP+ cells uncovered

Figure 2-2 (next page). Retinoic acid signaling enhances embryonic liver development.

(A-F) *In situ* hybridization for *lfabp* at 72 hpf reveals differences in liver size after chemical exposure at 18 hpf. ATRA treatment leads to greater *lfabp* expression, whereas DEAB treatment leads to reduced *lfabp* expression. First row, lateral view. Second row, dorsal view.

(G-I) Fluorescence microscopy of *lfabp:GFP* reporter fish at 72 hpf confirms *in situ* hybridization results in (A-F).

(J-L) Fluorescence microscopy of *cyp26a1:eYFP* reporter fish at 72 hpf demonstrates changes in RA signaling activity in chemically treated embryos. Arrowheads highlight the liver.

(M-O) BrdU whole mount immunostaining of 24 hpf embryos demonstrates that ATRA-treated embryos show higher levels of proliferation in the liver primordium (black rectangle) compared to DEAB and DMSO-treated controls.

(M'-O') Enlarged images of (M-O) illustrating individual proliferating cells in the liver primordium.

(P) Quantification of the number of BrdU+ cells/field (black rectangle in O).

(Q) FACS quantification of percent GFP+ cells in chemically treated *lfabp:GFP* embryos reveals that ATRA-treated embryos contain more hepatocytes and DEAB-treated embryos contain fewer hepatocytes than DMSO-treated controls.

(R) qPCR analysis reveals differences in the relative expression of the hepatocyte marker *transferrin* in ATRA and DEAB-treated embryos at 72 hpf compared to DMSO-treated controls (where control expression levels were normalized to 1.0).

Scale bars: 100 microns.

Figure 2-2 (continued)

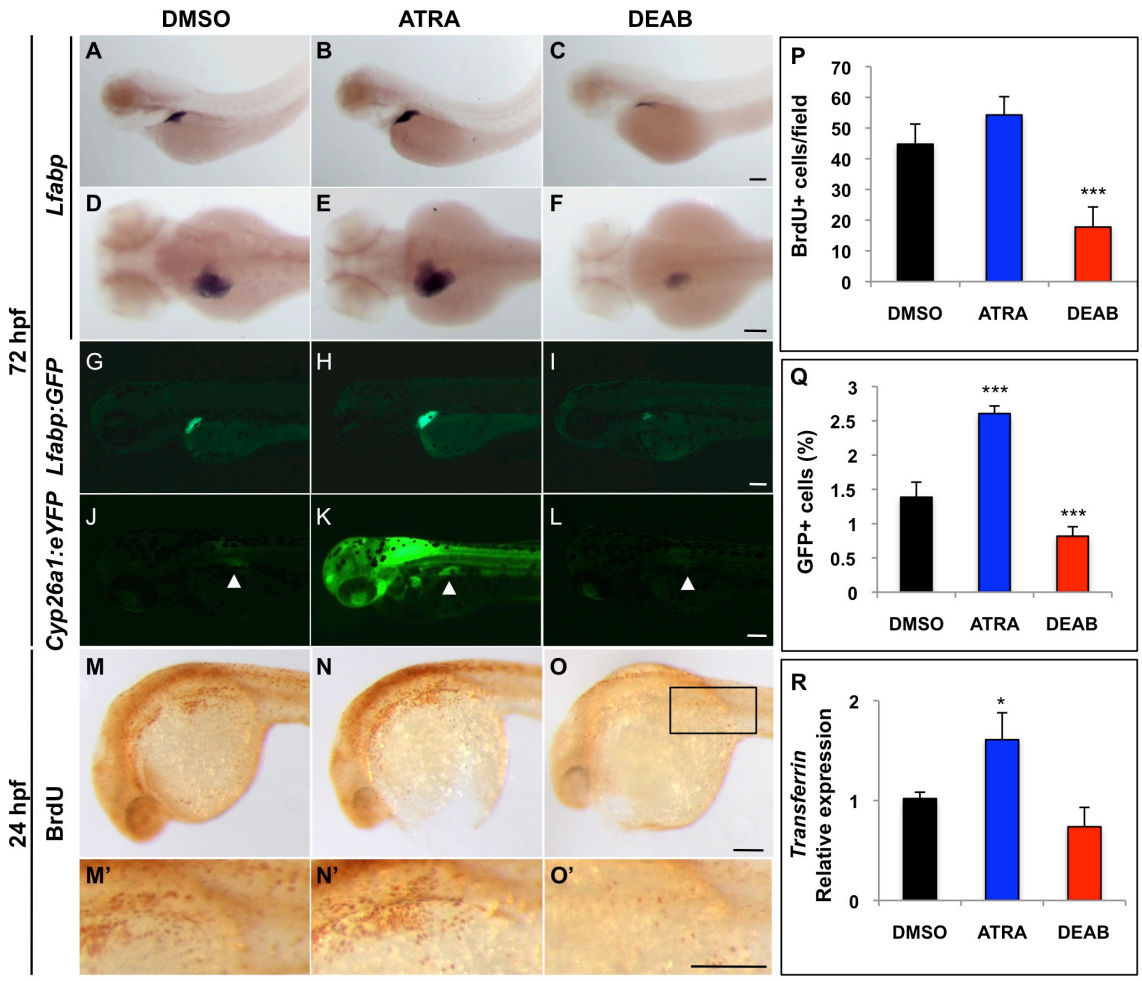

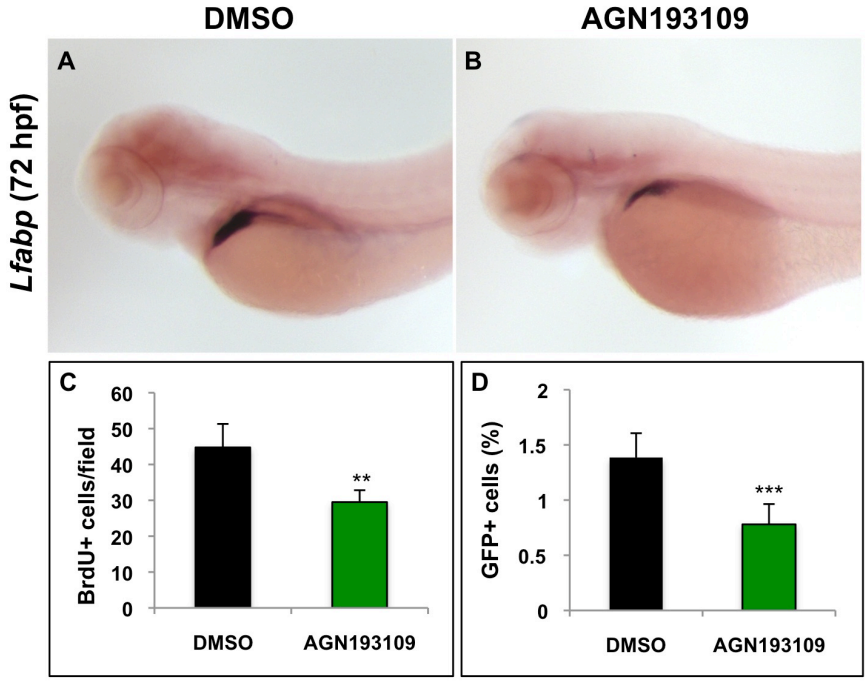

Figure 2-3. The pan-RAR antagonist AGN193109 reduces liver size and hepatic proliferation.

(A-B) Embryos treated with the RAR antagonist AGN193109 from 18-24 hpf develop smaller livers compared to DMSO-treated controls as shown by *lfabp* expression at 72 hpf. Lateral views.

(C) Quantification of the number of proliferating BrdU+ cells in the area of the liver primordium (see Figure 1, black rectangle) in AGN193109-treated embryos at 24 hpf.

(D) FACS quantification of percent GFP+ cells in chemically treated *lfabp:GFP* embryos reveals that AGN193109-treated embryos contain fewer hepatocytes than DMSO-treated controls.

significant changes in hepatocyte number in compound-treated embryos compared to controls (DMSO versus ATRA $p=2.0x10^{-5}$, DEAB $p=8.6x10^{-5}$, AGN193109 p=0.0002; ATRA versus DEAB $p=4.6x10^{-8}$, AGN $p=1.1x10^{-6}$; DEAB versus AGN p=0.69) (Figure 2-2Q, Figure 2-3D). TUNEL analysis confirmed that changes in liver size are not related to hepatic cell death (data not shown). qPCR analysis of embryos exposed to RA pathway compounds further demonstrated that liver size and hepatocyte number correlate with expression levels of the hepatocyte marker *transferrin* at 72 hpf, indicating that the observed changes are not specific to *lfabp* (Figure 2-2R) (DMSO versus ATRA: p=0.02; versus DEAB: 0.07; ATRA versus DEAB p=0.01). Together, these results demonstrate that RA signaling enhances embryonic liver growth.

Retinaldehyde dehydrogenase (Raldh) enzymes are responsible for converting retinaldehyde to RA. The zebrafish expresses three Raldhs – *raldh2*, *raldh3*, and *raldh4* (Begemann et al., 2001; Liang et al., 2008; Pittlik et al., 2008). Raldh2 is expressed in the lateral plate mesoderm during somitogenesis, and zebrafish and medaka *raldh2* mutants display defective liver development (Begemann et al., 2001; Alexa et al., 2009; Negishi et al., 2010). Raldh3 is expressed in the eye and is therefore unlikely to have a role in liver development. Raldh4 is expressed in the developing liver at 48 hpf (Liang et al., 2008), however targeted knockdown of *raldh4* has not been reported. To determine whether Raldh4 is required for normal liver development and whether its temporal requirement is distinct from that of Raldh2, we knocked down *raldh2* and *raldh4* using ATG start site morpholinos (MOs). Liver size was subsequently assessed by *in situ* for *prox1* at 30 and 48 hpf and *lfabp* at 72 hpf. At 30 hpf, 100% of *raldh2* knockdown embryos and 4% of *raldh4* knockdown embryos developed small livers compared to 6% in controls (n≥25/condition) (Figure 2-4, A-C). Similarly, at 48 hpf, 7% of control embryos, 100% of *raldh2* morphants, and 17% of *raldh4* morphants developed small livers (n≥18/condition) (Figure 2-4, D-F). When examined at 72 hpf, 0% of control

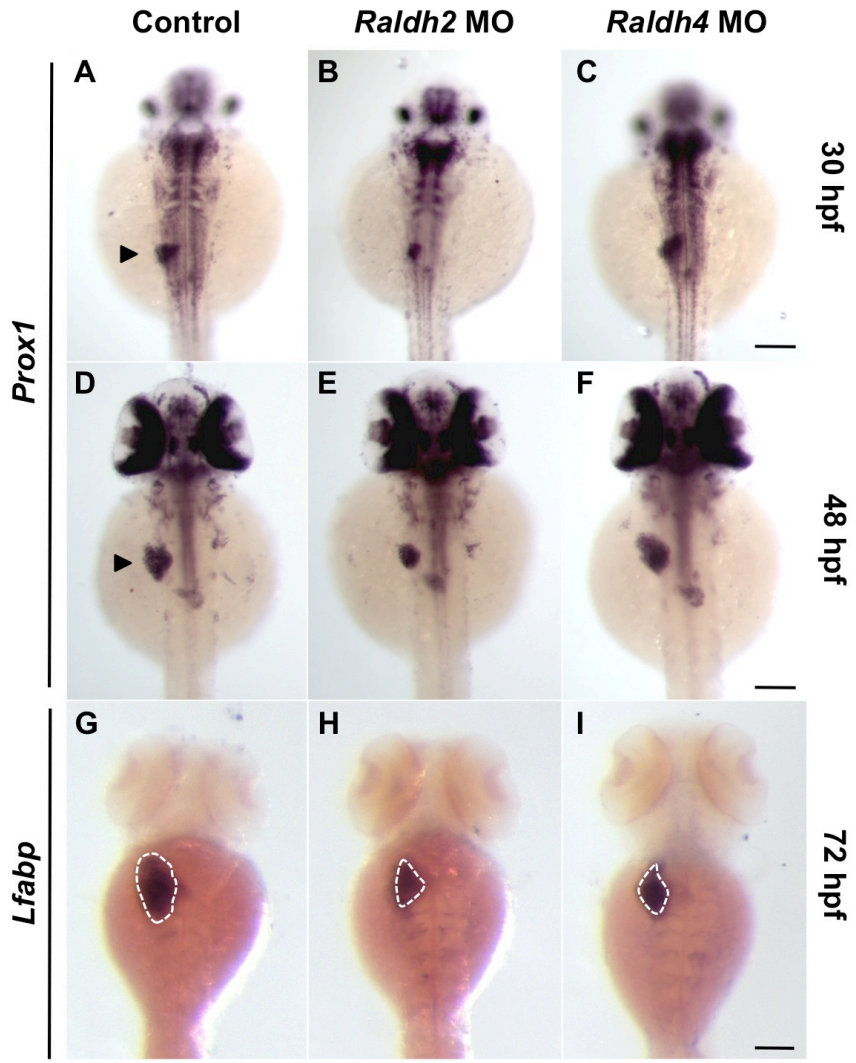

Figure 2-4. Raldhs 2 and 4 temporally regulate liver development.

(A-I) Wild type embryos were injected with *raldh2* or *raldh4* MO at the 1-cell stage, and liver development was assessed over the next 72 hours. *In situ* hybridization for the hepatoblast marker *prox1* at 30 hpf (A-C) and 48 hpf (D-F) and hepatocyte marker *lfabp* at 72 hpf (G-I) demonstrates distinct temporal requirements for Raldh2 and Raldh4 during liver development. Arrowheads denote the liver primordium, and the dotted lines outline the liver. Scale bars: 100 microns.

embryos, 80% of *raldh2* morphants, and 82% of *raldh4* morphants developed small livers (n≥40/condition) (Figure 2-4, G-I). Our results indicate that *raldh2* is required throughout hepatogenesis, whereas *raldh4* is primarily required following hepatocyte specification (after 48 hpf). Additionally, in a separate experiment in which we titered individual MO doses to prevent toxicity from double MO injection, we found that 0% of uninjected embryos, 31% of *raldh2* morphants, 21% of *raldh4* morphants, and 76% of *raldh2+4* double morphants developed small livers at 72 hpf (n≥14/condition). These data suggest that Raldh2 and 4 enzymes act sequentially and synergistically during hepatogenesis and corroborate our timed chemical exposure studies.

Retinoic acid signaling impacts liver size and laterality by receptor-specific mechanisms

The zebrafish expresses two RA receptor (RAR) α subtypes, *raraa* and *rarab*, and two RAR γ subtypes, *rarga* and *rargb* (Hale et al., 2006). No RAR β has been identified to date. Combinatorial RAR knockdowns result in defects in hindbrain, limb, and pharyngeal arch development (Linville et al., 2009), but receptor-specific roles in liver development have not been described. To elucidate individual receptor contributions to hepatogenesis, we knocked down each receptor using previously published MOs (Linville et al., 2009). Knockdown of *RARs aa*, *ab,* and *ga*, primarily resulted in smaller livers (*raraa*: 43% smaller livers, n=28; *rarab*: 15%, n=34; *rarga*: 47%, n=38) (Figure 2-5, A-D, G-J), suggesting that these receptors act redundantly during hepatic specification and/or hepatocyte proliferation. Interestingly, we found that knockdown of *rargb* caused embryos to develop bilateral livers (29%, n=105) (Figure 2-5, E and K), suggesting that this receptor regulates liver laterality. Combinatorial knockdown of all four RARs resulted in even smaller (82%), sometimes absent livers (18%, n=22), indicating that RARs are required for normal hepatic specification (Figure 2-5, F and L). These results are

Figure 2-5 (next page). Retinoic acid receptors differentially impact liver development and laterality.

(A-L) *Lfabp* expression at 72 hpf in RAR morphant embryos. Loss of RARs *raraa, rarab*, and *rarga* leads to a reduction in liver size (A-D, G-J), whereas loss of *rargb* causes embryos to develop bilateral livers (E, K, K'). Embryos simultaneously injected with a lower dose of all four RAR MOs develop small livers or none at all (F, L).

(M-P) Embryos treated with the RARγ antagonist MM11253 over the time points given develop bilateral livers, confirming genetic knockdown data.

(Q) FACS quantification of percent GFP+ cells in *lfabp:GFP* RAR morphant embryos reveals that *rargb* morphant embryos with bilateral livers contain significantly more GFP+ hepatocytes than control siblings. Embryos injected with *raraa, rarab, rarga*, and *rargb* in combination have roughly half as many GFP+ hepatocytes as control embryos.

Scale bars: 100 microns.

Figure 2-5 (continued)

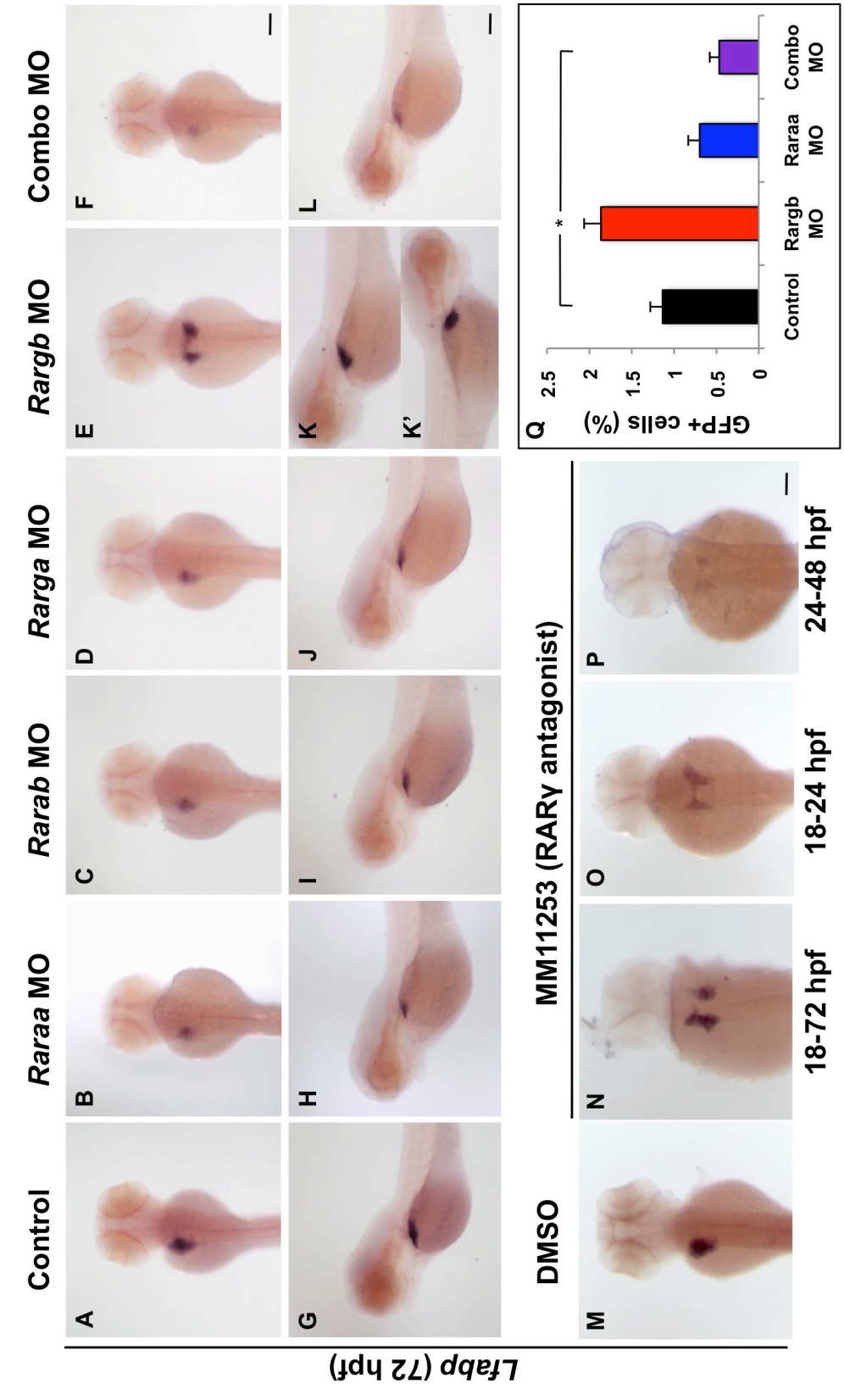

corroborated by the fact that single RAR knockout mice are viable, whereas double knockouts display a number of developmental defects (Mark et al., 2006).

To confirm our *rargb* knockdown results chemically, we treated embryos with a selective RARγ antagonist, MM11253, over the course of hepatogenesis (18-72 hpf). Whereas DMSO controls developed left-sided livers, 24% (n=33) of MM11253-treated embryos developed bilateral livers (Figure 2-5, M-N), confirming our MO knockdown results. Additionally, bilateral livers developed in embryos treated during shorter, early time windows (18-24 and 24-48 hpf) (Figure 2-5, O-P), suggesting that Rargb exerts its effect during hepatic specification. FACS quantification of RAR MO-injected *lfabp:GFP* reporter fish at 72 hpf demonstrated that *rargb* morphants with two livers have significantly more hepatocytes than their control siblings, whereas *raraa* knockdown embryos have fewer GFP+ hepatocytes than control siblings, and combinatorial knockdown embryos fewer still (Figure 2-5Q) (*rargb* MO versus control, p=0.00017; versus *raraa* MO, p=0.00023; versus combo MO, $p=2.40 \times 10^{-6}$). These data illustrate that individual RARs have specific effects on liver specification and laterality.

To further elucidate the timing of *rargb*'s effect on liver laterality, we injected *rargb* MO and assessed hepatic bud formation at 30 hpf using the hepatoblast marker *prox1* and at 48 hpf using the pan-endodermal marker *foxA3*. Whereas control embryos displayed left-sided liver buds at 30 hpf, 26% of *rargb* morphants (n=23) developed bilateral populations of hepatoblasts (Figure 2-6, A-B). This percentage corresponds to the number of bilateral livers seen at 72 hpf (29%). We also observed that some *rargb* morphants display midline liver buds at 30 hpf (21%, n=23). We did not observe midline livers at 72 hpf in *rargb* morphants, suggesting that midline populations of hepatoblasts ultimately resolve into unilateral hepatocyte populations or split into two liver buds. These results corroborate our early (18-24, 24-48 hpf) MM11253 treatments, demonstrating that *rargb* knockdown impacts liver laterality during hepatic specification.

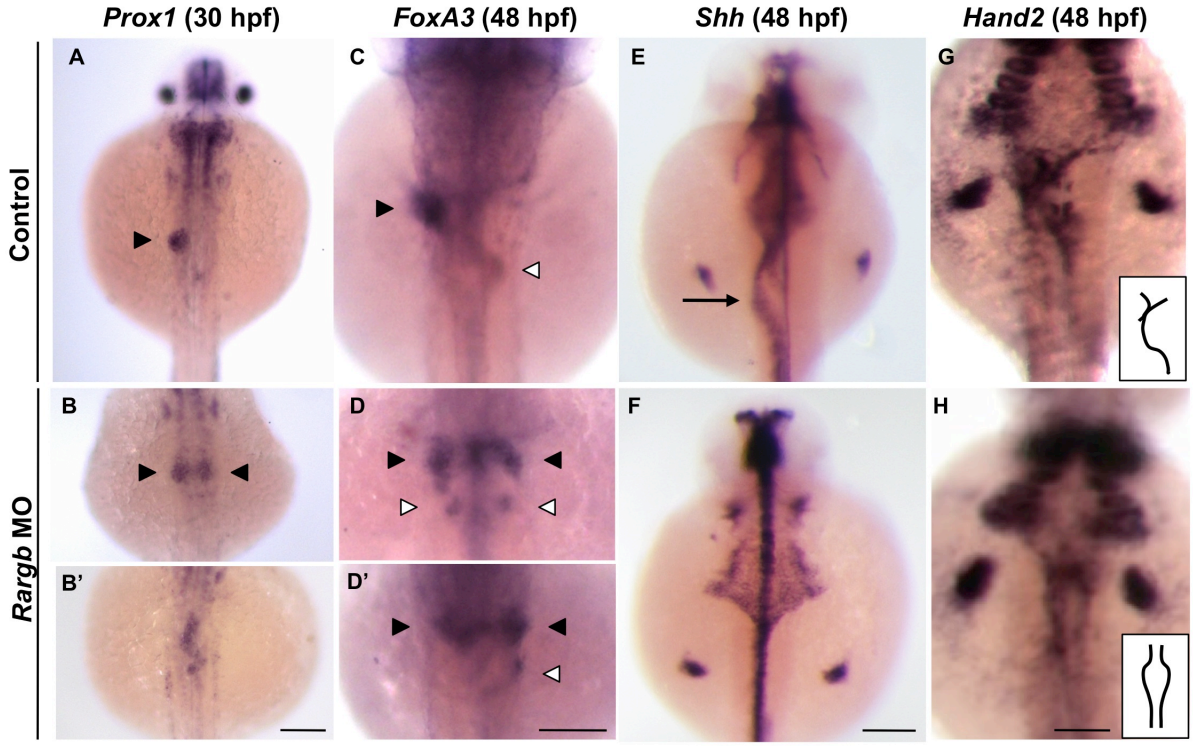

Figure 2-6. *Rargb* knockdown impacts the left-right asymmetry of visceral organs.

(A-B) *Prox1* expression demonstrates that hepatic progenitors normally migrate to the left of the midline at 30 hpf (A, black arrowhead). Loss of *rargb* results in bilateral (B) or midline (B') hepatoblast populations.

(C-D) *In situ* hybridization for the pan-endodermal marker *foxA3* at 48 hpf demonstrates that loss of *rargb* results in bilateral livers (black arrowheads) that are sometimes accompanied by bilateral pancreata (white arrowheads).

(E-F) *Rargb* morphants develop gut looping abnormalities (arrow), as demonstrated by *shh* expression at 48 hpf.

(G, H) *Hand2* expression at 48 hpf demonstrates aberrant LPM migration in *rargb* morphants (H). Insets in (G, H) highlight the differences in LPM phenotypes.

Scale bars: 100 microns.

Examination of *foxA3* expression at 48 hpf further confirmed that *rargb* knockdown leads to bilateral livers (Figure 2-6, C-D). In control embryos, the pan-endodermal marker *foxA3* marks the left-sided liver and right-sided pancreas. In *rargb* morphants, we identified bilateral livers in 30% of MO-injected embryos (n=28). We also discovered that in some cases, embryos with bilateral livers also developed bilateral pancreata (7%, n=28). Whereas most bilateral livers occurred in the presence of a normal right-sided pancreas, bilateral pancreata always occurred in conjunction with bilateral livers (Figure 2-6D). These results demonstrate that *rargb* knockdown impacts the laterality of the liver and other endoderm derivatives.

***Rargb* knockdown affects organ laterality**

In zebrafish, cardiac progenitors develop bilaterally, coalesce at the midline, then the nascent heart tube jogs asymmetrically to the left of the midline around 1 dpf (Bakkers et al., 2009). In mice, the cardiac mesoderm and septum transversum mesenchyme provide Fgf and Bmp signals to specify hepatic progenitors in the overlying endoderm (Jung et al., 1999; Rossi et al., 2001), and loss of these signals in zebrafish prevents hepatic specification (Shin et al., 2007). It is therefore possible that defective heart positioning and ectopic inductive cues precede the development of bilateral livers. We have observed the coincidence of heart and liver laterality defects in other contexts; double *in situ* hybridization for hepatoblast and cardiac markers *prox1* and *cmlc2*, respectively, revealed that cardia bifida mutants *miles apart* (*mil*) (Kupperman et al., 2000) also develop bilateral livers (Figure 2-7). Accordingly, to determine whether laterality defects in the endoderm are accompanied by heart jogging defects, we examined expression of the pan-cardiomyocyte marker *cmlc2* at 26 hpf. Control embryos developed left-sided heart tubes, whereas 33% of *rargb* morphants displayed midline heart tubes (n=33) (Figure 2-8, A and D). Knockdowns of RARs *raraa, rarab*,

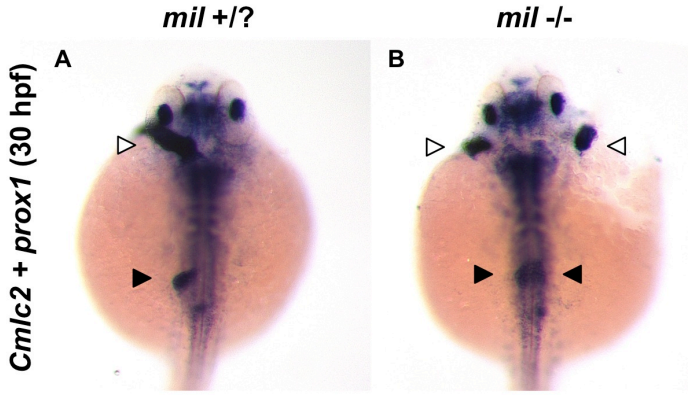

Figure 2-7. Cardia bifida mutants *miles apart* (*mil*) develop bilateral livers.

(A-B) *In situ* hybridization at 30 hpf for heart and hepatoblast markers *cmlc2* and *prox1*, respectively, demonstrates that cardia bifidia mutants *mil* develop two hearts (white arrowheads) and bilateral livers (black arrowheads).

Figure 2-8 (next page). Midline hearts and bilateral livers correlate in *rargb* morphants.

(A-F) Control embryos develop leftward jogging hearts as shown by the pan-cardiomyocyte marker *cmlc2* at 26 hpf (A) and chamber-specific markers *vmhc* and *amhc* at 30 hpf (B, C), whereas *rargb* morphants develop midline ventricles (D, E).

(G, H) Embryos treated with the RARγ antagonist MM11253 develop midline hearts, confirming genetic knockdown data.

(I) RARγ function is evolutionarily conserved. The midline heart phenotype of *rargb* morphant embryos is rescued by injection of mouse *Rarg* mRNA.

(J) Midline hearts and bilateral livers correlate in the same embryo. *Cmlc2:GFP* reporter fish injected with *rargb* MO were sorted by heart phenotype at 30 hpf, then liver laterality was assessed at 72 hpf by *lfabp* expression.

Scale bars: 100 microns.

Figure 2-8 (continued)

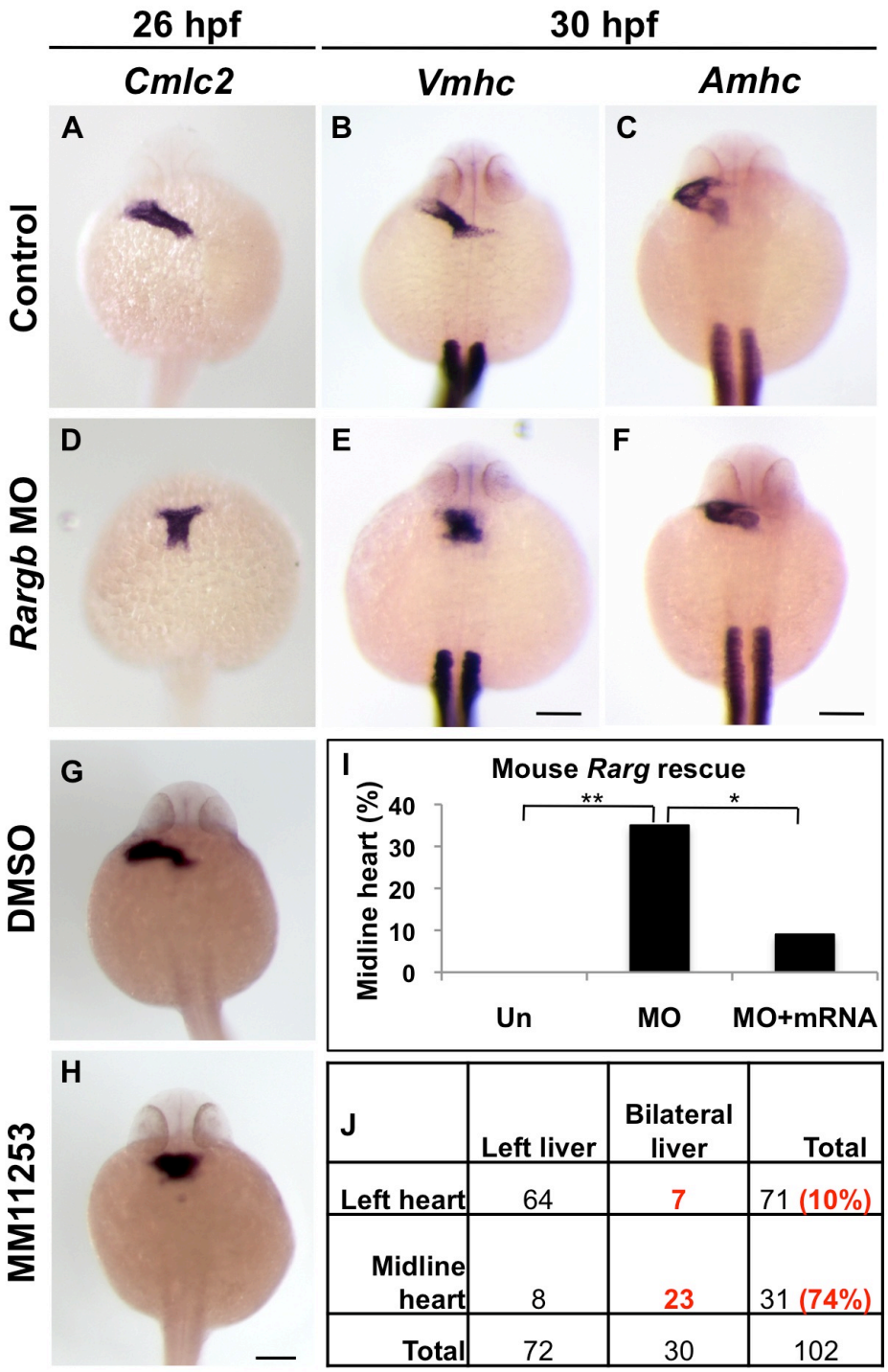

J	Left liver	Bilateral liver	Total
Left heart	64	7	71 (10%)
Midline heart	8	23	31 (74%)
Total	72	30	102

and *rarga* did not affect heart jogging (data not shown). Examination of chamber specific markers *atrial* and *ventricular myosin heavy chain* (*amhc* and *vmhc*, respectively) revealed that the ventricle is specifically affected by *rargb* knockdown (36%, n=28) (Figure 2-8, B-C and E-F). We also confirmed our genetic results chemically by treating embryos with the selective RARγ antagonist MM11253 over the course of cardiac jogging (14-26 hpf) and examining *cmlc2* expression at 26 hpf. MM11253-exposed embryos also displayed heart jogging defects (25%, n=24) (Figure 2-8, G-H), further indicating that loss of *rargb* perturbs heart laterality.

Just as zebrafish *rargb* morphants develop midline ventricles, dominant negative RARγE_{305} chimeric mice exhibit misaligned or unlooped ventricles (Iulianella and Lohnes, 2002), suggesting that RARγ functions similarly during vertebrate organogenesis. To demonstrate evolutionary conservation of RARγ function during cardiac development, we performed a rescue experiment in which zebrafish *rargb* MO was co-injected with mouse *Rarg* mRNA at the 1-cell stage, and *vmhc* expression was evaluated at 30 hpf. Compared to controls (0% midline ventricles, n=20), 35% (n=34) of *rargb* morphants developed a midline ventricle (control versus MO p=0.0019), whereas only 9% (n=22) of MO+mRNA co-injected embryos displayed this defect (MO versus MO+mRNA p=0.0315) (Figure 2-8I). We also examined *lfabp* expression at 72 hpf to determine whether mouse *Rargb* mRNA rescues the *rargb* morphant liver phenotype. All controls developed left-sided livers (n=23), whereas 22% (n=41) of *rargb* morphants (control versus MO p=0.0208) and 10% (n=30) of MO+mRNA co-injected embryos had bilateral livers (MO versus MO+mRNA p=0.218). Although we consistently see a reduction in the number of bilateral livers in co-injected embryos, we suspect that the rescue is less effective at a later stage due to persistent toxicity from the presence of two

exogenous nucleotide constructs. Together, our results demonstrate that RARγ function is conserved between fish and mammals.

To demonstrate that heart and endoderm defects are linked in the same embryo, we injected *rargb* MO into *cmlc2:GFP* reporter fish, sorted embryos by heart phenotype (left or midline) at 30 hpf by fluorescence microscopy, and assessed *lfabp* expression by *in situ* at 72 hpf. If heart and liver defects correlate in the same embryo, this would suggest a unifying underlying cause (e.g., gut looping defect) or that one defect precedes the other (e.g., altered cardiac asymmetry governs liver positioning). We found that heart and liver defects are significantly correlated in the same embryo ($p<0.0001$, Chi-squared analysis). Specifically, whereas only 10% of embryos with a left-sided heart developed bilateral livers (n=71), 74% of embryos with a midline heart developed bilateral livers (n= 31) (Figure 2-8J). Together, our results demonstrate that *rargb* knockdown impacts heart (ventricle) as well as endoderm laterality and suggest that these phenotypes are linked.

Because *rargb* morphants develop endoderm and cardiac defects, we reasoned that this might be due to an underlying cause such as aberrant LPM migration. Failed gut looping is often associated with bilateral endodermal organs (Chen et al., 2001), and zebrafish mutant for the bHLH transcription factor *hand2* exhibit failed LPM migration and develop gut looping defects and bilateral livers and pancreata (Yin et al., 2010). To assess this possibility, we examined whether gut looping is affected in *rargb* morphants by observing expression of *sonic hedgehog* (*shh*) and *hand2* at 48 hpf. We found that the gut, which normally loops leftward in control embryos, did not loop or remained at the midline in *rargb* morphant embryos (*shh*: 29% midline, 54% weak looping, n=24; *hand2*: 73%, n=22) (Figure 2-6, E-H). We tested additional markers for the thyroid, hypothalamus, and kidney (*nkx2.1a, slc20a1a, slc12a3*) and did not note any defects

(data not shown), indicating that *rargb* knockdown impacts only a subset of mesendodermal organs.

Nodal signaling is unaffected in *rargb* morphants

Nodal signaling is a master regulator of left-right asymmetry (Shen, 2007). Nodal signals originating in the node propagate anteriorly in the left LPM and impact endoderm and heart asymmetry. To determine whether laterality defects seen in *rargb* morphants are due to altered Nodal signaling, we examined the expression of the zebrafish Nodal signal *southpaw* (*spaw*), downstream effector *pitx2,* and Nodal antagonists *lefty1* and *lefty2* during somitogenesis (18-22 somites). Both control and *rargb* morphant embryos displayed normal left-sided expression of *spaw, pitx2*, and *lefty2*, and the molecular midline barrier *lefty1* remained intact (Figure 2-9), demonstrating that Rargb's impact on organ laterality is Nodal-independent. We also treated embryos with the RARγ antagonist MM11253 in two time windows targeting early development, 32 cell-2 somite and 2 somite-20 hpf, and found that Nodal signals remain left-sided in 91% (n=66) and 92% (n=51) of these embryos, respectively. The results of these chemical exposures further demonstrate that inhibition of *rargb* during early development does not impact Nodal signaling. It was recently shown that LPM migration defects in *hand2* mutants are not due to Nodal defects alone; in *spaw* morphants, the direction of LPM migration is randomized, whereas in *hand2* mutants, LPM migration does not occur at all (Yin et al., 2010). Furthermore, although previous studies have suggested that early inhibition of RA signaling (prior to the 2 somite stage) affects Nodal signaling, these embryos ultimately develop *situs inversus* rather than duplicated or midline organs (Huang et al., 2011), bolstering our observations that *rargb* morphant defects are likely due to defects in LPM migration rather than misexpression of global laterality signals.

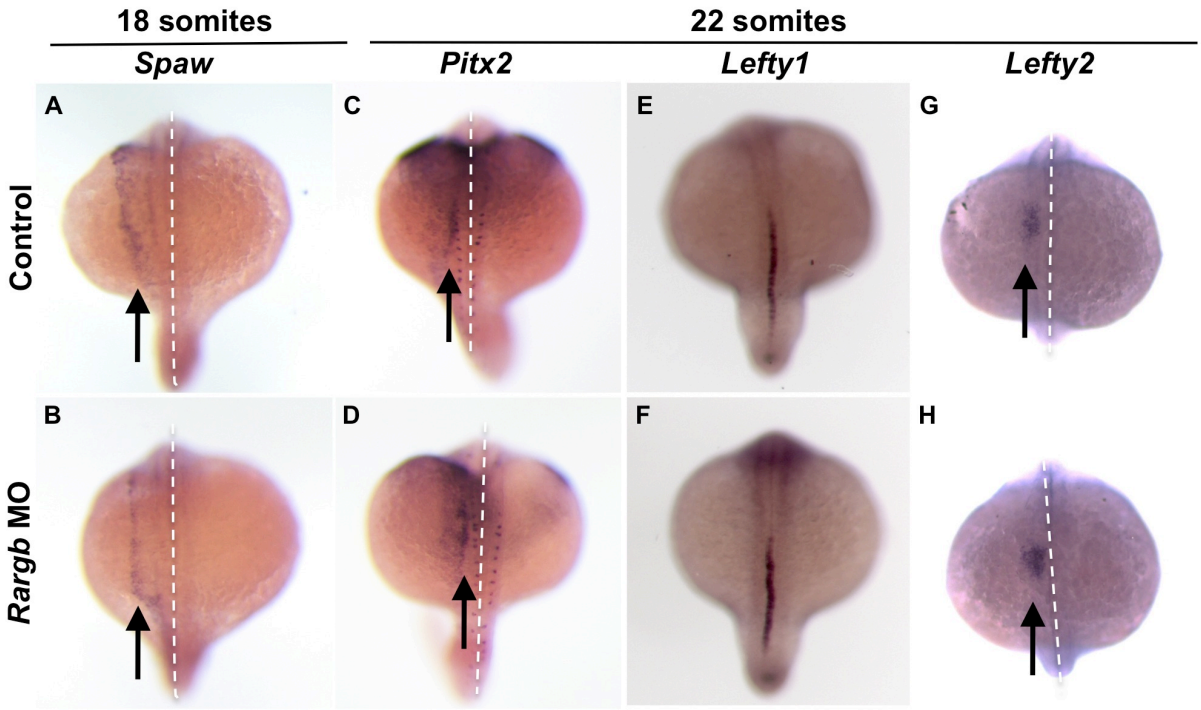

Figure 2-9. Loss of *rargb* does not affect Nodal signaling.

Rargb knockdown does not affect normal left-sided expression of Nodal signals *spaw* (A, B), *pitx2* (C, D), or *lefty2* (G, H) (arrows) or the molecular midline barrier *lefty1* (E, F). White dotted lines denote the midline.

Rargb affects Bmp signaling via altered phospho-Smad levels during organ laterality determination

Bmp4 is expressed asymmetrically in the left LPM between 20-22 somites, and this expression pattern leads to greater activation of phosphorylated Smads on the left side and is correlated with leftward cardiac jogging (Chen et al., 1997; Chocron et al., 2007; Smith et al., 2008). Because Bmp signaling is important for determining heart laterality, we investigated whether ectopic Bmp signaling perturbs liver laterality. We heat shocked inducible *hs:bmp2b* zebrafish embryos at 12 somites, prior to cardiac jogging and hepatic specification, and examined heart and liver development by *in situ* for *cmlc2* (30 hpf) and *lfabp* (72 hpf), respectively. At 30 hpf, 5% (n=100) of non heat shocked (hs-) control sibling embryos and 72% (n=79) of heat shocked embryos (hs+) displayed midline hearts (Figure 2-10A). Similarly, at 72 hpf, 4% (n=106) of hs- embryos compared to 33% (n=111) of hs+ embryos developed bilateral livers (Figure 2-10B). These data demonstrate that *rargb* knockdown and *bmp2b* overexpression result in the same phenotype, suggesting interplay between RA and Bmp signaling during laterality determination.

Given that loss of *rargb* or gain of *bmp2b* expression results in bilateral livers and midline hearts, we hypothesized that RA signaling antagonizes Bmp signaling during organ development (or vice versa). To determine whether RA inhibits Bmp signaling, we injected *rargb* MO at the 1-cell stage then treated these embryos with the Bmp inhibitor dorsomorphin from 14-17 hpf. At 72 hpf, we assessed whether Bmp inhibition rescued *rargb* morphants' bilateral liver phenotype. Whereas 3% of uninjected/DMSO-treated control embryos (n=101) and 1% of uninjected/dorsomoprhin-treated embryos (n=137) developed bilateral livers, 24% of *rargb* MO-injected/DMSO-treated embryos developed bilateral livers (n=144; p-value<0.0001 for MO/DMSO versus uninjected/DMSO). In contrast, 17% of *rargb* MO/dorsomorphin-treated embryos (n=163) developed bilateral

Figure 2-10 (next page). Rargb negatively regulates Bmp activity and localization *in vivo*.

(A-B) Overexpression of Bmp in heat shock inducible *hs:bmp2b* embryos results in midline hearts (A) and bilateral livers (B), paralleling the phenotype of *rargb* morphants.

(C) Treatment of *rargb* morphant embryos with the Bmp inhibitor dorsomorphin results in a reduction in the number of bilateral livers compared to DMSO-treated control *rargb* morphants.

(D) Western blot for Bmp effectors phospho-Smads 1/5/8 in uninjected control (Un) and *rargb* MO-injected embryos (MO) at 18 hpf. Band density values normalized to Actin demonstrate that loss of *rargb* results in increased expression of p-Smads 1/5/8. Embryos treated with the Bmp inhibitor dorsomorphin (DM) show reduced p-Smad 1/5/8 expression compared to DMSO-treated controls.

(E-H) Fluorescence microscopy of Bmp response element reporter fish *BRE:eGFP*. At 20 hpf, control embryos display greater Bmp activity on the left side (E), whereas *rargb* morphants display symmetrical Bmp activity (F). Altered Bmp localization at 20 hpf corresponds to heart laterality defects at 36 hpf in *rargb* morphants (H). White dotted lines denote the midline (E, F) or outline the heart tube (G, H).

Scale bars: 100 microns.

Figure 2-10 (continued)

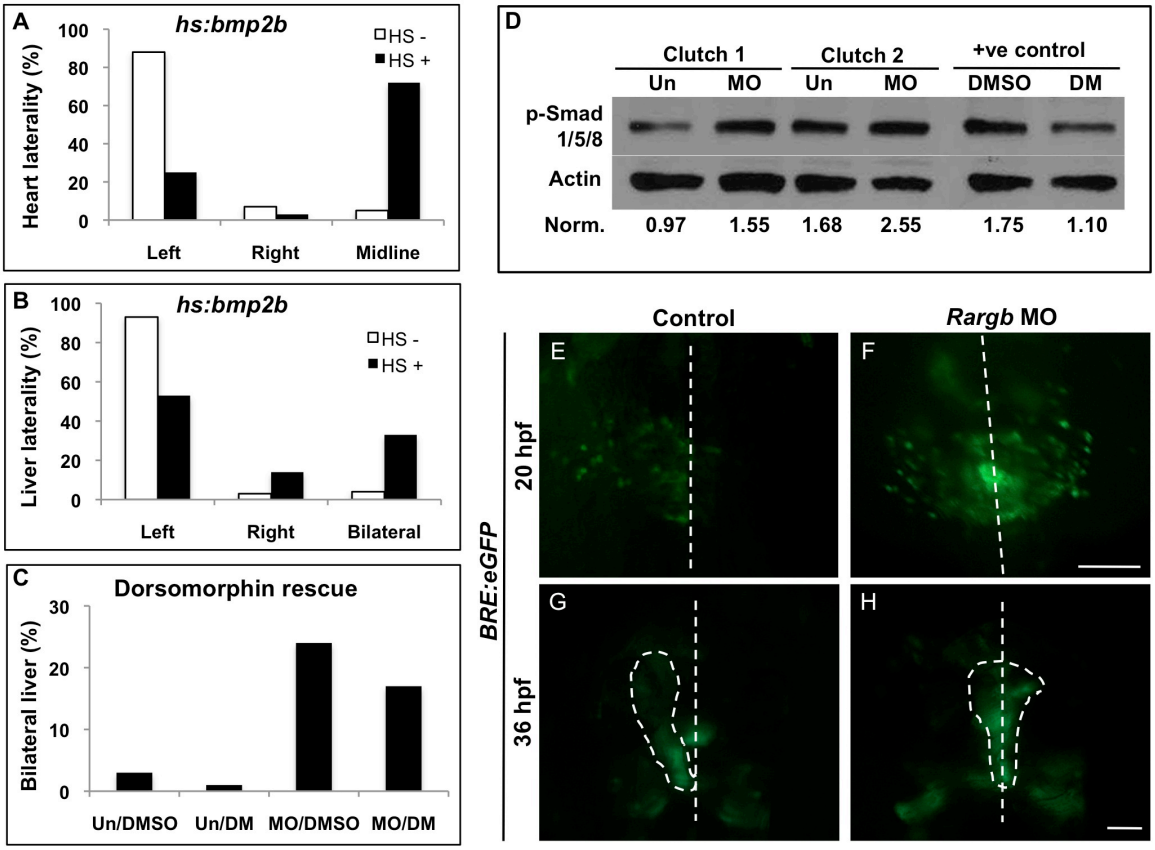

livers (Figure 2-10C; p-value = 0.1565 for MO/DMSO versus MO/dorsomorphin). These results represent six independent experiments in which the same rescue trend was noted in each. Together, these results demonstrate that inhibition of Bmp signaling rescues the *rargb* morphant phenotype and suggesting that Bmp acts downstream of Rargb during laterality determination.

We also performed the reverse experiment by first overexpressing Bmp then treating embryos with a RARγ agonist, CD1530. *Hs:bmp2b* transgenic embryos were heat-shocked at 12 somites then treated with CD1530 from 16-18 somites, and liver development was assessed at 72 hpf by *lfabp* expression. Whereas hs-/CD1530- and hs-/CD1530+ embryos did not display laterality defects, 25% of both hs+/CD1530- and hs+/CD1530+ embryos (n≥13/condition) developed bilateral livers (data not shown). These data further indicate that Rargb acts upstream of Bmp signaling to govern organ laterality.

Our *in vivo* data suggest that loss of *rargb* leads to an increase in Bmp signaling, since loss of *rargb* and overexpression of *bmp2b* result in the same laterality defects, and inhibition of Bmp signaling by dorsomorphin rescues the *rargb* morphant phenotype. To corroborate our *in vivo* findings, we examined expression levels of phosphorylated Smad1/5/8 (p-Smads), cytoplasmic effectors of Bmp signaling, in whole embryo lysates at 18 hpf. We found that *rargb* knockdown led to a ~60% increase in p-Smad1/5/8 expression levels compared to control embryos by Western blot analysis (Figure 2-10D). Whereas expression patterns of Bmp-related *smads 1/5* as well as that of co-Smad *smad4* are unchanged at the level of *in situ* hybridization (data not shown), total levels of Smad 1/5/8/9 proteins are also increased in *rargb* morphants as determined by Western blot analysis, indicative of decreased degradation (Figure 2-11). Together, our results indicate that Rargb normally inhibits Bmp signaling by reducing levels of active cytoplasmic Bmp effectors p-Smad1/5/8.

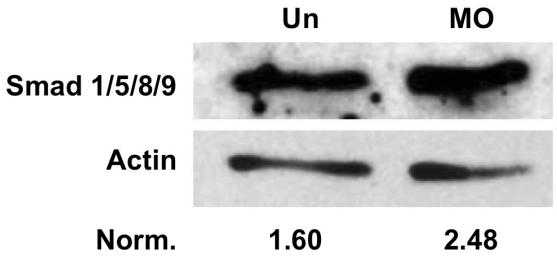

Figure 2-11. Levels of Smad 1/5/8/9 proteins are increased in *rargb* morphants. Western blot for Smad 1/5/8/9 on whole embryo lysates at 18 hpf. Loss of *rargb* (MO) results in increased Smad protein levels compared to uninjected controls (Un). Band density values normalized to Actin.

In addition to examining p-Smad1/5/8 levels in embryo lysates, we also investigated whether changes in Bmp signaling were visible in the cardiac field of living embryos using transgenic Bmp response element reporter fish *BRE:eGFP* that are responsive to Smad1/5 activity (Laux et al., 2011). In wild type embryos, Bmp signaling is active asymmetrically (Smith et al., 2008), with greater signaling occurring in the left LPM around the 20-22 somite stage, leading to a leftward jogging heart tube by 24 hpf. Compared to control embryos that displayed asymmetric Bmp activity (100%; 6 left, 1 right), 53% of *rargb* morphant embryos (n=15) exhibited symmetrical Bmp activity at 22 somites (Figure 2-10, E-F). We examined these same embryos at 30 hpf to assess whether changes seen in Bmp signaling at 22 somites ultimately affected heart tube development. Because Bmp remains active in the heart at this stage, the direction of cardiac jogging can be assessed in *BRE:eGFP* embryos. Both control and *rargb* morphant embryos' hearts jogged according to earlier sidedness of Bmp activity. Specifically, all control embryos developed asymmetrically jogged hearts (6 left, 1 right; 100% asymmetrical), whereas 40% of *rargb* morphant embryos developed midline hearts (6 midline, 7 left, 2 right; 60% asymmetrical) (Figure 2-10, G-H; p-value = 0.0225 for control versus *rargb* morphant embryos showing asymmetrical – left or right – versus symmetrical Bmp signaling). Correspondingly, we also found that control embryos displayed normal asymmetric expression of *bmp4* around the cardiac cone, whereas *bmp4* expression is symmetrical in *rargb* morphants as determined by *in situ* hybridization at 21 somites (Figure 2-12, A-B). Together, these results demonstrate *in vivo* that loss of *rargb* affects Bmp activity and ultimately organ laterality.

The zebrafish *rargb* morphant phenotype resembles human right atrial isomerism

Rargb morphant laterality defects are strikingly similar to the human heterotaxic syndrome left/right atrial isomerism in which patients display both a midline heart and a

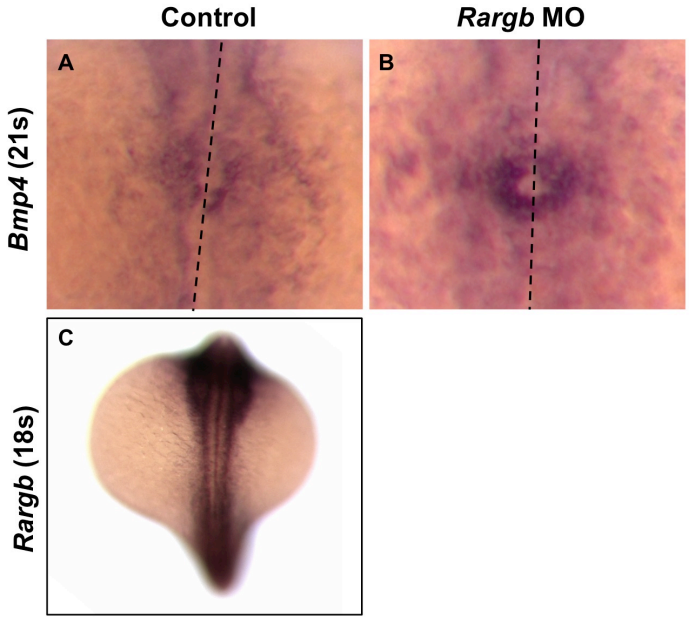

Figure 2-12. *Bmp4* is symmetrically expressed in *rargb* morphants.

(A, B) *In situ* hybridization for *bmp4* expression in the cardiac cone of control and *rargb* morphant embryos at 21 somites. Black dotted lines denote the midline.

(C) *Rargb* expression at 18 somites in wild type embryos.

duplicated or midline liver (Sutherland and Ware, 2009; Zhu et al., 2006). Biliary atresia, characterized by blocked or absent hepatic bile ducts, is another hallmark of the human heterotaxic condition (Sutherland and Ware, 2009) so we investigated whether *rargb* morphants also display biliary defects. We first examined *tp1bglob:eGFP* reporter fish in which the Epstein-Barr Virus *TP1* gene, placed upstream of the rabbit *β-globin* minimal promoter acts as a Notch-responsive element (Parsons et al. 2009). Notch signaling is required for normal bile duct specification and development and highlights the biliary tree as early as 76 hpf (Lorent et al., 2010; Lorent et al., 2004). Compared to control larvae that developed intrahepatic bile ducts with a normal latticework appearance, 56% (n=52) of *rargb* MO-injected larvae exhibited dysmorphic bile duct architecture characterized by reduced intrahepatic branching and connectivity (Figure 2-13, A-B). In addition to examining bile duct development *in vivo* in Notch reporter fish, we also investigated the expression of the bile duct cell marker 2F11 (Crosnier et al., 2005) by whole mount immunostain in 5 dpf larvae. Confocal projections of control embryos revealed a regular, highly branched network of intrahepatic bile ducts, whereas *rargb* morphant embryos displayed less extensive ductular networks and enlarged cell bodies at duct junctions (84%, n=19) (Figure 2-13, C-F), defects reminiscent of the human pathophysiology of biliary atresia. The etiology of biliary atresia remains unknown, however our results suggest that loss of *rargb* negatively impacts bile duct formation.

Patients with heterotaxia often exhibit asplenia or polyspenia (Ivemark, 1955; Sutherland and Ware, 2009), so we also investigated whether *rargb* morphants develop spleen defects by examining expression of *hox11* at 5 dpf. Thirty-four percent (n=58) of *rargb* morphants had a small or absent spleen, compared to only 3% of control embryos (n=33, p-value = 0.0005) (Figure 2-13, G-I), suggesting that loss of *rargb* results in a phenotype similar to human asplenia. Patients with right atrial isomerism, or Ivemark

Figure 2-13 (next page). *Rargb* morphants develop biliary defects.

(A-B) Fluorescence microscopy of Notch reporter fish *tp1bglob:eGFP* at 5 dpf. *Rargb* morphant embryos develop defective bile duct architecture (B, arrows) compared to the normal latticework appearance of the control embryo's biliary tree (A).

(C-F) Confocal microscopy of 2F11 whole mount immunostained embryos at 5 dpf. *Rargb* morphant embryos display enlarged cell bodies (D-E, white arrowheads) and reduced branching of intrahepatic bile duct networks (F) compared to control embryos (C). White dotted lines outline the liver. Images are taken at the same magnification.

(G-I) *In situ* hybridization for *hox11* at 5 dpf. *Rargb* morphants display small (H) or absent (I) spleens compared to control embryos (G). Black arrowheads denote the spleen.

Scale bars: 50 microns.

Figure 2-13 (continued)

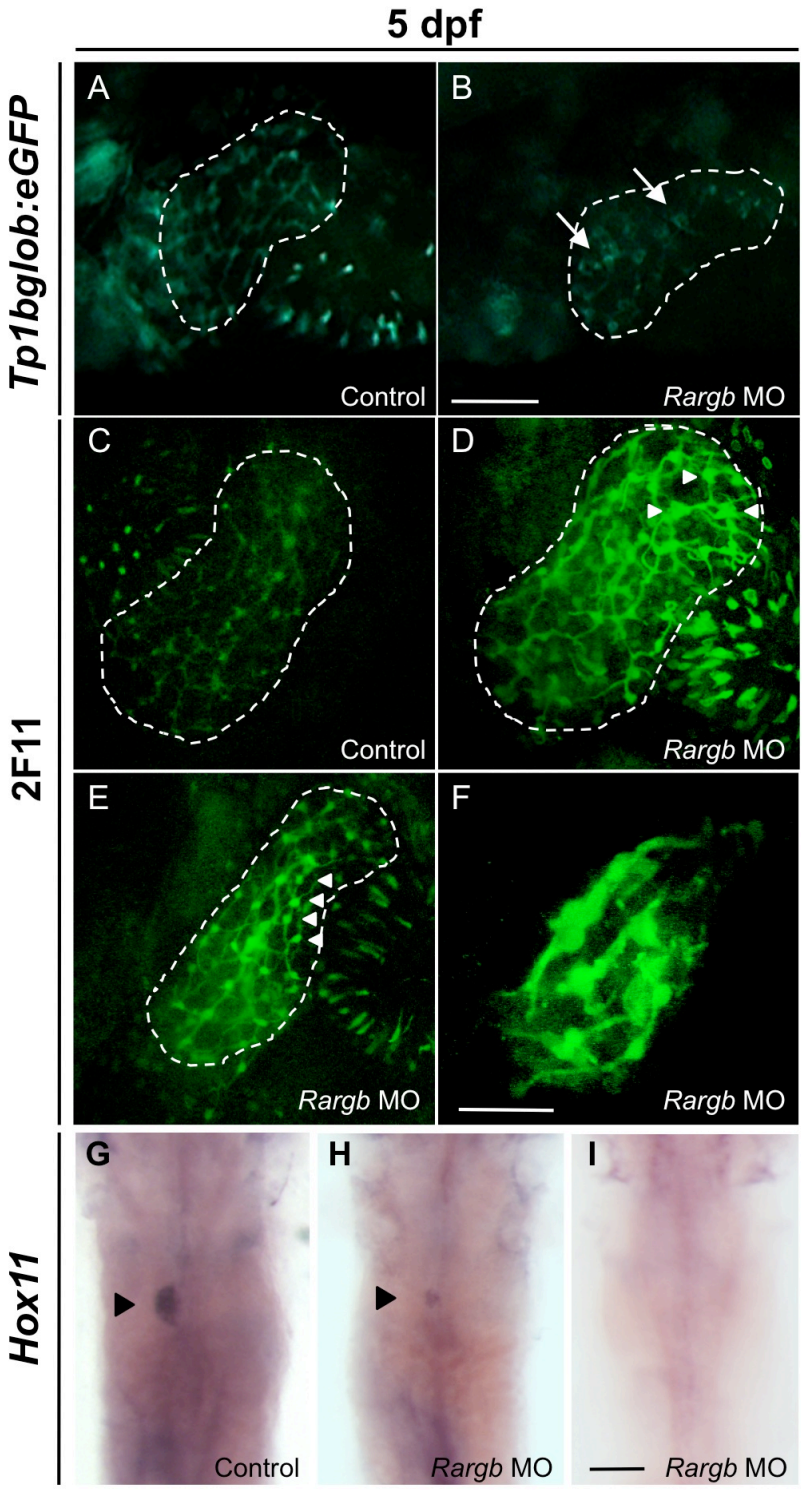

Syndrome, typically display apslenia (Ivemark, 1955), whereas patients with left atrial isomerism predominantly develop polyspenia (Zhu et al., 2006). Thus, the *rargb* morphant phenotype more closely resembles right atrial isomerism. Together, the laterality, biliary, and spleen defects seen in *rargb* morphants implicate RARγ in human heterotaxic syndromes and suggest that RA signaling is important for *situs solitus* of human organs.

DISCUSSION

In this study, we identified RA as a regulator of zebrafish hepatogenesis and elucidated roles for RA signaling in organ development and positioning. We have shown that RA synthesis by Raldh enzymes and downstream signal transduction by RARs are both important for proper liver development. RAR knockdowns reveal that individual receptors exert specific effects during organogensis. Loss of Rargb results in duplicated livers, midline hearts, and unlooped guts, and epistasis analyses demonstrate that Rargb functions upstream of Bmp to affect organ positioning. *Rargb* morphants also develop bile duct defects and asplenia, which in combination with their laterality phenotypes, parallel the human heterotaxic syndrome right atrial isomerism.

It has been suggested that RA signaling is involved in endoderm development (Stafford and Prince, 2002; Alexa et al., 2009; Negishi et al., 2010), however roles for specific RARs in liver development and positioning have not been described. Our finding that one receptor, Rargb, impacts organ laterality can be explained by differences in zebrafish RAR expression patterns and divergent RAR phylogenies (Waxman and Yelon, 2007). First, r*argb* is located on a different chromosome than *rarga*, suggesting that these may be different genes rather than splice variants. Furthermore, whereas *rarga* is not expressed maternally, *rargb* is expressed both maternally and zygotically. Phylogenetic analyses have also established that *rargb* is more closely related to mouse

and human *RARG*, supporting our results demonstrating evolutionary conservation of RARγ function. Knockdown of the RA transport protein Rbp4 results in the formation of two liver buds (Li et al., 2007), corroborating a role for RA signaling in liver progenitor positioning.

Although Nodal is known to be a master regulator of left-right asymmetry (Shen 2007), we did not find its expression affected by loss of *rargb*. It has previously been shown that blocking RA signaling before the 2 somite stage alters Nodal signaling in zebrafish (Huang et al. 2011), but organs are primarily reversed rather than duplicated or midline in these embryos. Furthermore, studies in other species have suggested that RA signaling can impact organ laterality without disrupting early left-right signals. In *Xenopus*, laterality defects manifest in embryos treated with DEAB after Nodal has established the left-right axis (Lipscomb et al., 2006), and *Raldh2* null mice develop unlooped hearts despite Nodal being unaffected (Niederreither et al., 2001). Characterization of the zebrafish mutant *heart and soul* (*has*), which displays failed gut looping and symmetrical visceral organs (Horne-Badovinac et al. 2001), revealed that these laterality defects are accompanied by normal *spaw* and *pitx2* expression (Horne-Badovinac et al., 2003), further suggesting that left-right patterning defects can manifest in the presence of normal Nodal signaling.

RA and Bmp signals intersect in other developmental contexts (Sheng et al. 2010; Shimono et al. 2011; Song et al., 2007; Tehrani and Lin, 2010), so we hypothesized that RA may exert its effect on organ development by regulating Bmp activity. In mice, Bmps generated adjacent to the cardiac mesoderm in the septum transversum mesenchyme induce hepatic progenitors in the nearby endoderm and promote outgrowth of the liver primordium (Jung et al., 1999; Rossi et al., 2001). Studies in mice and chick have demonstrated that RARG inhibits Bmp signaling by promoting degradation of phosphorylated Smad (Sheng et al. 2010; Shimono et al.

2011), further substantiating our finding that RA integrates with Bmp signaling via regulation of Bmp's downstream effectors.

Loss of *rargb* results in laterality defects of the liver, heart, and gut, but it is unclear whether all defects are linked. Gut looping occurs around 30 hpf (Horne-Badovinac et al., 2003), but we observe heart jogging defects as early as 26 hpf; accordingly, abnormal LPM migration can only account for visceral organ but not heart defects. It is possible that aberrant RA signaling affects both LPM migration and local Bmp signaling around the cardiac cone, thereby affecting multiple organs. It has recently been shown that zebrafish RARs often act as transcriptional activators rather than repressors (Waxman and Yelon, 2011), so it is also possible that *rargb* may preferentially activate another molecule on the right side that normally acts as a repressor of the hepatic fate. *Ntl, flh*, and *sur* mutants display midline hearts, loss of gut looping, and duplication of visceral organs, and it has been suggested that because these are loss-of-function mutations, the normally asymmetric liver results from suppression of hepatic activators on the right side (Chen et al., 2001). A previous study suggests that *rargb* is asymmetrically expressed in the neural crest cells of the hindbrain at 18 hpf (Linville et al., 2009), however *rargb* appears to be expressed equally on both left and right sides of the trunk during somitogenesis (Figure 2-12C), so it remains unclear how *rargb* exerts its affect on visceral organ laterality. It is possible that *in situ* hybridization is not sensitive enough to detect slight asymmetries in *rargb* expression that may impact downstream signaling.

Organ laterality and bile duct defects exhibited by *rargb* morphants are reminiscent of the human pathological condition right atrial isomerism in which patients display midline hearts, midline or duplicated livers, biliary atresia, and asplenia. Our data suggest that perturbed RA signaling may play a role in human heterotaxia and furthermore, that heterotaxia can result from mutations in genes other than Nodal. We

demonstrate that loss of Rargb and Bmp overexpression result in the same organ laterality defects, where Rargb functions upstream of Bmp signaling to regulate organ position, and that Rargb also impacts biliary development. Biliary abnormalities often result in obstructed bile flow, leading to pancreatitis and jaundice, and necessitate surgical intervention or liver transplantation in infants (Davenport, 2005; Haber and Russo, 2003). The etiology of biliary atresia remains unknown, but the fact that *rargb* morphants and left/right atrial isomerism patients develop organ *situs* and biliary defects suggests a common underlying mechanism. By understanding the role of RA and Bmp signaling in organ development and positioning, we may be able to better understand and treat patients with these life-threatening malformations.

METHODS

Zebrafish husbandry

Zebrafish were maintained according to IACUC protocols. *LF2.8-EGFP* (referred to as *Lfabp:GFP*) (Her et al., 2003), *cmlc2:GFP* (Huang et al., 2003), *cyp26a1:eYFP* (Hu et al., 2008), *miles apart* (*mil*) (Kupperman et al., 2000), *hs:bmp2b* (Chocron et al., 2007), *BRE:eGFP* (Laux et al., 2011) and *tp1bglob:eGFP* (Parsons et al., 2009) transgenic and mutant lines have been described previously.

Chemical exposures

Zebrafish embryos were exposed to 0.1 uM all trans retinoic acid (ATRA, Sigma), 1.0 uM 4-diethylaminobenzaldehyde (DEAB, Sigma), 1.0 uM AGN193109 (Toronto Research Chemicals), 1.0 uM MM11253 (Tocris), 25 uM dorsomorphin, or 0.1 uM CD1530 (Tocris) during the specified time windows. Stock solutions were diluted in E3 embryo water. Control embryos were concurrently exposed to 0.1% DMSO. After chemical exposure, embryos were washed 3-5x in E3 solution then fixed with 4% PFA at the appropriate

stages. The chemical genetic screen was performed as described previously (North et al., 2007). Wild type age-matched embryos were arrayed into 48-well plates and exposed to test compounds from 18-72 hpf. Compound libraries used include the NINDS Custom Collection (1,040 compounds), SpecPlus Collection (960) and BIOMOL ICCB Known Bioactives (480).

Whole mount *in situ* hybridization

Zebrafish embryos were fixed in 4% PFA at the specified stages, and *in situ* hybridization was performed according to established protocols (http://zfin.org/ZFIN/Methods/ThisseProtocol.html) using the following probes: (Endoderm) *lfabp, prox1, foxA3, shh*; (heart) *cmlc2, amhc, vmhc*; (spleen) *hox11*; (kidney) *slc20a1a, slc12a3*; (thyroid) *nkx2.1a*; (LPM) *hand2*; (Nodal) *spaw, pitx2, lefty1, lefty2*; (Bmp) *smad1, smad4, smad 5*. The number of embryos displaying a particular phenotype is presented as a percentage of the sample size, n.

Whole mount immunostaining

BrdU: Zebrafish embryos were incubated in 10 mM BrdU on ice for 20 minutes at 24 hpf, returned to warm embryo water for 5 minutes, then fixed in 4% PFA. Embryos were incubated with anti-BrdU primary (Roche) and goat anti-mouse peroxidase-conjugated secondary (Jackson ImmunoResearch) antibodies and visualized with DAB. BrdU+ cells were counted manually in a defined region of the embryo (n=5 embryos/chemical treatment).

2F11: Zebrafish larvae were fixed at 5 dpf and incubated in a 1:500 dilution of mouse monoclonal 2F11 primary antibody (Abcam) followed by 1:50 FITC rabbit anti-mouse IgG secondary antibody (Jackson ImmunoResearch).

Morpholino knockdown and mRNA rescue injections

Morpholinos (MOs; GeneTools) were designed against zebrafish *raldh2* (5' CAACTTCACTGGA GGTCATCGCGTC 3') (100 uM) and *raldh4* (5' GATATTTCATGTCTTTTGACATCGC 3') (200 uM), and previously published MOs were used against RA receptors *raraa, rarab, rarga,* and *rargb* (400-800 uM) (Linville et al., 2009). For the RARγ rescue experiment, 200 pg mouse *Rarg* mRNA (OriGene Technologies) was co-injected with 400 uM *rargb* MO at the 1-cell stage.

Flow cytometry analysis

Lfabp:GFP fluorescent embryos were exposed to chemicals or injected with MOs as described above, whole embryos were manually dissociated in 0.9x PBS, and %GFP+ cells were determined by flow cytometric analysis. ≥20,000 cells were analyzed per embryo, and ≥5 embryos were analyzed for each chemical treatment or MO injection using FlowJo software.

Microscopy

Live fluorescence microscopy was performed on *cmlc2:GFP*, *BRE:eGFP*, or *tp1bglob:eGFP* embryos anesthetized in 0.04 mg/ml Tricaine in E3 embryo water using a Zeiss Discovery V8 microscope. Once sorted by phenotype, embryos were washed several times and returned to E3 for further observation and/or until fixation. Embryos used in *in situ* hybridization or BrdU immunostaining experiments were visualized in glycerol. Confocal microscopy of 2F11 immunostained embryos was performed on a Zeiss LSM 510 Meta microscope. For each treatment group, images presented are shown at the same magnification. Scale bars represent 100 microns unless otherwise noted.

Smad Western blots

Protein lysates were isolated at 18 hpf from control, *rargb* morphant, and dorsomorphin-treated embryos by manual disruption in RIPA buffer. 1:1000 anti-pSmad/1/5/8 (Cell Signaling Technology) or 1 ug/ml anti-Smad 1/5/8/9 (Cayman Chemical) primary antibody was used, followed by 1:3000 anti-rabbit HRP secondary antibody (Abcam).

REFERENCES

Alexa, K., Choe, S. K., Hirsch, N., Etheridge, L., Laver, E., Sagerstrom, C. G., 2009. Maternal and zygotic aldh1a2 activity is required for pancreas development in zebrafish. PLoS One. 4, e8261.

Bakkers, J., Verhoeven, M. C., Abdelilah-Seyfried, S., 2009. Shaping the zebrafish heart: from left-right axis specification to epithelial tissue morphogenesis. Dev Biol. 330, 213-20.

Begemann, G., Schilling, T. F., Rauch, G. J., Geisler, R., Ingham, P. W., 2001. The zebrafish neckless mutation reveals a requirement for raldh2 in mesodermal signals that pattern the hindbrain. Development. 128, 3081-94.

Chazaud, C., Chambon, P., Dolle, P., 1999. Retinoic acid is required in the mouse embryo for left-right asymmetry determination and heart morphogenesis. Development. 126, 2589-96.

Chen, J. N., van Bebber, F., Goldstein, A. M., Serluca, F. C., Jackson, D., Childs, S., Serbedzija, G., Warren, K. S., Mably, J. D., Lindahl, P., Mayer, A., Haffter, P., Fishman, M. C., 2001. Genetic steps to organ laterality in zebrafish. Comp Funct Genomics. 2, 60-8.

Chen, J. N., van Eeden, F. J., Warren, K. S., Chin, A., Nusslein-Volhard, C., Haffter, P., Fishman, M. C., 1997. Left-right pattern of cardiac BMP4 may drive asymmetry of the heart in zebrafish. Development. 124, 4373-82.

Chocron, S., Verhoeven, M. C., Rentzsch, F., Hammerschmidt, M., Bakkers, J., 2007. Zebrafish Bmp4 regulates left-right asymmetry at two distinct developmental time points. Dev Biol. 305, 577-88.

Chung, W. S., Shin, C. H., Stainier, D. Y., 2008. Bmp2 signaling regulates the hepatic versus pancreatic fate decision. Dev Cell. 15, 738-48.

Crosnier, C., Vargesson, N., Gschmeissner, S., Ariza-McNaughton, L., Morrison, A., Lewis, J., 2005. Delta-Notch signalling controls commitment to a secretory fate in the zebrafish intestine. Development. 132, 1093-104.

Davenport, M., 2005. Biliary atresia. Semin Pediatr Surg. 14, 42-8.

Dersch, H., Zile, M. H., 1993. Induction of normal cardiovascular development in the vitamin A-deprived quail embryo by natural retinoids. Dev Biol. 160, 424-33.

Field, H. A., Dong, P. D., Beis, D., Stainier, D. Y., 2003. Formation of the digestive system in zebrafish. II. Pancreas morphogenesis. Dev Biol. 261, 197-208.

Haber, B. A., Russo, P., 2003. Biliary atresia. Gastroenterol Clin North Am. 32, 891-911.

Hale, L. A., Tallafuss, A., Yan, Y. L., Dudley, L., Eisen, J. S., Postlethwait, J. H., 2006. Characterization of the retinoic acid receptor genes raraa, rarab and rarg during zebrafish development. Gene Expr Patterns. 6, 546-55.

Her, G. M., Yeh, Y. H., Wu, J. L., 2003. 435-bp liver regulatory sequence in the liver fatty acid binding protein (L-FABP) gene is sufficient to modulate liver regional expression in transgenic zebrafish. Dev Dyn. 227**,** 347-56.

Horne-Badovinac, S., Lin, D., Waldron, S., Schwarz, M., Mbamalu, G., Pawson, T., Jan, Y., Stainier, D. Y., Abdelilah-Seyfried, S., 2001. Positional cloning of heart and soul reveals multiple roles for PKC lambda in zebrafish organogenesis. Curr Biol. 11**,** 1492-502.

Horne-Badovinac, S., Rebagliati, M., Stainier, D. Y., 2003. A cellular framework for gut-looping morphogenesis in zebrafish. Science. 302**,** 662-5.

Hu, P., Tian, M., Bao, J., Xing, G., Gu, X., Gao, X., Linney, E., Zhao, Q., 2008. Retinoid regulation of the zebrafish cyp26a1 promoter. Dev Dyn. 237**,** 3798-808.

Huang, C. J., Tu, C. T., Hsiao, C. D., Hsieh, F. J., Tsai, H. J., 2003. Germ-line transmission of a myocardium-specific GFP transgene reveals critical regulatory elements in the cardiac myosin light chain 2 promoter of zebrafish. Dev Dyn. 228**,** 30-40.

Huang, H., Ruan, H., Aw, M. Y., Hussain, A., Guo, L., Gao, C., Qian, F., Leung, T., Song, H., Kimelman, D., Wen, Z., Peng, J., 2008. Mypt1-mediated spatial positioning of Bmp2-producing cells is essential for liver organogenesis. Development. 135**,** 3209-18.

Huang, S., Ma, J., Liu, X., Zhang, Y., Luo, L., Retinoic acid signaling sequentially controls visceral and heart laterality in zebrafish. J Biol Chem. 286**,** 28533-43.
Iulianella, A., Lohnes, D., 2002. Chimeric analysis of retinoic acid receptor function during cardiac looping. Dev Biol. 247**,** 62-75.

Ivemark, B., 1955. Implications of agenesis of the spleen on the pathogenesis of conotruncus anomalies in childhood; an analysis of the heart malformations in the splenic agenesis syndrome, with fourteen new cases. Acta Paediatr Suppl. 44(Suppl 104), 7-110.

Jung, J., Zheng, M., Goldfarb, M., Zaret, K. S., 1999. Initiation of mammalian liver development from endoderm by fibroblast growth factors. Science. 284**,** 1998-2003.

Kupperman, E., An, S., Osborne, N., Waldron, S., Stainier, D. Y., 2000. A sphingosine-1-phosphate receptor regulates cell migration during vertebrate heart development. Nature. 406**,** 192-5.

Laux, D. W., Febbo, J. A., Roman, B. L., 2011. Dynamic analysis of BMP-responsive smad activity in live zebrafish embryos. Dev Dyn. 240**,** 682-94.

Li, Z., Korzh, V., Gong, Z., 2007. Localized rbp4 expression in the yolk syncytial layer plays a role in yolk cell extension and early liver development. BMC Dev Biol. 7**,** 117.

Liang, D., Zhang, M., Bao, J., Zhang, L., Xu, X., Gao, X., Zhao, Q., 2008. Expressions of Raldh3 and Raldh4 during zebrafish early development. Gene Expr Patterns. 8**,** 248-53.

Linville, A., Radtke, K., Waxman, J. S., Yelon, D., Schilling, T. F., 2009. Combinatorial roles for zebrafish retinoic acid receptors in the hindbrain, limbs and pharyngeal arches. Dev Biol. 325, 60-70.

Lipscomb, K., Schmitt, C., Sablyak, A., Yoder, J. A., Nascone-Yoder, N., 2006. Role for retinoid signaling in left-right asymmetric digestive organ morphogenesis. Dev Dyn. 235, 2266-75.

Lorent, K., Moore, J. C., Siekmann, A. F., Lawson, N., Pack, M., 2010. Reiterative use of the notch signal during zebrafish intrahepatic biliary development. Dev Dyn. 239, 855-64.

Lorent, K., Yeo, S. Y., Oda, T., Chandrasekharappa, S., Chitnis, A., Matthews, R. P., Pack, M., 2004. Inhibition of Jagged-mediated Notch signaling disrupts zebrafish biliary development and generates multi-organ defects compatible with an Alagille syndrome phenocopy. Development. 131, 5753-66.

Mark, M., Ghyselinck, N. B., Chambon, P., 2006. Function of retinoid nuclear receptors: lessons from genetic and pharmacological dissections of the retinoic acid signaling pathway during mouse embryogenesis. Annu Rev Pharmacol Toxicol. 46, 451-80.

Negishi, T., Nagai, Y., Asaoka, Y., Ohno, M., Namae, M., Mitani, H., Sasaki, T., Shimizu, N., Terai, S., Sakaida, I., Kondoh, H., Katada, T., Furutani-Seiki, M., Nishina, H., Retinoic acid signaling positively regulates liver specification by inducing wnt2bb gene expression in medaka. Hepatology. 51, 1037-45.

Niederreither, K., Vermot, J., Messaddeq, N., Schuhbaur, B., Chambon, P., Dolle, P., 2001. Embryonic retinoic acid synthesis is essential for heart morphogenesis in the mouse. Development. 128, 1019-31.

North, T. E., Goessling, W., Walkley, C. R., Lengerke, C., Kopani, K. R., Lord, A. M., Weber, G. J., Bowman, T. V., Jang, I. H., Grosser, T., Fitzgerald, G. A., Daley, G. Q., Orkin, S. H., Zon, L. I., 2007. Prostaglandin E2 regulates vertebrate haematopoietic stem cell homeostasis. Nature. 447, 1007-11.

Ober, E. A., Field, H. A., Stainier, D. Y., 2003. From endoderm formation to liver and pancreas development in zebrafish. Mech Dev. 120, 5-18.

Ober, E. A., Verkade, H., Field, H. A., Stainier, D. Y., 2006. Mesodermal Wnt2b signalling positively regulates liver specification. Nature. 442, 688-91.

Parsons, M. J., Pisharath, H., Yusuff, S., Moore, J. C., Siekmann, A. F., Lawson, N., Leach, S. D., 2009. Notch-responsive cells initiate the secondary transition in larval zebrafish pancreas. Mech Dev. 126, 898-912.

Pittlik, S., Domingues, S., Meyer, A., Begemann, G., 2008. Expression of zebrafish aldh1a3 (raldh3) and absence of aldh1a1 in teleosts. Gene Expr Patterns. 8, 141-7.
Reiter, J. F., Alexander, J., Rodaway, A., Yelon, D., Patient, R., Holder, N., Stainier, D. Y., 1999. Gata5 is required for the development of the heart and endoderm in zebrafish. Genes Dev. 13, 2983-95.

Reiter, J. F., Kikuchi, Y., Stainier, D. Y., 2001. Multiple roles for Gata5 in zebrafish endoderm formation. Development. 128**,** 125-35.

Rossi, J. M., Dunn, N. R., Hogan, B. L., Zaret, K. S., 2001. Distinct mesodermal signals, including BMPs from the septum transversum mesenchyme, are required in combination for hepatogenesis from the endoderm. Genes Dev. 15**,** 1998-2009.

Shen, M. M., 2007. Nodal signaling: developmental roles and regulation. Development. 134**,** 1023-34.

Sheng, N., Xie, Z., Wang, C., Bai, G., Zhang, K., Zhu, Q., Song, J., Guillemot, F., Chen, Y. G., Lin, A., Jing, N., Retinoic acid regulates bone morphogenic protein signal duration by promoting the degradation of phosphorylated Smad1. Proc Natl Acad Sci U S A. 107**,** 18886-91.

Shimono, K., Tung, W. E., Macolino, C., Chi, A. H., Didizian, J. H., Mundy, C., Chandraratna, R. A., Mishina, Y., Enomoto-Iwamoto, M., Pacifici, M., Iwamoto, M., Potent inhibition of heterotopic ossification by nuclear retinoic acid receptor-gamma agonists. Nat Med. 17**,** 454-60.

Shin, D., Shin, C. H., Tucker, J., Ober, E. A., Rentzsch, F., Poss, K. D., Hammerschmidt, M., Mullins, M. C., Stainier, D. Y., 2007. Bmp and Fgf signaling are essential for liver specification in zebrafish. Development. 134**,** 2041-50.

Smith, K. A., Chocron, S., von der Hardt, S., de Pater, E., Soufan, A., Bussmann, J., Schulte-Merker, S., Hammerschmidt, M., Bakkers, J., 2008. Rotation and asymmetric development of the zebrafish heart requires directed migration of cardiac progenitor cells. Dev Cell. 14**,** 287-97.

Song, J., Kim, H. J., Gong, Z., Liu, N. A., Lin, S., 2007. Vhnf1 acts downstream of Bmp, Fgf, and RA signals to regulate endocrine beta cell development in zebrafish. Dev Biol. 303**,** 561-75.

Stafford, D., Prince, V. E., 2002. Retinoic acid signaling is required for a critical early step in zebrafish pancreatic development. Curr Biol. 12**,** 1215-20.

Sutherland, M. J., Ware, S. M., 2009. Disorders of left-right asymmetry: heterotaxy and situs inversus. Am J Med Genet C Semin Med Genet. 151C**,** 307-17.

Tehrani, Z., Lin, S., Antagonistic interactions of hedgehog, Bmp and retinoic acid signals control zebrafish endocrine pancreas development. Development. 138**,** 631-40.
Waxman, J. S., Yelon, D., Zebrafish retinoic acid receptors function as context-dependent transcriptional activators. Dev Biol. 352**,** 128-40.

Waxman, J. S., Yelon, D., 2007. Comparison of the expression patterns of newly identified zebrafish retinoic acid and retinoid X receptors. Dev Dyn. 236**,** 587-95.

Yin, C., Kikuchi, K., Hochgreb, T., Poss, K. D., Stainier, D. Y., Hand2 regulates extracellular matrix remodeling essential for gut-looping morphogenesis in zebrafish. Dev Cell. 18**,** 973-84.

Zhu, L., Belmont, J. W., Ware, S. M., 2006. Genetics of human heterotaxias. Eur J Hum Genet. 14**,** 17-25.

CHAPTER 3

Estrogen inhibits hepatoblast differentiation in an Esr2-dependent manner

Maija K. Garnaas[1], Claire C. Cutting[1], Casey A. Gifford[3,4], Kelli J. Carroll[2], Daniel A. Gorelick[5], Marnie E. Halpern[5], Alexander Meissner[3,4], Trista E. North[2,3], Wolfram Goessling[1,3]

[1]Genetics Division, Brigham and Women's Hospital, Harvard Medical School, Brigham and Women's Hospital, Boston, MA, USA. [2]Department of Pathology, Beth Israel Deaconess Medical Center, Harvard Medical School, Boston, MA, USA. [3]Harvard Stem Cell Institute, Cambridge, MA, USA. [4]Broad Institute of MIT and Harvard, Cambridge, MA, USA. [5]Carnegie Institute for Science, Baltimore, MD, USA.

This chapter contains the manuscript entitled "Estrogen inhibits hepatoblast differentiation in an Esr2-dependent manner", in preparation for submission to *Genes & Development*. It has been modified to fit the style of this dissertation. Author attributions: MKG devised, executed, and analyzed experiments and wrote the manuscript. MKG and CCC performed chemical exposures and morpholino knockdowns. CAG and AM carried out human ESC differentiation protocols and ChIP-seq and RNA-seq analyses. MKG and KJC executed enzyme immunoassay. KJC and TEN performed mouse husbandry and dissections. DAG and MEH graciously provided *ERE:GFP* transgenic zebrafish. WG and TEN devised experiments and analyzed data.

ABSTRACT

Exposure to environmental estrogens has increased dramatically over the past decade and is correlated with hepatic dysfunction and cancer. In a chemical genetic screen in zebrafish, we identified estrogen as a negative regulator of hepatogenesis. Embryos treated with estradiol develop fewer hepatoctyes, resulting in a small liver phenotype. Genetic knockdown of each of the three estrogen receptors revealed that embryonic estrogen signaling exerts its effect through the Esr2 receptor subtype. Estradiol exposure does not impact the hepatoblast progenitor population, and endogenous estrogen levels are reduced concomitant with the initial appearance of differentiated hepatocytes, suggesting that estrogen signaling prevents hepatoblast differentiation rather than specification. Removal of estradiol from embryo water following early exposure results in the delayed appearance of hepatocytes, further indicating that estrogen signaling negatively affects hepatic differentiation. In mammals, *5α-reductase* mutant mice producing excess estrogen develop less differentiated livers compared to their wild type siblings. In addition, in human hepatocytes, the activating epigenetic mark H3K4me1 is diminished at the *ERβ* locus compared to undifferentiated embryonic stem cells and endodermal precursors, resulting in reduced expression of *ERβ*. Together, our findings define a novel role for estrogen signaling in regulating hepatic differentiation.

INTRODUCTION

The role of sex hormones in reproductive development is well established, however the function of estrogens in non-gonadal organogenesis is less understood. Exposure to exogenous estrogens has increased dramatically over the past decade (Fucic et al., 2012; Waring et al., 2008; Wolstenholme et al., 2011) and is associated with liver dysfunction, suggesting that strict control of estrogen signaling is required for proper hepatic development and homeostasis. Estrogenic compounds are able to cross the placenta (Vandenberg et al., 2007) and may thereby directly impact organogenesis during embryonic development, and the liver, being a first-pass metabolic filter, is particularly susceptible to toxic estrogenic insult.

Women taking oral contraceptives are at increased risk for developing hepatic adenomas, and there is significant correlation between estrogen exposure *in utero* and carcinogenesis (Giannitrapani et al., 2006; Harris and Waring, 2012; Laronda et al., 2012). Cirrhotic men overexpress estrogen receptors (De Maria et al., 2002), further suggesting a correlation between unregulated estrogen levels and liver disease. Nevertheless, hepatocellular carcinoma (HCC) is more prevalent in males than females in both humans and mice (Buch et al., 2008; Kalra et al., 2008; Parkin et al., 2005), and administering estrogen to male mice reduces HCC incidence (Kalra et al., 2008; Li et al., 2012). These reports suggest that estrogen signaling influences hepatic growth, but there is no consensus on the precise role of estrogens during liver development.

Estrogen hormones including estradiol (E2), the primary physiological estrogen, estrone (E1), and estriol (E3) are steroid hormones derived from cholesterol. Estradiol synthesis culminates in conversion of testosterone to E2 by the enzyme aromatase, also known as Cyp19a1. Typically, estrogens bind and activate cytoplasmic estrogen receptors (ESRs) that translocate to the nucleus and bind estrogen response elements (EREs) at DNA promoters to regulate downstream transcriptional targets (Nelson and

Habibi, 2013), although recent studies have also suggested that estrogens can exert their cellular effects by non-genomic mechanisms (Thomas, 2012). Xenoestrogens are a class of synthetic compounds that includes plastic monomers, surfactants, and pesticides that mimic or inhibit physiological estrogen action (Colborn et al., 1993; McLachlan, 2001; Soto et al., 1994). Xenoestrogens often persist in the environment long after their initial use and have thus become major health concerns in recent years (Watson et al., 2013). Bisphenol A (BPA), for example, a polycarbonate compound found in plastic water bottles and food can liners, has been linked to a number of human diseases including cancer (Vinas and Watson, 2010). Plant-derived estrogens, or phytoestrogens, are found in many soy-based products and also exhibit estrogenic activity; their impact on human health has accordingly also been the subject of numerous investigations (Brownson et al., 2002; Cornwell et al., 2004; Jeng et al., 2009; Jeng and Watson, 2009; Whitten et al., 1995).

Zebrafish express three cytoplasmic ESRs, *esr1, esr2a*, and *esr2b*, which are orthologous to mammalian ERα and ERβ (Bardet et al., 2002; Chandrasekar et al., 2010), and a less well characterized membrane receptor, G-protein coupled receptor 1 (GPER) (Liu et al., 2009). Of all adult zebrafish organs, including the ovaries and testes, ESRs are most highly expressed in the liver (Chandrasekar et al., 2010), however their embryonic expression and function in non-reproductive organs such as the liver has not been investigated in detail.

In zebrafish, hepatic progenitors, first identifiable by *prox1* expression at 18 hours post fertilization (hpf), aggregate and emerge as a nascent liver bud between 24 and 48 hpf. After 48 hpf, the liver starts to function, as hepatoblasts begin to differentiate into hepatocytes that express mature markers such as *liver fatty acid binding protein* (*lfabp*) (Her et al., 2003) and *transferrin* (Fraenkel et al., 2009). Members of the hepatic nuclear factor (Hnf), Gata, and FoxA families of transcription factors are known to direct hepatic

specification and coordinate hepatoblasts' transition into mature hepatocytes (Zaret, 2002), but nuclear hormone regulation of hepatic development has not been characterized as extensively. Previous studies have demonstrated unique roles for individual retinoic acid receptors during hepatogenesis (Garnaas et al., 2012), suggesting that nuclear receptors may regulate several diverse aspects of liver development.

In this report, we elucidate a role for estrogen signaling during hepatic differentiation. We first identified estrogen signaling as a regulator of normal liver development through our prior chemical genetic screen (Garnaas et al., 2012). Zebrafish treated with estradiol (E2) or xeno- and phytoestrogens from 18-72 hours post-fertilization (hpf) develop smaller livers at 72 hpf. The livers of embryos treated with estrogenic compounds are rescued by co-treatment with fulvestrant, an estrogen receptor (ESR) antagonist, indicating estrogenic compounds exert their effects via ESRs. Chemical inhibition or genetic knockdown of *esr2a* and *esr2b* but not *esr1* results in bigger livers, demonstrating that the Esr2 receptor subtype governs estrogen's effect on hepatogenesis. E2 treatment from 18-72 hpf does not significantly impact the hepatoblast population, suggesting that E2 does not prevent hepatic specification but rather differentiation. Embryonic estrogen levels decline precipitously from 30-72 hpf, thereby allowing liver differentiation to proceed normally. In mammals, we demonstrate that *srd5a1* mutant mice that synthesize excess estrogen *in utero* develop less differentiated livers compared to their wild type siblings, confirming the negative impact of estrogen on liver maturation. Furthermore, we find that H3K4 methylation is significantly diminished at the *ERβ* locus in human hepatocytes compared to undifferentiated embryonic stem or pan-endodermal cells. RNA-seq transcriptome analysis of these cell populations confirms that the *ERβ* locus is not highly expressed in differentiated human liver cells, and the E2-degrading enzyme *Cyp1a* is upregulated

while the E2-synthesizing enzyme *Cyp19a1* is downregulated in mature hepatocytes. Together, our results demonstrate that endogenous estrogen is under strict temporal control to prevent hepatoblasts' differentiation into hepatocytes.

RESULTS

Estrogen signaling negatively impacts embryonic liver development

We previously performed a chemical genetic screen to identify novel regulators of liver development (Garnaas et al., 2012) and uncovered seven estrogen-related compounds that affect hepatogenesis (Figure 3-1). Physiological estrogens 17β-estradiol (E2) and estriol, synthetic estrogens 17α-ethynylestradiol (EE) and diethylstilbestrol, and the phytoestrogen quercetin decreased liver size, whereas the aromatase inhibitor chrysin and estrogen receptor antagonist tamoxifen increased liver size, suggesting that estrogen signaling negatively impacts liver growth.

To substantiate our chemical screen findings, we treated wild type and *lfabp:GFP* transgenic reporter embryos with 1 uM E2 from 18-72 hpf and consistently noted small or absent livers by *lfabp in situ* hybridization (67↓/74) and fluorescence microscropy (37↓/42), respectively (Figure 3-2, A-D). It has previously been determined that this is a non-toxic dose that does not impact gross embryo morphology (Chandrasekar et al., 2010). We confirmed these findings by examining expression of *transferrin*, another hepatocyte marker; its expression is also reduced in E2-exposed embryos (33↓/35) (Figure 3-3, A-B), demonstrating that E2's negative effect on liver development is not specific to *lfabp* expression. Shorter (6 or 24 hour time window) E2 exposures between 18 and 72 hpf similarly inhibited liver formation (Figure 3-3, E-H), suggesting that hepatic progenitors are highly sensitive to estrogen over the course of embryonic liver development. Embryos exposed to the xenoestrogen bisphenol A (BPA) (48↓/51) or the phytoestrogen genistein (27↓/33) also develop smaller livers, whereas exposure to

A

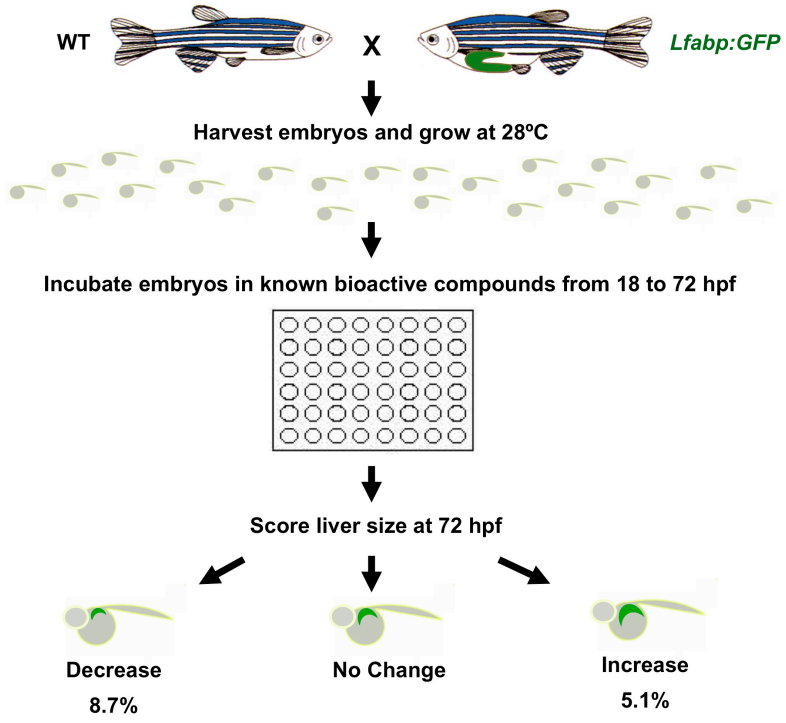

B

Compound	Effect on liver size
Estradiol (E2)	↓
Estriol (E3)	↓
17 alpha-ethynylestradiol (EE)	↓
Diethylstilbestrol	↓
Quercetin	↓
Chrysin	↑
Tamoxifen	↑

Figure 3-1. A chemical genetic screen identifies estrogen signaling as a negative regulator of embryonic zebrafish liver development.

(A) Chemical genetic screen workflow. Wild type (WT) or *lfabp:GFP* transgenic reporter fish were exposed to individual compounds from a library of 2640 known bioactives over the course of embryonic liver development (18-72 hpf). Alterations in liver size were detected by fluorescence microscopy and *in situ* hybridization for *lfabp*.

(B) Seven compounds were identified in the screen. Estrogenic compounds 17β-estradiol (E2), estriol (E3), 17α-ethynylestradiol (EE), diethylstilbestrol, and quercetin decreased liver size, whereas the aromatase inhibitor chrysin and estrogen receptor antagonist tamoxifen increased liver size.

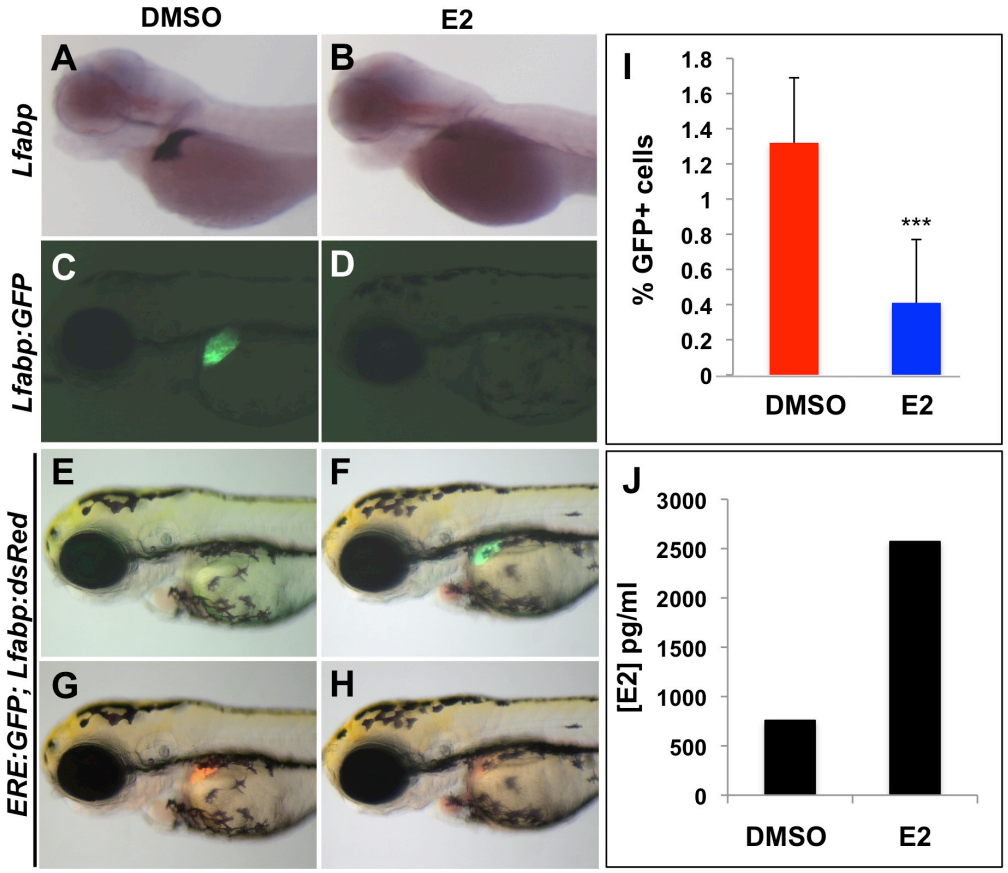

Figure 3-2. Estrogen signaling negatively impacts embryonic liver development.

(A-D) Compared to DMSO-treated controls, embryos exposed to estradiol (E2) from 18-72 hpf develop smaller livers at 72 hpf as determined by *in situ* hybridization for the hepatocyte marker *lfabp* (A, B) and live fluorescence microscopy of *lfabp:GFP* transgenic reporter fish (C,D).

(E-H) Dual transgenic *ERE:GFP;Lfabp:dsRed* reporter fish exposed to E2 display activated estrogen signaling in the liver (F) which occurs concomitantly with a smaller liver (H) at 72 hpf.

(I) FACS quantification of percent GFP+ cells in chemically treated *lfabp:GFP* embryos reveals that E2-treated embryos contain fewer hepatocytes than DMSO-treated controls.

(J) E2 exposure results in a three-fold increase in endogenous E2 concentrations at 30 hpf as determined by enzyme immunoassay.

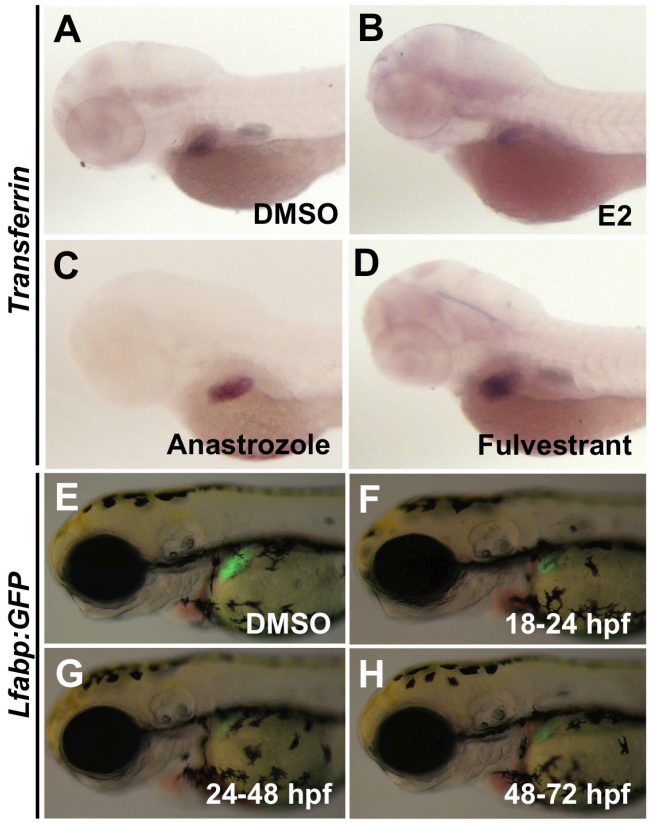

Figure 3-3. Estrogen exposure inhibits liver development.

(A-D) *In situ* hybridization for the hepatocyte marker *transferrin* at 72 hpf. Embryos exposed to E2 from 18-72 hpf develop smaller livers (B), whereas exposure to anastrozole, an aromatase inhibitor (C), or fulvestrant, an ESR antagonist (D), enhances liver development compared to controls (A).

(E-H) *Lfabp:GFP* transgenic embryos treated with E2 during shorter exposure windows develop smaller livers compared to control siblings at 72 hpf.

testosterone (2↑/18) or progesterone (5↓/31) does not significantly impact liver development (Figure 3-4, A-F), indicating the inhibitory effect is specific to estrogenic compounds. Exposing embryos to anastrozole, an aromatase inhibitor, results in the development of bigger livers (28↑/39) (Figure 3-3C), further illustrating the negative impact of estrogen on hepatogenesis. Using a bigenic estrogen response element (ERE) (Gorelick and Halpern, 2011) and hepatocyte transgenic reporter line *ERE:GFP;lfabp:dsRed*, we observed greater GFP fluorescence in the liver primordium of embryos treated with E2 from 18-72 hpf (Figure 3-2, E-H), demonstrating that the liver is estrogen responsive, and E2 exposure increases estrogen signaling in the liver. To substantiate this finding, we performed an enzyme immunoassay for endogenous estrogen levels at 30 hpf. Estrogen exposure from 18-30 hpf approximately triples the endogenous estrogen concentration compared to DMSO controls (Figure 3-2J), indicating that exogenous estrogen exposure alters the bioavailability of estrogen in the embryo within the physiological range.

To determine whether changes in liver size correspond to changes in hepatocyte cell number, we performed FACS quantification of *lfabp:GFP* reporter fish at 72 hpf. Compared to DMSO-treated control siblings (1.32±0.37% GFP+), we observed a 70% decrease in hepatocytes in E2-treated embryos (0.41±0.36% GFP+, $p<0.001$) compared to controls (Figure 3-2I), while liver cell size, as determined by forward and side scatter, was not affected. These results demonstrate that estrogen signaling negatively impacts embryonic liver development by reducing the number of hepatocytes.

Estrogen exerts its effect on liver development via Esr2

To determine whether estrogen exerts its negative effect on hepatogenesis via its nuclear receptors, we treated *lfabp:GFP* embryos with fulvestrant, an estrogen receptor (ESR) antagonist from 18-72 hpf. Compared to control siblings, fulvestrant treated

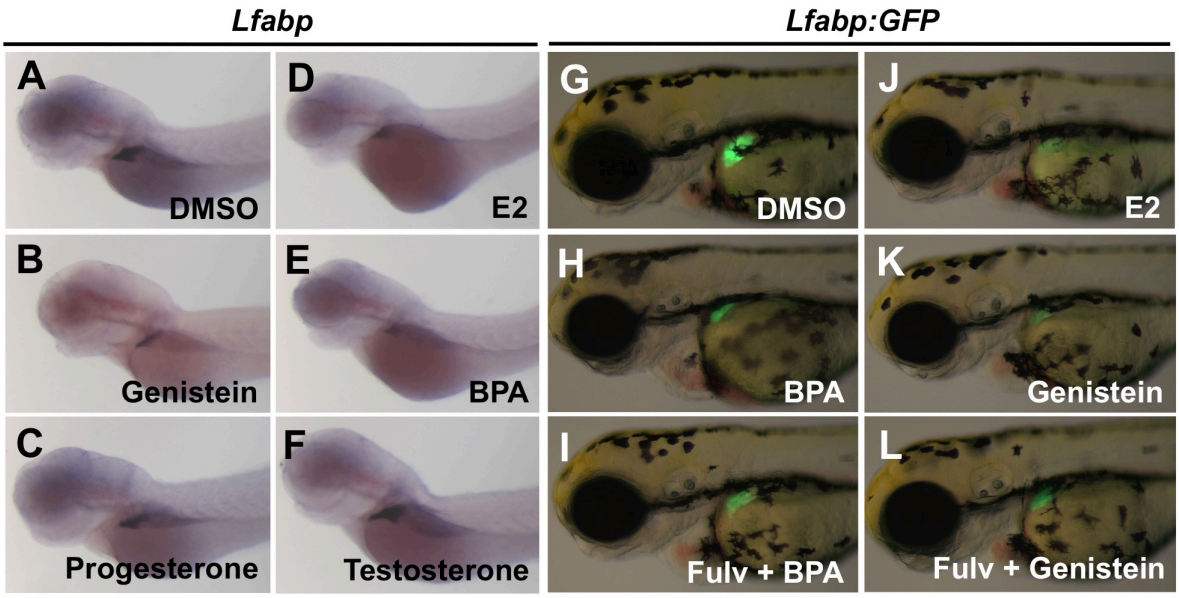

Figure 3-4. Non-physiological estrogens exert their effect on liver development via ESRs.

(A-F) Embryos exposed to the phytoestrogen genistein (B) and the xenoestrogen bisphenol A (BPA) (E) from 18-72 hpf develop smaller livers compared to control siblings (A). Androgen exposure does not impact liver development as demonstrated by normal *lfabp* expression in progesterone (C) and testosterone-treated (F) embryos.

(G-L) Liver development is rescued in *lfabp:GFP* embryos co-treated with estrogenic compounds E2, BPA, or genistein and the ESR antagonist fulvestrant (Fulv).

embryos displayed a marked increase in liver size (35↑/47). Furthermore, co-treating embryos exposed to E2, BPA, or genistein with fulvestrant rescues the small liver phenotype (Figure 3-4, G-L; Figure 3-5, A-C), suggesting that all estrogenic compounds examined exert their effects on liver development via ESRs.

The zebrafish expresses three ESRs: *esr1*, an ortholog of mammalian *ERα*, and *esr2a* and *esr2b*, duplicated orthologs of mammalian *ERβ*. *In situ* hybridization for the three cytoplasmic zebrafish ESRs reveals that Esr2a is expressed in the area of the liver primoridum at 72 hpf (Figure 3-6), suggesting that the Esr2 isoform is responsible for mediating estrogen's effect on liver development. All three zebrafish ESRs are expressed prior to the midblastula transition indicating that they are originally maternally deposited, and they continue to be expressed to varying degrees throughout embryonic development (Bardet et al., 2002; Tingaud-Sequeira et al., 2004). To further elucidate which receptors impact liver size, we exposed embryos to specific ESR agonists and antagonists from 18-72 hpf and scored *lfabp* expression at 72 hpf. Embryos treated with the Esr2 agonist DPN develop smaller livers (100↓/113), while the Esr1 agonist PPT has no effect (91/101 normal). Conversely, embryos exposed to the Esr2 antagonist PHTPP develop bigger livers (30↑/33), whereas the Esr1 antagonist MPP has a lesser effect (35/46 normal) (Figure 3-5, D-I).

To confirm our chemical exposure results genetically, we knocked down ESRs individually and in combination using antisense morpholino (MO) technology and assessed liver development at 72 hpf. Knockdown of *esr2a* (15↑/105) or *esr2b* (30↑/100) results in bigger livers while loss of *esr1* has no effect (5↓/70) compared to controls (Figure 3-5, J-M). Double receptor knockdown of *esr2a+2b* resulted in a greater proportion of embryos with enlarged livers (45↑/100) than any individual receptor knockdown alone (Figure 3-5N), further indicating that the Esr2 subtype governs estrogen's effect on liver development. In addition, whereas E2 exposure alone

Figure 3-5 (next page). Estrogen exerts its effect on liver development via Esr2 receptors.

(A-C) *Lfabp:GFP* embryos exposed to E2 (B) develop smaller livers compared to controls (A), whereas liver size is rescued in embryos co-treated with E2 and the ESR antagonist fulvestrant (E2+Fulv) (C).

(D-I) Embryos exposed to the Esr1 agonist PPT (E) and Esr1 antagonist MPP (H) from 18-72 hpf develop normal livers at 72 hpf compared to DMSO-treated controls (D) as determined by *lfabp in situ*. In contrast, embryos exposed to the Esr2 agonist DPN (F) develop small livers, and embryos exposed to the Esr2 antagonist PHTPP (I) develop larger livers compared to controls.

(J-M) Morpholino (MO) knockdowns of *esr2a* and *esr2b* result in bigger livers at 72 hpf (L, M), while loss of *esr1* has little effect on liver size (K) compared to controls (J).

(N) Quantification of individual and double ESR knockdowns. Knockdown of *esr2a* and *esr2b* in combination results in a greater percentage of embryos with larger livers than that of each ESR knockdown alone. Liver size is partially rescued in *esr2a* and *esr2b* morphant embryos challenged with E2 from 18-72 hpf.

Figure 3-5 (continued)

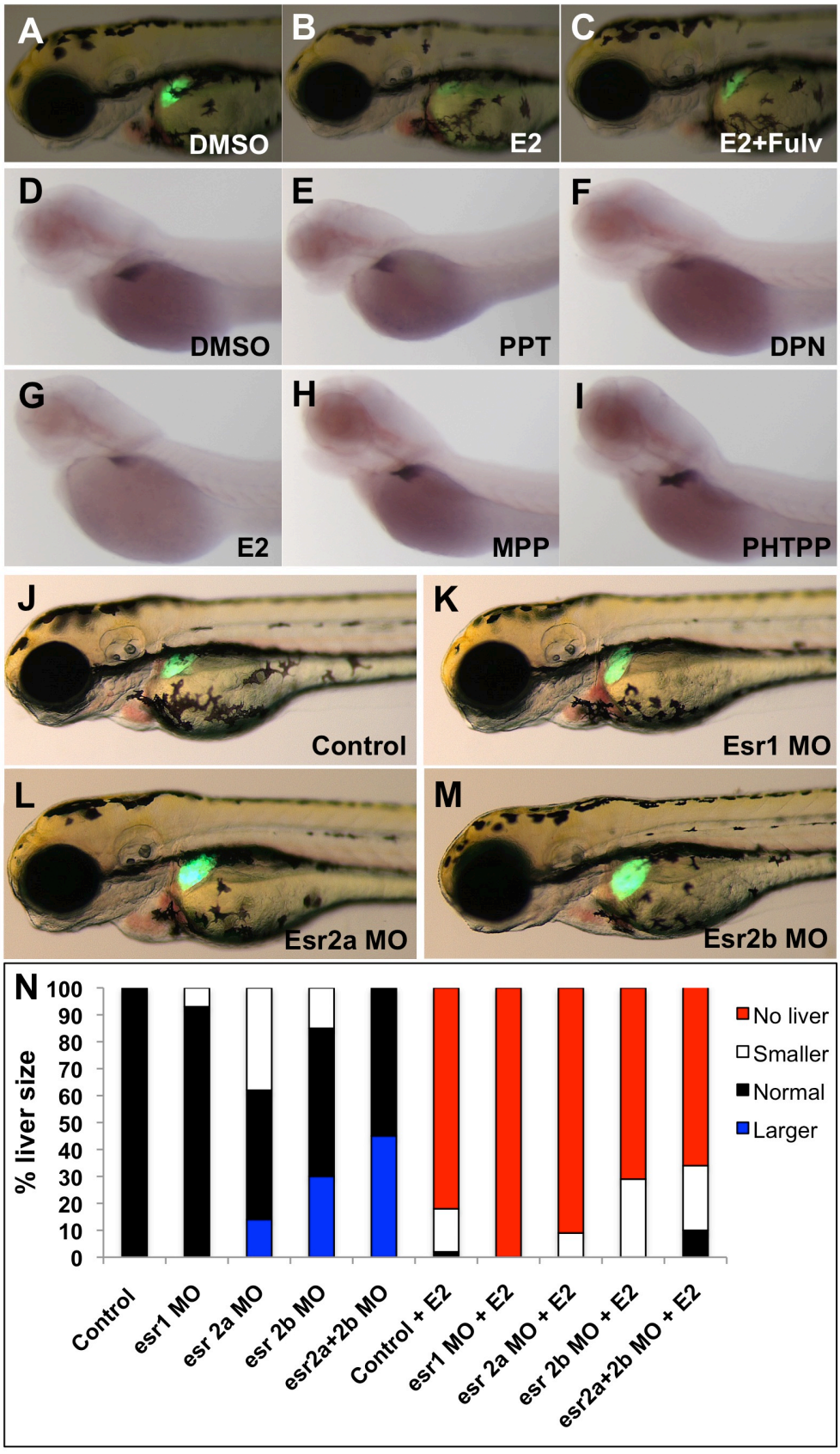

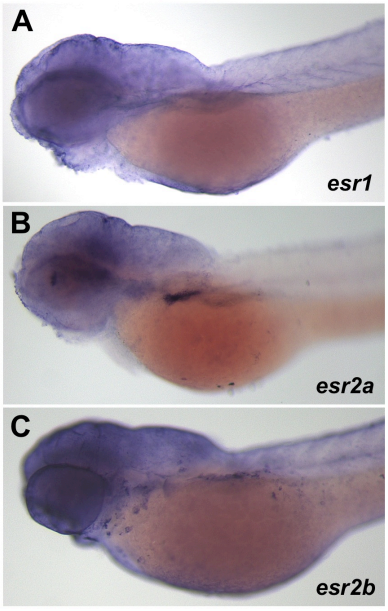

Figure 3-6. Esr2a is expressed in the liver primordium.

(A-C) Expression patterns of *esr1*, *esr2a*, and *esr2b* at 72 hpf by *in situ* hybridization.

results in small or absent livers, a proportion of E2-treated embryos injected with *esr2* MOs are protected against E2's negative effects (Figure 3-5N). These results indicate that exogenous estrogens negatively impact liver development, and their effect is mediated via Esr2 isoforms. Moreover, the fact that loss of *esr2a* and *esr2b* results in larger livers in the absence of exogenous estrogen suggests that endogenous estrogen is normally required to limit liver growth or maturation in the embryo, and this regulation is similarly achieved through the Esr2 receptor subtype.

E2 exposure prevents hepatoblasts from differentiating into hepatocytes

To determine whether the small or absent liver phenotype of E2-exposed embryos results from hepatoblast depletion or impaired differentiation into hepatocytes, we treated *lfabp:GFP* embryos with E2 from 18-72 hpf, removed E2 at 72 hpf, then followed liver development in individual embryos from 72-120 hpf using live fluorescence microscopy (10 embryos/treatment) (Figure 3-7, A-F). At 72 hpf, 100% of E2-exposed embryos display small or absent livers. At 96 hpf, 60% of embryos' livers show enhanced fluorescence indicative of recovery, and by 120 hpf, 80% of the embryos have livers that have recovered to normal size. These data suggest that estrogen exposure does not deplete the hepatic progenitor population but rather prevents hepatoblasts from differentiating into mature hepatocytes. To directly demonstrate that estrogen exerts different effects on hepatoblast and hepatocyte populations, we treated embryos with DMSO or E2 from 18-72 hpf and assessed expression of hepatoblast (*prox1*) and hepatocyte (*lfabp*) markers at 72 hpf by *in situ* hybridization. E2 exposure does not impact hepatic progenitors but results in a loss of mature hepatocytes (Figure 3-7, H-K). We also performed chemical treatments during shorter, earlier time windows (18-24 and 24-48 hpf) and examined *prox1* expression at each exposure's end point (24 and 48 hpf, respectively) and *lfabp* at 72 hpf since it is not expressed earlier. In all cases, *prox1*

Figure 3-7 (next page). Estrogen inhibits hepatoblast differentiation into hepatocytes.

(A-F) Livers of *lfabp:GFP* embryos exposed to E2 from 18-72 hpf (D-F) recover to control liver size (A-C) by 120 hpf after E2 removal at 72 hpf.

(G) Endogenous E2 levels (pg/ml) as quantified by enzyme immunoassay. E2 concentration declines between 30 and 72 hpf, concurrent with hepatocyte differentiation.

(H-K) *In situ* hybridization for the hepatoblast marker *prox1* (H, J) and the hepatocyte marker *lfabp* (I, K) at 72 hpf. *Lfabp* expression is lost in embryos treated with E2 from 18-72 hpf (K), however *prox1* expression remains unchanged (J) compared to DMSO-treated controls (H, I).

(L) Embryos treated with E2 during 18-24, 24-48, or 18-72 hpf exposure windows develop small or absent livers as determined by *lfabp* at 72 hpf, whereas the *prox1*+ hepatoblast population remains largely unaffected by E2 treatments. Embryos assayed for *lfabp* expression were stopped at 72 hpf, whereas embryos assayed for *prox1* expression were stopped at the end of each exposure window.

Figure 3-7 (continued)

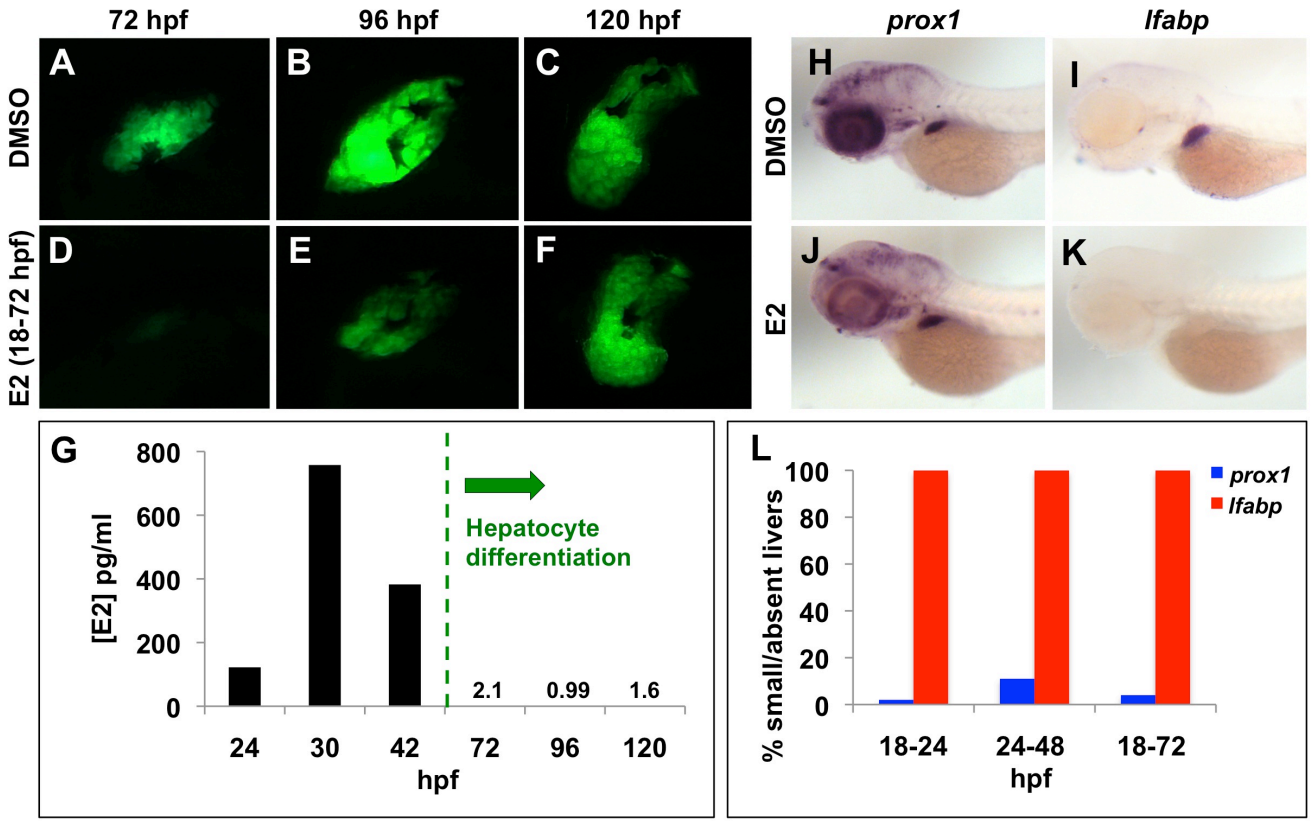

expression was unaffected by E2 exposure, whereas *lfabp* expression was diminished or absent (Figure 3-7L). These data further indicate that estrogen does not impact the nascent hepatoblast population but inhibits their differentiation into hepatocytes.

Given estrogen's ability to inhibit hepatocyte differentiation, we quantified endogenous levels of E2 over the course of embryonic liver development to establish whether changes in E2 levels correlate with hepatic differentiation. Using an enzyme immunoassay, we determined that endogenous E2 levels rise between 24 and 30 hpf (Figure 3-7G), likely due to the onset of embryonic estrogen synthesis following depletion of maternal deposits, as expression of the zebrafish aromatase gene *cyp19a1b* increases between 24-48 hpf (Mouriec et al., 2009). Levels of endogenous estrogen then decline precipitously until E2 is no longer detectable at 72 hpf. The decline of endogenous estrogen occurs concomitantly with the timing of hepatocyte maturation and proliferation, suggesting that endogenous estrogen may act to prevent hepatoblasts from differentiating into hepatocytes too early or before liver function is required. Expression of the estrogen-degrading enzyme *cyp1a* increases after 72 hpf (Jones et al., 2010), indicating one mechanism by which E2 levels are downregulated. In addition, *aromatase*/*cyp19a1b* contains an ERE in its promoter (Tong and Chung, 2003) and is upregulated in the presence of excess estrogen (Cheshenko et al., 2007), suggesting reduced endogenous estrogen levels also moderate this autoregulatory feedback loop.

E2 exposure affects hepatic differentiation in mammals

To determine whether estrogen's effect on hepatic differentiation in zebrafish is conserved in mammals, we examined embryonic liver development in *5α-reductase* mutant mice (*Srd5a1-/-*) (Mahendroo et al., 1997). During androgen and estrogen biosynthesis, testosterone is converted irreversibly into either dihydrotestosterone by 5α-

reductase or estradiol by aromatase. Loss of 5α-reductase results in a metabolic imbalance in which excess estradiol is produced. We compared fetal livers of mutant and wild type siblings at E14.5 since hepatoblasts normally begin to differentiate into mature hepatocyte and biliary lineages by E13.0 (Crawford et al., 2010). We found that mutant livers are less organized than wild type controls as determined by H&E stain (Figure 3-8, A-B), suggestive of a less differentiated, immature liver. We also performed immunohistochemistry to determine whether expression of hepatic markers alpha-fetoprotein (AFP), hepatic nuclear factor 4α (HNF4α), and albumin (Alb) was altered in *Srd5a1-/-* embryos. The murine liver is specified by E9.0, at which time hepatoblasts begin to express AFP and HNF4α (Crawford et al., 2010). Whereas AFP expression diminishes from E9.0 onwards (Hata et al., 2007), Alb, the predominant marker of mature hepatocytes, begins around E12.0 and increases into adulthood (Tilghman and Belayew, 1982). We noted marked increases in HNF4α and AFP expression in mutant livers at E14.5 (Figure 3-8, C-F), but there was no difference in Alb expression at this timepoint (data not shown). These results further underscore that *Srd5a1* mutant livers are less differentiated than their wild type siblings' given the greater and persistent expression hepatic progenitor markers.

In addition to elucidating the effect of excess estrogen on mouse hepatic development, we examined epigenetic modifications on human *ERα* and *ERβ* coding sequences in human cells. We specifically investigated epigenetic changes at these loci in pluripotent embryonic stem cells (ESCs), differentiated endodermal cells, and mature hepatocytes to determine whether modifications accompany cell differentiation. The pattern of H3K4 methylation (H3K4me1), an activating histone mark, remained relatively unchanged at the *ERα* locus across all cell types (Figure 3-9A). In contrast, H3K4me1 is significantly diminished at the *ERβ* locus in hepatocytes compared to undifferentiated

Figure 3-8 (next page). *Srd5a1* mutant mouse livers are less differentiated than wild type sibling controls.

(A, B) H&E staining of sectioned mouse livers at E14.5. *Srd5a1 -/-* livers (B) are less organized and compact and contain more hepatoblasts than wild type sibling livers (A). (A',B') Magnifications of the boxed areas in (A, B). Boxed area in B' highlights an immature hepatoblast.

(C-F) Immunohistochemistry for hepatic markers HNF4α (C, D) and alpha-fetoprotein (AFP) (E, F) demonstrates that *Srd5a1* -/- mice retain more hepatoblasts than wild type livers at E14.5.

Figure 3-8 (continued)

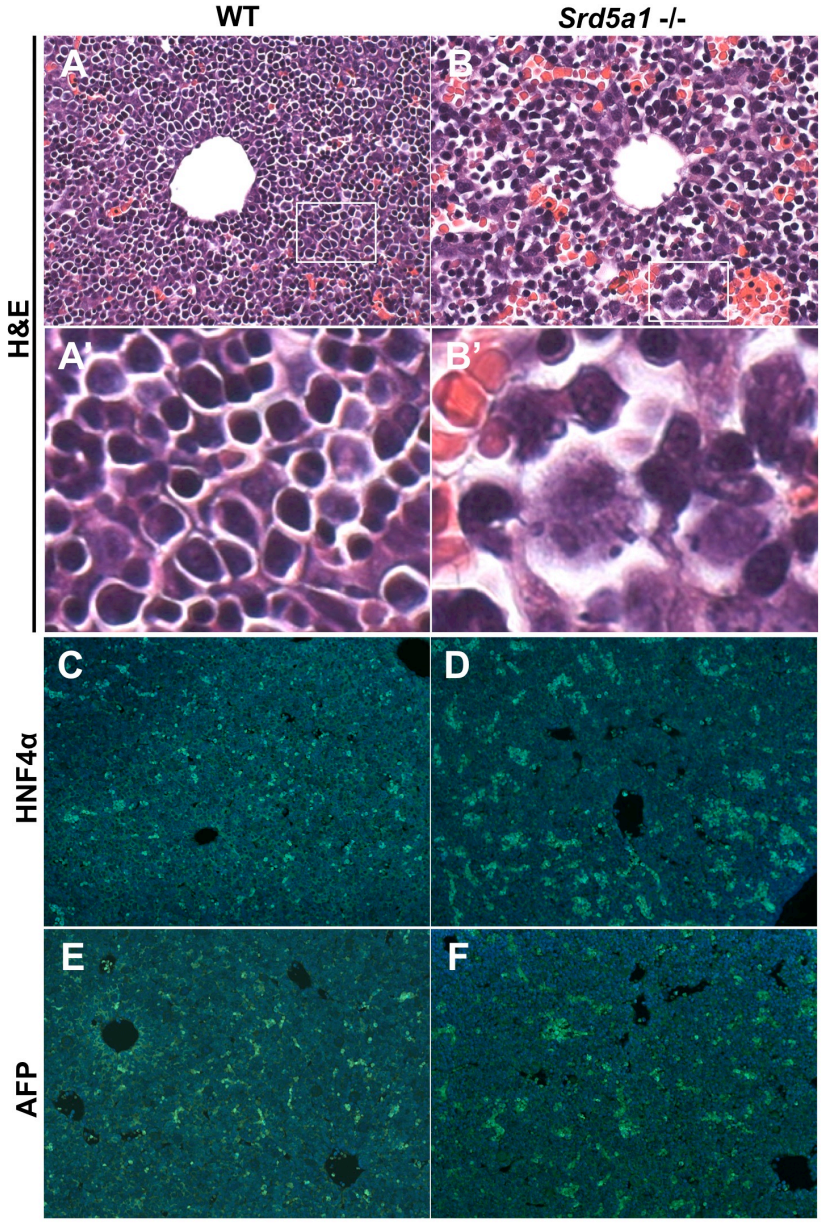

Figure 3-9 (next page). Estrogen receptors are downregulated during hepatic differentiation.

(A) Histone methylation changes at the human estrogen receptor *ER*α and *ER*β loci during embryonic stem cell differentiation. The activating methylation mark H3K4me1 is lost at the *ER*β locus in mature hepatocytes.

(B) RNA expression values of estrogen signaling pathway components and hepatic markers in ESCs (teal), endoderm (purple), hepatoblasts (yellow), and hepatocytes (green). Expression values were measured as fragments per kilobase of exon per million fragments mapped (FPKM).

(C) Changes in expression of zebrafish *esr1, esr2a,* and *esr2b* in *foxA3*+ endodermal cells at 2 and 4 dpf.

Figure 3-9 (continued)

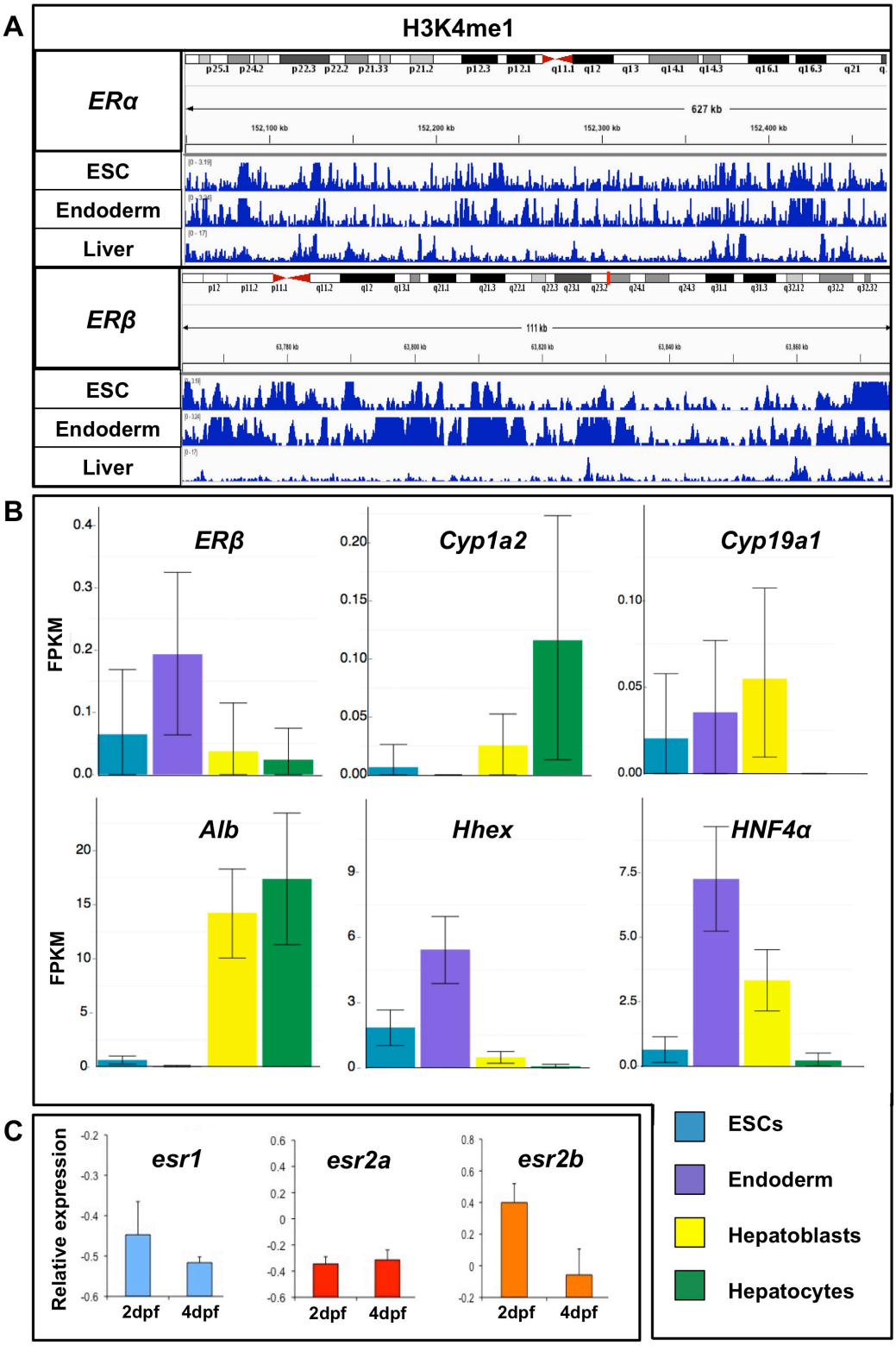

ESCs or endodermal cells (Figure 3-9A), and this epigenetic change correlates with decreased expression of *ERβ* (Figure 3-9B). RNA-seq transcriptome analyses of all cell types also revealed that the E2-degrading enzyme *Cyp1a2* is augmented and the E2-synthesizing enzyme *Cyp19a1/aromatase* is reduced in hepatocytes compared to expression levels in less differentiated precursors (Figure 3-9B), further demonstrating that estrogen signaling is downregulated in differentiating liver cells. Expression of known hepatic markers *Albumin* (*Alb*), *Hhex*, and *HNF4*α confirmed cell type identity (Figure 3-9B) and corroborate our mouse data indicating that *Srd5a1-/-* mutant livers improperly overexpress hepatoblast markers (Figure 3-8, C-F). The fact that *ERβ* expression is downregulated in hepatic cells substantiates our hypotheses that estrogen signaling functions via Esr2/ERβ and normally functions as a negative regulator of hepatoblasts' differentiation into hepatocytes.

To determine whether zebrafish not only downregulate the estrogen ligand but also ESR expression during hepatic differentiation, we analyzed publicly available microarray profiles of FACS-sorted endodermal (*foxA3*+) cells (Stuckenholz et al., 2009) between 2 and 4 dpf. We found that there is a general trend of decreased ESR expression between these stages, which coincides with the timing of hepatic differentiation. In particular, both *esr1* and *esr2b* expression is reduced between 2 and 4 dpf in zebrafish, while *esr2a* expression remains relatively unchanged (Figure 3-9C). These data demonstrate that ESR expression is modulated in endodermal tissues during liver development and align with our findings that estrogen signaling is downregulated concomitant with hepatocyte differentiation. Given that the Esr2 subtype regulates embryonic hepatogenesis, reduced expression of *esr2b* after 2 dpf may act to further mitigate estrogen's inhibition of hepatic differentiation. Although we do not find that Esr1 contributes significantly to liver development, its reduced expression may be indicative of declining levels of endogenous E2, as an ERE has been identified in the promoter region

of Esr1 in zebrafish (Menuet et al., 2004). Collectively, our data identify a regulatory role for the Esr2/ERβ subtype in embryonic liver differentiation across species.

DISCUSSION

In this report, we identified estrogen signaling as a negative regulator of embryonic liver development and demonstrated that estradiol (E2) exerts its effects via the estrogen receptor 2 (Esr2) subtype. Removal of E2 following embryonic exposure results in the delayed appearance of hepatocytes, however embryos ultimately form a normal-sized liver. Exposure to E2 does not impact the *prox1*+ hepatoblast population, indicating that hepatic progenitors remain in the presence of estrogen and retain their ability to differentiate into mature hepatocytes. Assessment of endogenous E2 levels revealed that downregulation of E2 by 72 hpf occurs concomitantly with hepatic differentiation. Mammalian studies corroborate our zebrafish findings: in mice, excess estrogen results in an undifferentiated liver phenotype, and in human cells, differentiated hepatocytes show reduced *ERβ* expression relative to undifferentiated ESCs, endodermal cells, and hepatoblasts.

The zebrafish expresses three ESRs – Esr1, orthologous to mammalian ERα, and Esr2a and Esr2b, which resulted from a zebrafish genome duplication event and are each equally related to mammalian ERβ (Bardet et al., 2002). It is clear that mammalian ERs exert distinct biological functions as differences in receptor expression patterns and knockout phenotypes are well documented in mice (Harris, 2007; Zhao et al., 2008). In humans, ERα binds E2 with four times greater affinity than ERβ, and it is considered the primary mediator of estrogen's effects on classical target tissues such as the reproductive organs, mammary glands, skeleton, and hypothalamus (Harris, 2007; Hawkins and Thomas, 2004). Interestingly, in a number of fish species including *Danio*

rerio, Esr2 binds E2 with higher affinity than Esr1 (Menuet et al., 2002; Xia et al., 2000), suggesting that Esr2 receptor may be the primary mediator of estrogen signaling in teleosts.

Using an enzyme immunoassay to quantify endogenous E2 concentrations in zebrafish, we uncovered a significant drop in estrogen levels after 30 hpf, corresponding to the onset of hepatocyte differentiation. In human cells, we determined that there are fewer activating H3K4 methylation marks at the ERβ locus in hepatic cells, similarly demonstrating that reduced estrogen signaling is required for hepatocyte differentiation. A recent study demonstrated that zebrafish embryos exposed to E2 at 3 and 4 dpf show reduced expression of *lfabp* (*fabp10a*) compared to earlier timepoints (Hao et al., 2013), validating our results that demonstrate that estrogen has a negative effect on differentiating hepatocytes. Together, our results suggest that zebrafish and mammals accomplish hepatic differentiation via similar mechanisms – both downregulate ESR/ER expression, and zebrafish additionally downregulate the estradiol ligand. ESR expression has been shown to increase in response to E2 exposure (Chandrasekar et al., 2010), suggesting that the estrogen ligand mediates receptor expression in an autoregulatory feedback loop. Expression of *cyp1a*, an E2-degrading enzyme, has been shown to markedly increase between 72 and 96 hpf (Jones et al., 2010), suggesting that this may be one of the primary temporal mechanisms by which E2 levels are abated. By decreasing global levels of E2, the embryo may thereby also downregulate receptor expression to ensure proper signaling levels during development. An estrogen response element (ERE) has been identified in the promoter region of ERα in rainbow trout (Le Drean et al., 1995) and an imperfect ERE site found in Esr1 in zebrafish (Menuet et al., 2004). Mammalian embryos develop *in utero* and are therefore continuously exposed to factors in their mother's circulation, so downregulating ERs rather than the estrogen ligand may be the most effective mechanism to control

embryonic estrogen signaling activity. Conversely, teleosts are externally fertilized and, excepting initial deposition of maternal factors in the yolk, must regulate their development independently; this may explain why zebrafish employ redundant mechanisms to regulate estrogen signaling.

Exogenous estrogen treatment inhibits hepatocyte differentiation, and hepatocyte differentiation naturally corresponds with diminishing levels of endogenous E2 in the embryo. It is conceivable that the embryo normally uses estrogen signaling as a means to prevent liver differentiation from occurring too early, as this could have deleterious effects on development. For example, premature differentiation may reduce the number of specified hepatic progenitors and consequently the pool of mature hepatic cell types. In addition, creating an organ before its function is required would result in unnecessary energy expenditure that may prove detrimental to a newly formed embryo's continued growth and survival.

Given ESRs' roles as transcriptional activators, it is possible that estrogen activates downstream factors responsible for establishing or maintaining the hepatoblast population. In ESC-derived endoderm, continuous expression of *Hex* leads to decreased levels of the hepatocyte marker *Albumin*, suggesting that prolonged *Hex* expression inhibits hepatic differentiation (Kubo et al., 2010). Uncovering the downstream targets of estrogen signaling in liver development will not only be crucial to understanding how estrogen exerts its inhibitory effects on hepatogenesis but may aid our understanding of hepatoblastoma, a malignant liver cancer that contains proliferating hepatic progenitors. Overexpression of a number of growth factors including IGF and c-MET is correlated with less differentiated tumors (Kim et al., 2005; Akmal et al., 1995; von Schweinitz et al., 2002), so it would be informative to assess estrogen regulation in this setting.

Our finding that human ERβ undergoes epigenetic modification during hepatic differentiation suggests that chromatin remodeling is an important aspect of embryonic organogenesis and furthermore, that aberrant methylation may contribute to developmental defects and adult disease. The promoter regions of mammalian ERs have been shown to be subject to extensive epigenetic regulation, and changes in methylation at the ERβ locus have been linked with cancer onset and progression in the breast and kidney (Dulaimi et al., 2004; Mirza et al., 2012; Zhao et al., 2008).

In addition to elucidating the role for endogenous estrogens during embryonic hepatogenesis, we also demonstrated the negative impact of exogenous estrogen exposure on the developing liver. Embryos treated with xeno- or phytoestrogens from 18-72 hpf display decreased liver size, and this effect is rescued by co-treatment with fulvestrant, indicating that these estrogenic compounds also exert their effects via ESRs. Steroid hormone receptors have been identified in ancestral non-vertebrate taxonomies and are believed to have originated as environmental toxin sensors (Keay and Thornton, 2009; Paris et al., 2008; Thornton et al., 2003), so it is not surprising that non-physiological estrogens can act agonistically at ESRs. In recent years, estrogenic compounds have appeared in increasing concentrations in our environment (ethinyl estradiol in oral contraceptives, dichlorodiphenyltricloroethane/DDT in insecticides, nonylphenol in oil dispersants), plastic products (bisphenol A/BPA), and diet (genistein and daidzein in soy), and it is therefore imperative that we continue to explore the effects of exogenous estrogen exposure on organ development. Future investigations into estrogen's role during normal embryonic hepatogenesis will further uncover its developmental importance and improve our understanding of liver growth and differentiation in disease states.

METHODS

Zebrafish husbandry

Zebrafish were maintained according to IACUC protocols. *LF2.8-EGFP* (referred to as *lfabp:GFP*) (Her et al., 2003)*, lfabp:dsRed* (Korzh et al., 2008), and *5xERE:GFP* (*ERE:GFP*) (Gorelick and Halpern, 2011) transgenic lines have been described previously.

Chemical exposures

Zebrafish embryos were exposed to 1 μM E2, 10 μM fulvestrant, 1 μM anastrozole, 20 μM DPN, 20 μM PHTPP, 20 μM PPT, 20 μM MPP, 5 μM BPA, and 5 μM genistein during specified time windows. Stock solutions were diluted in embryo water. Control embryos were concurrently exposed to 0.1% DMSO. After chemical exposure, embryos were washed 3-5x in embryo water then fixed with 4% PFA at the appropriate stages. The chemical genetic screen was performed as described previously (Garnaas et al., 2012).

Whole mount *in situ* hybridization

Zebrafish embryos were fixed in 4% PFA at the specified stages, and *in situ* hybridization was performed according to established protocols (http://zfin.org/ZFIN/Methods/ThisseProtocol.html) using *lfabp*, *prox1*, *esr1, esr2a*, and *esr2b* probes.

Morpholino knockdown

Morpholinos (MOs; GeneTools) were designed against zebrafish *esr1* (5' AGGAAGGTTCCTCCAGGGCTTCTCT 3') (20 uM) (Pang and Thomas, 2010), *esr2a*

(5’ ACATGGTGAAGGCGGATGAGTTCAG 3’) (10 uM) (Froehlicher et al., 2009), and *esr2b* (5' AGCTCATGCTGGAGAACACAAGAGA 3') (10 uM) and injected at the 1 cell stage. When injected in combination, MO doses were halved to prevent morphological defects due to toxicity.

Flow cytometry analysis

Lfabp:GFP fluorescent embryos were exposed to chemicals as described above. Whole embryos were manually dissociated in 0.9x PBS, and %GFP+ cells were determined by flow cytometric analysis. ≥20,000 cells were analyzed per embryo, and ≥5 embryos were analyzed for each chemical treatment using FlowJo software.

Microscopy

Live fluorescence microscopy was performed on *lfabp:GFP* and *ERE:GFP; lfabp:dsRed* embryos anesthetized in 0.04 mg/ml Tricaine in embryo water using a Zeiss Discovery V8 microscope. After visual examination, embryos were washed several times and returned to embryo water for further observation and/or until fixation. Embryos used in *in situ* hybridization experiments were visualized in glycerol.

Estradiol immunoassay

A commercially available estradiol enzyme immunoassay (EIA) kit (Cayman Chemical) was used. Embryos were treated with DMSO or estradiol (E2) as above, and 30 embryos were pooled at each timepoint for assessment of endogenous estrogen levels.

5α-reductase type 1 (*Srd5a1*) mice

Female B6;129S7-*Srd5a1*^{tm1Mahe}/J mice (Jackson Laboratory) from timed heterozygous incross matings were sacrificed at E14.5, and embryonic livers were isolated by microdissection in 1x PBS and fixed in 4% PFA for histological analyses.

Immunohistochemistry

Mouse livers were isolated at E14.5, fixed in 4% PFA, embedded in paraffin and sectioned. Alternating sections were H&E stained or used for immunohistochemistry. Sections were incubated in 1:1000 HNF4α (Abcam) or 1:100 AFP (Thermo Scientific) rabbit anti-mouse primary antibody followed by 1:100 Cy3-conjugated donkey anti-rabbit IgG secondary antibody (Jackson ImmunoResearch) and counterstained with DAPI (Vector Laboratories).

ESC differentiation, ChIP-seq, and RNA-seq

Human ESCs were cultured according to published procedures (Bock et al., 2011; De La Forest et al., 2011), and ChIP-seq and RNA-seq libraries were prepared and analyzed according to established protocols (Gifford et al., 2013; personal communication, Alexander Meissner). Hepatocytes isolated from adults were used in ChIP-seq experiments, and hepatocytes differentiated from ESCs were analyzed in RNA-seq experiments.

REFERENCES

Bardet, P. L., Horard, B., Robinson-Rechavi, M., Laudet, V. and Vanacker, J. M. (2002). Characterization of oestrogen receptors in zebrafish (Danio rerio). J Mol Endocrinol 28, 153-63.

Bock, C., Kiskinis, E., Verstappen, G., Gu, H., Boulting, G., Smith, Z. D., Ziller, M., Croft, G. F., Amoroso, M. W., Oakley, D. H. et al. (2011). Reference Maps of human ES and iPS cell variation enable high-throughput characterization of pluripotent cell lines. Cell 144, 439-52.

Brownson, D. M., Azios, N. G., Fuqua, B. K., Dharmawardhane, S. F. and Mabry, T. J. (2002). Flavonoid effects relevant to cancer. J Nutr 132, 3482S-3489S.

Buch, S. C., Kondragunta, V., Branch, R. A. and Carr, B. I. (2008). Gender-based outcomes differences in unresectable hepatocellular carcinoma. Hepatol Int 2, 95-101.

Chandrasekar, G., Archer, A., Gustafsson, J. A. and Andersson Lendahl, M. (2010). Levels of 17beta-estradiol receptors expressed in embryonic and adult zebrafish following in vivo treatment of natural or synthetic ligands. PLoS One 5, e9678.

Cheshenko, K., Brion, F., Le Page, Y., Hinfray, N., Pakdel, F., Kah, O., Segner, H. and Eggen, R. I. (2007). Expression of zebra fish aromatase cyp19a and cyp19b genes in response to the ligands of estrogen receptor and aryl hydrocarbon receptor. Toxicol Sci 96, 255-67.

Colborn, T., vom Saal, F. S. and Soto, A. M. (1993). Developmental effects of endocrine-disrupting chemicals in wildlife and humans. Environ Health Perspect 101, 378-84.
Cornwell, T., Cohick, W. and Raskin, I. (2004). Dietary phytoestrogens and health. Phytochemistry 65, 995-1016.

Crawford, L. W., Foley, J. F. and Elmore, S. A. (2010). Histology atlas of the developing mouse hepatobiliary system with emphasis on embryonic days 9.5-18.5. Toxicol Pathol 38, 872-906.

De La Forest, A., Nagaoka, M., Si-Tayeb, K., Noto, F.K., Konopka, G., Battle, M.A., and Duncan, S.A. (2011). HNF4A is essential for specification of hepatic progenitors from human pluripotent stem cells. Development 138, 4143-53.

De Maria, N., Manno, M. and Villa, E. (2002). Sex hormones and liver cancer. Mol Cell Endocrinol 193, 59-63.

Dulaimi, E., Ibanez de Caceres, I., Uzzo, R. G., Al-Saleem, T., Greenberg, R. E., Polascik, T. J., Babb, J. S., Grizzle, W. E. and Cairns, P. (2004). Promoter hypermethylation profile of kidney cancer. Clin Cancer Res 10, 3972-9.

Fraenkel, P. G., Gibert, Y., Holzheimer, J. L., Lattanzi, V. J., Burnett, S. F., Dooley, K. A., Wingert, R. A. and Zon, L. I. (2009). Transferrin-a modulates hepcidin expression in zebrafish embryos. Blood 113, 2843-50.

Froehlicher, M., Liedtke, A., Groh, K., Lopez-Schier, H., Neuhauss, S. C., Segner, H. and Eggen, R. I. (2009). Estrogen receptor subtype beta2 is involved in neuromast development in zebrafish (Danio rerio) larvae. Dev Biol 330, 32-43.

Fucic, A., Gamulin, M., Ferencic, Z., Katic, J., Krayer von Krauss, M., Bartonova, A. and Merlo, D. F. (2012). Environmental exposure to xenoestrogens and oestrogen related cancers: reproductive system, breast, lung, kidney, pancreas, and brain. Environ Health 11 Suppl 1, S8.

Garnaas, M. K., Cutting, C. C., Meyers, A., Kelsey, P. B., Jr., Harris, J. M., North, T. E. and Goessling, W. (2012). Rargb regulates organ laterality in a zebrafish model of right atrial isomerism. Dev Biol 372, 178-89.

Giannitrapani, L., Soresi, M., La Spada, E., Cervello, M., D'Alessandro, N. and Montalto, G. (2006). Sex hormones and risk of liver tumor. Ann N Y Acad Sci 1089, 228-36.

Gifford, C. A., Ziller, M. J., Gu, H., Trapnell, C., Donaghey, J., Tsankov, A., Shalek, A. K., Kelley, D. R., Shishkin, A. A., Issner, R. et al. (2013). Transcriptional and epigenetic dynamics during specification of human embryonic stem cells. Cell 153, 1149-63.

Gorelick, D. A. and Halpern, M. E. (2011). Visualization of estrogen receptor transcriptional activation in zebrafish. Endocrinology 152, 2690-703.

Hao, R., Bondesson, M., Singh, A. V., Riu, A., McCollum, C. W., Knudsen, T. B., Gorelick, D. A. and Gustafsson, J. A. (2013). Identification of Estrogen Target Genes during Zebrafish Embryonic Development through Transcriptomic Analysis. PLoS One 8, e79020.

Harris, H. A. (2007). Estrogen receptor-beta: recent lessons from in vivo studies. Mol Endocrinol 21, 1-13.

Harris, R. M. and Waring, R. H. (2012). Diethylstilboestrol--a long-term legacy. Maturitas 72, 108-12.

Hata, S., Namae, M. and Nishina, H. (2007). Liver development and regeneration: from laboratory study to clinical therapy. Dev Growth Differ 49, 163-70.

Hawkins, M. B. and Thomas, P. (2004). The unusual binding properties of the third distinct teleost estrogen receptor subtype ERbetaa are accompanied by highly conserved amino acid changes in the ligand binding domain. Endocrinology 145, 2968-77.

Her, G. M., Yeh, Y. H. and Wu, J. L. (2003). 435-bp liver regulatory sequence in the liver fatty acid binding protein (L-FABP) gene is sufficient to modulate liver regional expression in transgenic zebrafish. Dev Dyn 227, 347-56.

Jeng, Y. J., Kochukov, M. Y. and Watson, C. S. (2009). Membrane estrogen receptor-alpha-mediated nongenomic actions of phytoestrogens in GH3/B6/F10 pituitary tumor cells. J Mol Signal 4, 2.

Jeng, Y. J. and Watson, C. S. (2009). Proliferative and anti-proliferative effects of dietary levels of phytoestrogens in rat pituitary GH3/B6/F10 cells - the involvement of rapidly activated kinases and caspases. BMC Cancer 9, 334.

Jones, H. S., Panter, G. H., Hutchinson, T. H. and Chipman, J. K. (2010). Oxidative and conjugative xenobiotic metabolism in zebrafish larvae in vivo. Zebrafish 7, 23-30.
Kalra, M., Mayes, J., Assefa, S., Kaul, A. K. and Kaul, R. (2008). Role of sex steroid receptors in pathobiology of hepatocellular carcinoma. World J Gastroenterol 14, 5945-61.

Keay, J. and Thornton, J. W. (2009). Hormone-activated estrogen receptors in annelid invertebrates: implications for evolution and endocrine disruption. Endocrinology 150, 1731-8.

Korzh, S., Pan, X., Garcia-Lecea, M., Winata, C. L., Wohland, T., Korzh, V. and Gong, Z. (2008). Requirement of vasculogenesis and blood circulation in late stages of liver growth in zebrafish. BMC Dev Biol 8, 84.

Kubo, A., Kim, Y. H., Irion, S., Kasuda, S., Takeuchi, M., Ohashi, K., Iwano, M., Dohi, Y., Saito, Y., Snodgrass, R. et al. (2010). The homeobox gene Hex regulates hepatocyte differentiation from embryonic stem cell-derived endoderm. Hepatology 51, 633-41.

Laronda, M. M., Unno, K., Butler, L. M. and Kurita, T. (2012). The development of cervical and vaginal adenosis as a result of diethylstilbestrol exposure in utero. Differentiation 84, 252-60.

Le Drean, Y., Lazennec, G., Kern, L., Saligaut, D., Pakdel, F. and Valotaire, Y. (1995). Characterization of an estrogen-responsive element implicated in regulation of the rainbow trout estrogen receptor gene. J Mol Endocrinol 15, 37-47.

Li, Z., Tuteja, G., Schug, J. and Kaestner, K. H. (2012). Foxa1 and Foxa2 are essential for sexual dimorphism in liver cancer. Cell 148, 72-83.

Mahendroo, M. S., Cala, K. M., Landrum, D. P. and Russell, D. W. (1997). Fetal death in mice lacking 5alpha-reductase type 1 caused by estrogen excess. Mol Endocrinol 11, 917-27.

McLachlan, J. A. (2001). Environmental signaling: what embryos and evolution teach us about endocrine disrupting chemicals. Endocr Rev 22, 319-41.

Menuet, A., Le Page, Y., Torres, O., Kern, L., Kah, O. and Pakdel, F. (2004). Analysis of the estrogen regulation of the zebrafish estrogen receptor (ER) reveals distinct effects of ERalpha, ERbeta1 and ERbeta2. J Mol Endocrinol 32, 975-86.

Menuet, A., Pellegrini, E., Anglade, I., Blaise, O., Laudet, V., Kah, O. and Pakdel, F. (2002). Molecular characterization of three estrogen receptor forms in zebrafish: binding characteristics, transactivation properties, and tissue distributions. Biol Reprod 66, 1881-92.

Mirza, S., Sharma, G., Parshad, R., Srivastava, A., Gupta, S. D. and Ralhan, R. (2012). Clinical significance of promoter hypermethylation of ERbeta and RARbeta2 in tumor and serum DNA in Indian breast cancer patients. Ann Surg Oncol 19, 3107-15.

Mouriec, K., Lareyre, J. J., Tong, S. K., Le Page, Y., Vaillant, C., Pellegrini, E., Pakdel, F., Chung, B. C., Kah, O. and Anglade, I. (2009). Early regulation of brain aromatase (cyp19a1b) by estrogen receptors during zebrafish development. Dev Dyn 238, 2641-51.

Nelson, E. R. and Habibi, H. R. (2013). Estrogen receptor function and regulation in fish and other vertebrates. Gen Comp Endocrinol 192, 15-24.

Pang, Y. and Thomas, P. (2010). Role of G protein-coupled estrogen receptor 1, GPER, in inhibition of oocyte maturation by endogenous estrogens in zebrafish. Dev Biol 342, 194-206.

Paris, M., Pettersson, K., Schubert, M., Bertrand, S., Pongratz, I., Escriva, H. and Laudet, V. (2008). An amphioxus orthologue of the estrogen receptor that does not bind estradiol: insights into estrogen receptor evolution. BMC Evol Biol 8, 219.

Parkin, D. M., Bray, F., Ferlay, J. and Pisani, P. (2005). Global cancer statistics, 2002. CA Cancer J Clin 55, 74-108.

Soto, A. M., Chung, K. L. and Sonnenschein, C. (1994). The pesticides endosulfan, toxaphene, and dieldrin have estrogenic effects on human estrogen-sensitive cells. Environ Health Perspect 102, 380-3.

Stuckenholz, C., Lu, L., Thakur, P., Kaminski, N. and Bahary, N. (2009). FACS-assisted microarray profiling implicates novel genes and pathways in zebrafish gastrointestinal tract development. Gastroenterology 137, 1321-32.

Thomas, P. (2012). Rapid steroid hormone actions initiated at the cell surface and the receptors that mediate them with an emphasis on recent progress in fish models. Gen Comp Endocrinol 175, 367-83.

Thornton, J. W., Need, E. and Crews, D. (2003). Resurrecting the ancestral steroid receptor: ancient origin of estrogen signaling. Science 301, 1714-7.

Tilghman, S. M. and Belayew, A. (1982). Transcriptional control of the murine albumin/alpha-fetoprotein locus during development. Proc Natl Acad Sci U S A 79, 5254-7.

Tingaud-Sequeira, A., Andre, M., Forgue, J., Barthe, C. and Babin, P. J. (2004). Expression patterns of three estrogen receptor genes during zebrafish (Danio rerio) development: evidence for high expression in neuromasts. Gene Expr Patterns 4, 561-8.

Tong, S. K. and Chung, B. C. (2003). Analysis of zebrafish cyp19 promoters. J Steroid Biochem Mol Biol 86, 381-6.

Vandenberg, L. N., Hauser, R., Marcus, M., Olea, N. and Welshons, W. V. (2007). Human exposure to bisphenol A (BPA). Reprod Toxicol 24, 139-77.

Vinas, R. and Watson, C. S. (2010). Mixtures of xenoestrogens disrupt estradiol-induced non-genomic signaling and downstream functions in pituitary cells. Environ Health 12, 26.

Waring, R. H., Ayers, S., Gescher, A. J., Glatt, H. R., Meinl, W., Jarratt, P., Kirk, C. J., Pettitt, T., Rea, D. and Harris, R. M. (2008). Phytoestrogens and xenoestrogens: the contribution of diet and environment to endocrine disruption. J Steroid Biochem Mol Biol 108, 213-20.

Watson, C. S., Hu, G. and Paulucci-Holthauzen, A. A. (2013). Rapid actions of xenoestrogens disrupt normal estrogenic signaling. Steroids.

Whitten, P. L., Lewis, C., Russell, E. and Naftolin, F. (1995). Potential adverse effects of phytoestrogens. J Nutr 125, 771S-776S.

Wolstenholme, J. T., Rissman, E. F. and Connelly, J. J. (2011). The role of Bisphenol A in shaping the brain, epigenome and behavior. Horm Behav 59, 296-305.

Xia, Z., Gale, W. L., Chang, X., Langenau, D., Patino, R., Maule, A. G. and Densmore, L. D. (2000). Phylogenetic sequence analysis, recombinant expression, and tissue distribution of a channel catfish estrogen receptor beta. Gen Comp Endocrinol 118, 139-49.

Zaret, K. S. (2002). Regulatory phases of early liver development: paradigms of organogenesis. Nat Rev Genet 3, 499-512.

Zhao, C., Dahlman-Wright, K. and Gustafsson, J. A. (2008). Estrogen receptor beta: an overview and update. Nucl Recept Signal 6, e003.

CHAPTER 4

Ongoing and Future Work

ESTROGEN SIGNALING DURING LIVER DEVELOPMENT

Estrogen exhibits biphasic effects on liver development

In addition to demonstrating the impact of embryonic estradiol (E2) exposure on zebrafish liver development (see Chapter 3), we will also examine the effect of estrogen signaling on later larval development. We have preliminary data suggesting that estrogen signaling exerts a biphasic effect on hepatogenesis; that is, it inhibits embryonic liver development but enhances larval liver development. As we demonstrated previously, E2 treatment from 18-72 hpf leads to a marked decrease in liver size and hepatocyte number (Figure 3-2; Figure 4-1, A-C). Interestingly, E2 treatment from 120-144 hpf has a positive effect on liver growth at 144 hpf, where 83% of embryos (n=54) have bigger livers compared to DMSO-treated controls (Figure 4-1, D-F). FACS quantification of hepatocytes sorted from *lfabp:GFP* reporter larvae confirms that increased liver size is due to a greater number of hepatocytes (1.99±0.37% GFP+ control versus 2.8±0.49% E2-exposed embryos). Larval fulvestrant exposure results in embryos with smaller livers (Figure 4-1G), providing further evidence that later stage estrogen signaling enhances liver development.

To further investigate estrogen's effect on larval liver development, we will characterize which cell populations are impacted by E2 exposure from 120-144 hpf and identify the molecular mechanisms by which this occurs. Specifically, we will assess whether enhanced liver development in E2-treated larvae is accompanied by changes in the hepatic gene program (*hhex, prox1, lfabp*) by *in situ* hybridization (ISH) and qPCR analyses. We will evaluate cell viability and proliferation using TUNEL and BrdU assays, respectively, and determine whether cell cycle and proliferation markers (*cyclin D1*, *c-myc*) are altered in E2-exposed larvae. Similar to our study of estrogen's role in embryonic liver development, we will also elucidate the contribution of receptor subtypes to this phenotype by chemical and genetic modulation. Finally, we will identify

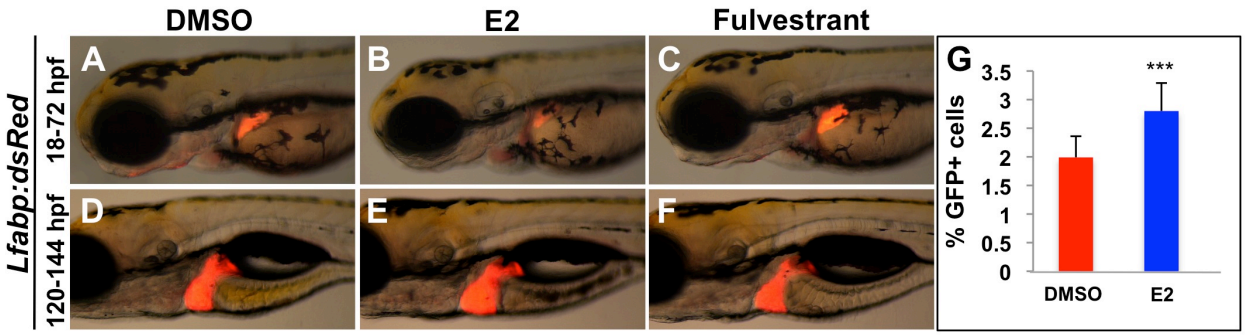

Figure 4-1. Estrogen signaling exerts a biphasic effect on liver development.

(A-C) *Lfabp:dsRed* transgenic reporter embryos exposed to estrogen pathway compounds from 18-72 hpf. Embryos exposed to estradiol (E2) during embryonic development develop smaller livers (B) compared to DMSO-treated controls (A). Conversely, embryos exposed to the estrogen receptor antagonist fulvestrant develop larger livers (C).

(D-F) *Lfabp:dsRed* larvae exposed to estrogen pathway compounds from 120-144 hpf. In contrast to embryonic exposures, larvae treated with E2 develop bigger livers (E) compared to DMSO-treated controls (D). Fulvestrant exposure does not significantly impact liver size (F).

(G) FACS quantification of percent GFP+ cells in chemically treated *lfabp:GFP* larvae reveals that zebrafish exposed to E2 from 120-144 hpf contain more hepatocytes than DMSO-treated controls.

downstream transcriptional targets of the estrogen receptors and compare target genes to those identified at embryonic stages (see below).

Identification of downstream transcriptional targets of estrogen signaling

The signaling pathways directly impacted by estrogen exposure during liver development have not been elucidated, and we have undertaken a ChIP-seq experiment to address this gap in knowledge. Specifically, to identify estrogen receptor targets in hepatic progenitors and mature hepatocytes, we performed ChIP-seq on cells isolated from 1 and 5 dpf embryos injected with *esr2a* or *esr2b-myc* constructs. These time points correspond to embryonic and larval stages during which estrogen exerts alternate effects. As demonstrated in Chapter 3, the Esr2 subtype mediates estrogen's effect on early embryonic development (Figure 3-5), so we pursued transcriptional targets of Esr2a and Esr2b. We created Myc-labeled ESRs to pull down estrogen receptor-bound chromatin using a Myc antibody, as no Esr2 antibodies exist with sufficient cross-reactivity to zebrafish, and Myc-based ChIP has been successfully executed in the zebrafish (Xu et al., 2012). Following sequence data analysis, novel estrogen targets will be validated by genetic knockdown or overexpression experiments. We will inject target gene MO or mRNA constructs into *lfabp:GFP* reporter fish to evaluate hepatocyte development in live embryos and further corroborate these data with *in situ* hybridization for hepatoblast (*prox1, hhex*) and mature hepatocyte markers (*lfabp, transferrin*) at the appropriate stages. If estrogen functions upstream of an identified target, embryos injected with a target MO should not respond to E2 treatments during hepatogenesis. Conversely, overexpressing the target gene by mRNA injection should mimic the effect of estrogen exposure. We hypothesize that ESRs bind to different target gene promoters during embryonic and larval stages, thus facilitating estrogen's biphasic effect on liver development. In conjunction with our investigation in Chapter 3, these studies

will further illuminate the role of estrogen signaling during hepatic differentiation and outgrowth stages.

NUCLEAR RECEPTOR SIGNALING AND LIVER REGENERATION

Genetic programs regulating organogenesis in the embryo may be recycled during adult tissue repair and regeneration. The liver is one of a few human organs (skin, intestine, blood) that is able to regularly regenerate. Previous work in the laboratory has shown that Wnt signals affecting hepatic progenitor cells in zebrafish embryos also govern adult liver regeneration in zebrafish and mouse (Goessling et al., 2008). Clinical studies have shown that hepatocyte transplants can reestablish liver function following organ failure, however expanding hepatocyte populations in cell culture has proven difficult (Zaret and Grompe, 2008). Our investigation of the role of nuclear receptor signaling in adult liver homeostasis may thus have important consequences for designing therapeutics for improving liver growth and function following trauma associated with liver disease and cancer.

Retinoic acid signaling inhibits liver regeneration

To investigate the role of nuclear receptor signaling in adult liver regeneration, we employ a surgical resection (1/3 partial hepatectomy) model established by the laboratory (Goessling et al., 2008). Liver regeneration studies in mammals suggest an antagonistic role for RA signaling in adult tissue repair (Hu et al., 1994; Ozeki and Tsukamoto, 1999), and our preliminary studies also indicate this to be the case in zebrafish. In our initial experiment, ATRA treatment following partial hepatectomy inhibits liver regeneration, whereas DEAB enhances liver regeneration compared to DMSO controls (5 fish/treatment) (Figure 4-2, A-C). We will repeat these experiments to solidify our observations. We will also test the effect of additional RA pathway

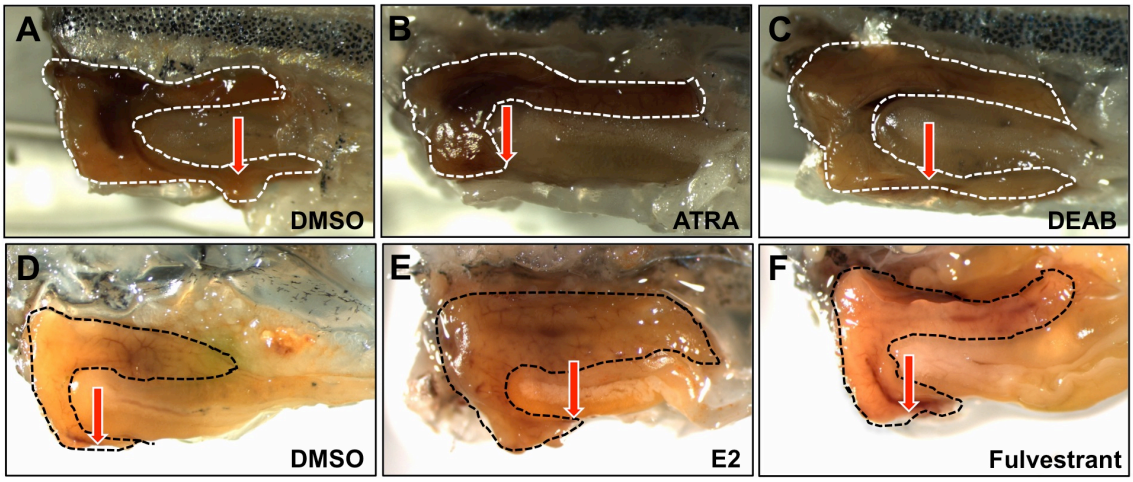

Figure 4-2. Retinoic acid and estrogen signaling inhibit liver regeneration following partial hepatectomy.

(A-F) Adult zebrafish liver regeneration capacity was evaluated by measuring the liver lobe:remnant ratio following surgical resection and chemical treatment. Compared to DMSO-treated control livers (A), ATRA-treated livers do not regenerate (B), whereas DEAB-treated livers show accelerated regeneration (C). Estradiol (E2) treatment caused cessation of liver growth at the resection margin and enhanced growth in the remaining lateral liver lobes, whereas fulvestrant treatment did not negatively impact liver regrowth (F). Red arrows indicate the point of resection. Livers are outlined by dotted lines.

compounds and analyze heterozygotes from our RA pathway mutant lines *neckless* and *giraffe* (*raldh2* and *cyp26a1* mutants, respectively; homozygotes are not viable past embryogenesis) to determine whether particular RA pathway members are required during adult liver regeneration. We will analyze histological sections of livers for BrdU incorporation to demonstrate whether chemical treatment enhances the proliferative response of liver cells following resection and perform TUNEL staining on liver sections to evaluate the extent of cell death. Expression of RA pathway members in the liver will be assessed by ISH to determine whether particular genes are required in the regenerating tissue. Together, these experiments will elucidate the impact of RA on adult liver regeneration and highlight the continued impact of RA on hepatocyte proliferation.

Estradiol differentially affects regenerating and uninjured liver lobes

Our preliminary data suggest that adult zebrafish livers exposed to E2 following resection are larger overall compared to DMSO-treated controls ($n \geq 10$ fish/treatment), results that are consistent with liver weight calculations in mouse experiments (Dixit et al., 1991). Interestingly, E2 treatment completely inhibits regrowth at the resection site on the lower lobe but results in excess growth in the upper lobes (Figure 4-2, D-F). In addition, the patterning of the hepatic and vascular tissue in the upper lobes is altered compared to controls. We will assess liver regeneration in the presence of various modulators of estrogen signaling, with particular interest in addressing the requirement for particular receptor subtypes in the regenerative process. Given E2's disparate effect on the resected and upper lobes, we hypothesize that distinct localization of receptor subtypes governs this atypical regenerative response. To further characterize this regenerative phenotype, we will also isolate RNA from tissue dissected from the resected and upper lobes for analysis of estrogen pathway, cell cycle, hepatic, and

vascular genes by qPCR. Proliferation and cell cycle analyses will be performed as described above. Because levels of circulating estrogen differ between males and females, we will stratify all data by gender. Based on our preliminary results, we expect that females will exhibit faster regenerative kinetics relative to males. These studies will inform our understanding of the impact of estrogens, both physiological and environmental, on adult liver regrowth.

Assays for liver function

We anticipate that NR pathway compounds affecting liver regrowth will also affect liver function, so we will examine serum protein levels in adult zebrafish following surgical resection. In humans, liver damage can be detected by evaluating serum levels of liver-specific enzymes, such as aminotransferases, bilirubin, and alkaline phosphatase (Ozer et al., 2008). Alanine aminotransferase (ALT) is the most frequently relied upon marker of hepatotoxicity. ALT plays roles in amino acid metabolism and gluconeogenesis, and its presence in the blood is indicative of hepatocyte damage. Bilirubin is a product of hemoglobin degradation, and its presence in the serum is suggestive of hepatobiliary defects, such as cholestasis. Enhanced levels of alkaline phosphatase (AP) also indicate hepatobiliary damage (Goessling and Friedman, 2005). Following liver resection and chemical exposures, zebrafish blood will be harvested by cardiac puncture using microcapillary tubes and serum proteomic analysis will be carried out in Dr. Wolfram Goessling's clinical laboratory. Liver-specific enzyme levels will be compared between chemically treated and DMSO-treated control fish. We expect chemicals that accelerate liver regeneration to similarly enhance restoration of liver function, however it is possible that some NR pathway compounds may simply induce hyperplasia of non-functional cells. Such results would indicate that these compounds are responsible for proliferation of cells that either are not specified hepatocytes or biliary

cells, or are hepatocytes or biliary cells but simply not functional. These possibilities can be assessed by histology and ISH for progenitor (*hhex, prox1*), hepatocyte (*lfabp, transferrin*), and biliary markers (*ck19*). These experiments will demonstrate whether modulation of NR signaling affects liver function in addition to liver regeneration.

Alternative approaches

It is possible that surgical resections don't recapitulate liver trauma associated with human liver disease or cancer, therefore lessening the potential therapeutic utility of our studies. To determine whether NR pathway compounds affect other forms of liver injury, we can also use an acetominophen-based toxicity model developed by Drs. Wolfram Goessling and Leonard Zon (North et al., 2010). Liver injury can be induced in adult zebrafish prior to or concomitant with chemical exposure, after which liver regeneration can be assessed by the parameters described above. It will also be informative to treat unresected fish with RA or E2-related compounds to determine whether NR signaling works similarly during normal liver growth and injury repair. We can also employ a more quantitative approach to assess the effect of chemical treatments on cell proliferation and number during regeneration by performing chemical exposures on *lfabp:GFP* reporter fish, which will allow hepatocyte number and BrdU incorporation or TUNEL staining to be quantified by FACS. These assays will bolster and broaden our evidence demonstrating that NR signaling influences adult liver regeneration.

ESTROGEN AND LIVER CANCER

There is strong clinical correlation between estrogen exposure and cancer (Giannitrapani et al., 2006; Harris and Waring, 2012; Laronda et al., 2012), so we will investigate the effect of estrogen exposure on hepatic tumor formation and progression

in adult zebrafish. First, we will assess the impact of long-term embryonic and larval estrogen exposure on adult liver histology. We will expose zebrafish biweekly to E2 and selected xenoestrogens from 3 days to 6 weeks old, then allow the fish to mature to adulthood. Estrogen and DMSO-exposed control animals will be sacrificed at 3, 6, and 12 months of age, and livers will be examined for any histological changes. We will perform trichrome and oil red O staining to detect fibrosis and steatosis, respectively, and look for evidence of hepatic dysplasia or cancer. At each time point, we will euthanize an equal number of male and female fish to delineate any gender-specific effects.

It is possible that estrogen exposure alone will not be sufficient to induce hepatic tumor formation, so we will also perform the above experiment using *APC +/-* fish (Hurlstone et al., 2003) and dimethylbenzanthracene (DMBA), a known liver carcinogen (Spitsbergen et al., 2000). In addition to regular estrogen exposure, juvenile fish will be exposed to DMBA at 3 and 4 weeks old to accelerate and increase the frequency of tumor formation. Fish will be sacrificed beginning at 3 months of age, and livers will be examined for tumor development. We will determine whether the expression of estrogen pathway members such as aromatase and ESRs is altered in cancerous livers as well as investigate whether expression of particular pathway components correlates with lesion subtypes (hepatocellular carcinoma, cholangiocarcinoma, combination tumors, dysplastic nodules). It has been reported that ESR expression is increased in livers with cirrhosis or hepatocellular carcinoma (HCC), so we anticipate similar overexpression phenotypes in our fish studies. We will perform immunohistochemistry for cell cycle markers (Cyclin D1, PCNA, Phospho-H3) to examine the proliferation state of liver samples and nuclear β-catenin to assess Wnt activation, commonly associated with HCC. We predict overlap between areas of enhanced estrogen and Wnt activity in hepatic tumor samples. Finally, in addition to exploring the effect of estrogenic

compounds on tumor incidence, we will also expose tumorogenic fish to estrogen pathway inhibitors to determine whether these compounds alter tumor progression. Wild type and *APC* +/- fish will be exposed to DMBA as above then treated with fulvestrant or tamoxifen and sacrificed at regular intervals to assess cancer incidence and progression. Experiments may require that we follow individual fish over time to assess disease progression or regression, so we will also employ ultrasound biomicroscopy on live zebrafish, a method previously developed by the laboratory (Goessling et al., 2007). The above experiments can also be performed in *lfabp:GFP* or *ERE:GFP* transgenic reporter lines to facilitate visualization of the liver and localized estrogen pathway activation. These studies will uncover the impact of estrogen exposure during embryonic, larval, and adult stages on adult liver homeostasis and enhance our understanding of the impact of estrogen signaling on hepatic pathologies.

METHODS

Larval chemical exposures

Lfabp:dsRed transgenic reporter zebrafish larvae were exposed to 1 μM E2 and 10 μM fulvestrant from 120-144 hpf, and liver development was assessed by live fluorescence microscopy. Stock solutions were diluted in E3 embryo water, and control embryos were treated with 0.1% DMSO.

Flow cytometry analysis

Lfabp:GFP fluorescent embryos were exposed to estrogen pathway compounds, whole embryos were manually dissociated in 0.9x PBS, and %GFP+ cells were determined by flow cytometric analysis. ≥20,000 cells were analyzed per embryo, and ≥5 embryos were analyzed for each chemical treatment using FlowJo software.

ChIP-seq

Esr2a and *esr2b* were cloned from embryonic zebrafish cDNA, and Myc-tagged Esr constructs were created using Gateway cloning technology (Life Technologies). 1,500 embryos were injected with 1 nl of 25 ng/μl *esr2a-myc* or *esr2b-myc* mRNA at the 1-cell stage for each timepoint. Chromatin immunoprecipitation was carried out as described previously (Lee et al., 2006; Xu et al., 2012) using whole embryo lysates and magnetic beads loaded with anti-Myc antibody (Abcam). Purified DNA was prepared using the Illumina Genomic DNA kit and sequenced on the Illumina Genome Analyzer.

1/3 partial hepatectomy

Adult wild type fish (>3 months old) were anesthetized with tricaine, and 1/3 partial hepatectomy was performed using brightfield imaging as previously described (Goessling et al., 2008). An incision was made on the abdomen just posterior to the heart with microdissection scissors, and forceps were used to resect the exposed left liver lobe. Fish were allowed to recover in system water for 6 hours and then exposed to chemical compounds or DMSO for 18 hours. Following chemical treatment, fish were placed in fresh water for an additional 48 hours. Three days after the time of resection, fish were euthanized, and livers were dissected for analysis. The ratio of total liver lobe length to regrowing lobe length (lobe:remnant) is used to provide a normalized measure of regenerative capacity and was calculated for all control and chemically-treated fish.

ATTRIBUTIONS

Partial hepatectomy: Maija Garnaas (retinoic acid) and Claire Cutting (estrogen). Larval estrogen exposures: Maija Garnaas and Claire Cutting. ChIP-seq: Maija Garnaas and Kristen Alexa.

REFERENCES

Dixit, A., Baquer, N.Z. and Rao, A.R. (1991). Effect of 17 beta-estradiol and ovariectomy on enzymes of carbohydrate metabolism in regenerating mouse liver. *Biochem Int* 24: 649-59.

Giannitrapani, L., Soresi, M., La Spada, E., Cervello, M., D'Alessandro, N. and Montalto, G. (2006). Sex hormones and risk of liver tumor. *Ann N Y Acad Sci* 1089, 228-36.

Goessling, W. and Friedman, L.S. (2005). Increased liver chemistry in an asymptomatic patient. *Clin Gastroenterol Hepatol* 3, 852-8.

Goessling, W., North, T. E., Lord, A. M., Ceol, C., Lee, S., Weidinger, G., Bourque, C., Strijbosch, R., Haramis, A. P., Puder, M. et al. (2008). APC mutant zebrafish uncover a changing temporal requirement for wnt signaling in liver development. *Dev Biol* 320, 161-74.

Goessling, W., North, T. E. and Zon, L. I. (2007). Ultrasound biomicroscopy permits in vivo characterization of zebrafish liver tumors. *Nat Methods* 4, 551-3.

Harris, R. M. and Waring, R. H. (2012). Diethylstilboestrol--a long-term legacy. *Maturitas* 72, 108-12.

Hu, Z., Fujio, K., Marsden, E. R., Thorgeirsson, S. S. and Evarts, R. P. (1994). Hepatic regeneration in vitamin A-deficient rats: changes in the expression of transforming growth factor alpha/epidermal growth factor receptor and retinoic acid receptors alpha and beta. *Cell Growth Differ* 5, 503-8.

Hurlstone, A. F., Haramis, A. P., Wienholds, E., Begthel, H., Korving, J., Van Eeden, F., Cuppen, E., Zivkovic, D., Plasterk, R. H. and Clevers, H. (2003). The Wnt/beta-catenin pathway regulates cardiac valve formation. *Nature* 425, 633-7.

Laronda, M. M., Unno, K., Butler, L. M. and Kurita, T. (2012). The development of cervical and vaginal adenosis as a result of diethylstilbestrol exposure in utero. *Differentiation* 84, 252-60.

Lee, J. E., Wu, S. F., Goering, L. M. and Dorsky, R. I. (2006). Canonical Wnt signaling through Lef1 is required for hypothalamic neurogenesis. *Development* 133, 4451-61.

North, T. E., Babu, I. R., Vedder, L. M., Lord, A. M., Wishnok, J. S., Tannenbaum, S. R., Zon, L. I. and Goessling, W. (2010). PGE2-regulated wnt signaling and N-acetylcysteine are synergistically hepatoprotective in zebrafish acetaminophen injury. *Proc Natl Acad Sci U S A* 107, 17315-20.

Ozeki, A. and Tsukamoto, I. (1999). Retinoic acid repressed the expression of c-fos and c-jun and induced apoptosis in regenerating rat liver after partial hepatectomy. *Biochim Biophys Acta* 1450, 308-19.

Ozer, J., Ratner, M., Shaw, M., Bailey, W. and Schomaker, S. (2008). The current state of serum biomarkers of hepatotoxicity. *Toxicology* 245, 194-205.

Spitsbergen, J. M., Tsai, H. W., Reddy, A., Miller, T., Arbogast, D., Hendricks, J. D. and Bailey, G. S. (2000). Neoplasia in zebrafish (Danio rerio) treated with 7,12-dimethylbenz[a]anthracene by two exposure routes at different developmental stages. *Toxicol Pathol* 28, 705-15.

Xu, C., Fan, Z. P., Muller, P., Fogley, R., DiBiase, A., Trompouki, E., Unternaehrer, J., Xiong, F., Torregroza, I., Evans, T. et al. (2012). Nanog-like regulates endoderm formation through the Mxtx2-Nodal pathway. *Dev Cell* 22, 625-38.

Zaret, K. S. and Grompe, M. (2008). Generation and regeneration of cells of the liver and pancreas. *Science* 322, 1490-4.

CHAPTER 5

Concluding Discussion

SUMMARY

The liver is a vital organ responsible for a myriad of functions including hormone and bile secretion, detoxification, and metabolic regulation. Liver and overall embryonic development must occur in tandem, particularly because an organism's ability to grow is directly correlated with its capacity to process nutrients and avoid exposure to harmful toxins. Moreover, in mammals the liver is a site of early hematopoieisis. As such, any aberrations in liver development may directly impact successful establishment of circulation, reducing the likelihood of embryo survival. Similarly, because the liver governs many normal physiological processes throughout an organism's life, liver diseases such as cirrhosis, steatosis, and cancer result in high rates of morbidity and mortality. Liver disease is the fourth leading cause of death in the United States in middle-aged adults (Si-Tayeb et al., 2010). When a significant portion of the liver is irreparably damaged and hepatic function is lost, liver failure ensues, and patients require immediate intensive care without which the mortality rate reaches 60-90% (Larson 2008; Lee and Seremba, 2008).

Understanding the genetic programs driving liver development and homeostasis will yield insight into the mechanisms fundamental to hepatogenesis and liver disease. Additionally, knowledge gained from investigations of embryonic liver development can be directly applied to the burgeoning field of stem cell biology. The discrepancy between the number of livers required for transplant and their availability necessitates that alternative approaches be taken to create replacement tissues. Studies identifying developmental genes that control hepatic specification and differentiation will immediately impact research aiming to create viable and functional hepatocytes from pluripotent stem cells. In the same vein, the prospect of *in situ* regeneration of damaged adult tissues will undoubtedly be aided by the characterization of hepatic developmental factors.

Harnessing the power of zebrafish genetics, I have expanded our understanding of two nuclear receptor signaling pathways in embryonic liver development and outlined future investigations to characterize these developmental signals in the adult in normal, cancerous, and regenerative states. In Chapter 2, I elucidated the role of a number of retinoic acid (RA) signaling pathway factors including RA-synthesizing Raldh enzymes and individual RA receptors (RARs) during hepatogenesis. I demonstrated a unique function for Rargb in governing left-right asymmetry of the liver and adjacent tissues and identified its mechanism of regulation via Bmp signaling. I also situated RA signaling in the context of human disease, as *rargb* knockdown phenotypes closely resemble the human heterotaxic syndrome right atrial isomerism (Ivemark Syndrome). In Chapter 3, I characterized the function of estrogen signaling during hepatic differentiation. I discovered that both naturally occuring and environmental estrogens negatively impact liver growth, delaying hepatocyte differentation, and demonstrated that the Esr2 receptor isoform mediates this effect. Importantly, I also determined that estrogen's effect on liver development is conserved in mouse and humans, highlighting the applicability of our zebrafish studies to higher vertebrate species and making them directly relevant to human physiology.

FINAL REMARKS

Development is comprised of a complex network of hundreds of regulatory pathways, which themselves are inherently complicated. Why? Considering one organ – the liver – there are a series of events that must occur in highly regulated fashion for a liver, and ultimatey an embryo, to come to be. First, hepatic progenitors must be specified in the right place at the right time. A number of organs arise from the foregut endoderm, so whether a cell becomes liver or something else, such as the pancreas, necessitates intricate coordination. Second, liver differentiation and growth

must be coincident with other organs and the embryo as a whole. Third, mature hepatic cells must know when and to what extent they should begin performing their endocrine, exocrine, and metabolic functions. These requirements, their essential nature, and the fact that each developmental program does not occur in a vacuum but within the context of the whole organism, justify development's complexity. And perhaps most importantly, because embryo survival is the ultimate goal of development, having redundancy or molecular fail safes is the most effective way to achieve this end.

In terms of initiating liver development, it is clear that RA signaling plays an integral role in determining whether and where hepatic cells are specified. Loss of RA signaling by globally repressing RA synthesis or downstream signal transduction results in small or no livers. Interestingly, we found that whether specification occurs and its spatial regulation are each governed by a subset of RARs in zebrafish – Raraa, Rarab, and Rarga regulate the "if", and Rargb regulates the "where". Our results suggest that there is a hierarchy of RAR function during hepatogenesis. Specifically, the first three receptors must be required prior to Rargb in order for liver specification to occur and in the appropriate location. If an embryo does not express Raraa, Rarab, or Rarga, it will not specify liver cells, in which case Rargb expression is immaterial as there are no hepatic progenitors to be localized to either side of the midline in the first place. This concept is corroborated by our data demonstrating that knockdown of all RARs in combination results only in very small or absent livers but not bilateral livers. Finally, the fact that three receptors govern hepatic specification while just one governs hepatic position is a seemingly evolutionarily advantageous allocation; that is, an embryo is better off creating an organ in the wrong location than having no organ at all.

Following specification, subsequent hepatic differentiation allows the developing organ to begin perfoming its requisite functions. We have demonstrated that estrogen signaling functions during this step of hepatogenesis: exogenous estrogen exposure

negatively impacts liver differentiation, and changing levels of endogenous estrogen signaling in the embryo coincide with the timing of differentiation. Specifically, it appears as though the embryo takes advantage of an inherent decline in endogenous estrogen levels to allow liver differentiation to proceed. The liver develops in concert with the rest of the embryo, and every organ must be specified at the correct moment to ensure proper body plan organization, tissue connections, and efficiency of function. It is tempting to speculate that the embryo employs estrogen to delay hepatic differentiation to prevent unwanted energy expenditure before liver function, carried out by differentiated hepatocytes and bile duct cells, is required. For instance, the hematopoietic system originates prior to initiation of liver function. This makes developmental sense, since only after the embryo establishes its hematopoietic system and blood flow is initiated can the liver act to detoxify it. Similarly, it would be inefficient to commence bile secretion, an exocrine function of the liver, before the embryo has exhausted its yolk supply and digestion of externally supplied nutrition has begun.

Retinoic acid and estrogen signaling are just two of the countless signaling pathways that regulate liver development. Each pathway is elaborate and impacts different aspects of liver development, as do individual components within each pathway, underscoring the complexity of hepatogenesis. Certainly, RA and estrogen signaling are not the only mechanisms by which liver specification, laterality, and differentiation are regulated, but this fact further emphasizes the intricate nature of embryonic development. What the embryo loses in efficiency by employing a multitude of overlapping, if not completely redundant, signaling pathways, it gains in ensuring its survival – the ultimate goal of development.

REFERNCES

Larson, A.M. (2008). Acute liver failure. Dis Mon 54, 457-485.

Lee, W.M., and Seremba, E. (2008). Etiologies of acute liver failure. Curr Opin Crit Care 14, 198-201.

Si-Tayeb, K., Lemaigre, F.P., and Duncan, S. A. (2010). Organogenesis and development of the liver. Dev Cell 18, 175-189.

APPENDIX

Genome-wide association and functional follow-up reveals new loci for kidney function

Cristian Pattaro[1]*, Anna Kottgen[2,3]*, Alexander Teumer[4]*, Maija K. Garnaas[5]*, Carsten Boeger[6]*, et al. *Equal contribution.

[1]Institute of Genetic Medicine, European Academy of Bozen/Bolzano (EURAC) and Affiliated Institute of the University of Lubeck, Bolzano, Italy, [2]Department of Epidemiology, Johns Hopkins Bloomberg School of Public Health, Baltimore, Maryland, USA, [3]Renal Division, Freiburg University Clinic, Freiburg, Germany, [4]Interfaculty Institute for Genetics and Functional Genomics, University of Greifswald, Greifswald, Germany, [5]Division of Genetics, Department of Medicine, Brigham and Women's Hospital, Harvard Medical School, Boston, MA, USA, [6]Department of Internal Medicine II, University Medical Center, Regensburg, Regensburg, Germany.

This appendix contains the manuscript entitled "Genome-wide association and functional follow-up reveals new loci for kidney function", originally published in *PLoS Genetics* on March 29, 2012 (8(3): e1002584). Author attributions: Over 100 authors contributed to this study as part of a collaboration among institutes affiliated with the National Institutes of Health National Heart, Lung, and Blood Institute (NHLBI)/Framingham Heart Study and the Candidate Gene Association Resource (CARe) consortium. Detailed author attributions are included at the end of the manuscript. MKG devised, executed, and analyzed all zebrafish experiments and wrote the zebrafish-related portions of the manuscript.

INTRODUCTION

In collaboration with the NHLBI/Framingham Heart Study and the CARe consortium, I investigated the developmental importance of genes implicated in human chronic kidney disease (CKD) by genome-wide association studies (GWAS). To gain insight into the functional implications of associated loci, I knocked down corresponding genes in the zebrafish and assessed kidney gene expression, structure, and function. Single nucleotide polymorphisms (SNPs) in the human genes *MPPED2* and *CASP9* were correlated with defective estimated glomerular filtration rate (eGFR), and I found that loss of these genes in zebrafish results in aberrant glomerular gene expression and filtration capacity. The following report demonstrates a role for *mpped2* and *casp9* in kidney development, indicating that cross-species modeling in zebrafish is feasible for genes associated with chronic human disease.

RELATED PROJECTS

The following manuscripts are examples of additional studies in which zebrafish were used to perform functional assessments of loci associated with human CKD:

Liu, C.*, Garnaas, M.*, Tin, A., Kottgen, A., Franceschini, N. et al. (2011). Genetic association for renal traits among participants of African ancestry reveals new loci for renal function. PLoS Genetics 7(9): e1002264. *Equal contribution.

Gorski, M.*, Tin, A.*, Garnaas, M.K.*, McMahon, G. M., Chu, A. Y. et al. (2013). Genome-wide association study reveals two novel loci associated with kidney function decline: the CKDGen Corsortium. Submitted, PLoS Genetics. *Equal contribution.

McMahon, G. M., Olden, M., Garnaas, M. K., Yang, Q., Hwang, S., Larson, M. G., CKDGen Corsortium, Goessling, W., and Fox, C.S. (2013). Sequencing of LRP2 Reveals Multiple Rare Variants associated with Urinary Trefoil Factor-3. Submitted, JASN.

Genome-Wide Association and Functional Follow-Up Reveals New Loci for Kidney Function

Cristian Pattaro[1☯], Anna Köttgen[2,3☯], Alexander Teumer[4☯], Maija Garnaas[5☯], Carsten A. Böger[6☯], Christian Fuchsberger[7], Matthias Olden[8,9], Ming-Huei Chen[10,11], Adrienne Tin[2], Daniel Taliun[1], Man Li[2], Xiaoyi Gao[12], Mathias Gorski[13,14], Qiong Yang[15], Claudia Hundertmark[16], Meredith C. Foster[17], Conall M. O'Seaghdha[17,18], Nicole Glazer[19], Aaron Isaacs[20,21], Ching-Ti Liu[22], Albert V. Smith[23,24], Jeffrey R. O'Connell[25], Maksim Struchalin[26], Toshiko Tanaka[27], Guo Li[28], Andrew D. Johnson[17], Hinco J. Gierman[29], Mary Feitosa[12], Shih-Jen Hwang[17], Elizabeth J. Atkinson[30], Kurt Lohman[31], Marilyn C. Cornelis[32], Åsa Johansson[33], Anke Tönjes[34,35], Abbas Dehghan[36], Vincent Chouraki[37], Elizabeth G. Holliday[38,39], Rossella Sorice[40], Zoltan Kutalik[41,42], Terho Lehtimäki[43], Tõnu Esko[44,45], Harshal Deshmukh[46], Sheila Ulivi[47], Audrey Y. Chu[48], Federico Murgia[49], Stella Trompet[50], Medea Imboden[51], Barbara Kollerits[52], Giorgio Pistis[53], CARDIoGRAM Consortium, ICBP Consortium, CARe Consortium, Wellcome Trust Case Control Consortium 2 (WTCCC2), Tamara B. Harris[54], Lenore J. Launer[54], Thor Aspelund[23,24], Gudny Eiriksdottir[23], Braxton D. Mitchell[25], Eric Boerwinkle[55], Helena Schmidt[56], Margherita Cavalieri[57], Madhumathi Rao[58], Frank B. Hu[32], Ayse Demirkan[20], Ben A. Oostra[20], Mariza de Andrade[30], Stephen T. Turner[59], Jingzhong Ding[60], Jeanette S. Andrews[61], Barry I. Freedman[62], Wolfgang Koenig[63], Thomas Illig[64], Angela Döring[14,64], H.-Erich Wichmann[14,65,66], Ivana Kolcic[67], Tatijana Zemunik[67], Mladen Boban[67], Cosetta Minelli[1], Heather E. Wheeler[68,69], Wilmar Igl[33], Ghazal Zaboli[33], Sarah H. Wild[70], Alan F. Wright[71], Harry Campbell[70], David Ellinghaus[72], Ute Nöthlings[72,73], Gunnar Jacobs[72,73], Reiner Biffar[74], Karlhans Endlich[75], Florian Ernst[4], Georg Homuth[4], Heyo K. Kroemer[76], Matthias Nauck[77], Sylvia Stracke[78], Uwe Völker[4], Henry Völzke[79], Peter Kovacs[80], Michael Stumvoll[34,35], Reedik Mägi[44,81], Albert Hofman[36], Andre G. Uitterlinden[82], Fernando Rivadeneira[82], Yurii S. Aulchenko[36], Ozren Polasek[83], Nick Hastie[84], Veronique Vitart[84], Catherine Helmer[85,86], Jie Jin Wang[87,88], Daniela Ruggiero[40], Sven Bergmann[42], Mika Kähönen[89], Jorma Viikari[90], Tiit Nikopensius[45], Michael Province[12], Shamika Ketkar[12], Helen Colhoun[46], Alex Doney[91], Antonietta Robino[92], Franco Giulianini[48], Bernhard K. Krämer[93], Laura Portas[49], Ian Ford[94], Brendan M. Buckley[95], Martin Adam[51], Gian-Andri Thun[51], Bernhard Paulweber[96], Margot Haun[97], Cinzia Sala[53], Marie Metzger[98], Paul Mitchell[87], Marina Ciullo[40], Stuart K. Kim[29,68], Peter Vollenweider[99], Olli Raitakari[100], Andres Metspalu[44,45], Colin Palmer[101], Paolo Gasparini[92], Mario Pirastu[49], J. Wouter Jukema[50,102,103,104], Nicole M. Probst-Hensch[51], Florian Kronenberg[52], Daniela Toniolo[53], Vilmundur Gudnason[23,24], Alan R. Shuldiner[25,105], Josef Coresh[2,106], Reinhold Schmidt[57], Luigi Ferrucci[27], David S. Siscovick[28], Cornelia M. van Duijn[20], Ingrid Borecki[12], Sharon L. R. Kardia[107], Yongmei Liu[31], Gary C. Curhan[108], Igor Rudan[70], Ulf Gyllensten[33], James F. Wilson[70], Andre Franke[72], Peter P. Pramstaller[1], Rainer Rettig[109], Inga Prokopenko[81], Jacqueline C. M. Witteman[36], Caroline Hayward[84], Paul Ridker[48,110], Afshin Parsa[111], Murielle Bochud[112], Iris M. Heid[113,114], Wolfram Goessling[115,116¶], Daniel I. Chasman[48,110¶], W. H. Linda Kao[2,106*¶], Caroline S. Fox[17,117*¶]

1 Institute of Genetic Medicine, European Academy of Bozen/Bolzano (EURAC) and Affiliated Institute of the University of Lübeck, Bolzano, Italy, **2** Department of Epidemiology, Johns Hopkins Bloomberg School of Public Health, Baltimore, Maryland, United States of America, **3** Renal Division, Freiburg University Clinic, Freiburg, Germany, **4** Interfaculty Institute for Genetics and Functional Genomics, University of Greifswald, Greifswald, Germany, **5** Division of Genetics, Department of Medicine, Brigham and Women's Hospital, Harvard Medical School, Boston, Massachusetts, United States of America, **6** Department of Internal Medicine II, University Medical Center Regensburg, Regensburg, Germany, **7** Center for Statistical Genetics, Department of Biostatistics, University of Michigan, Ann Arbor, Michigan, United States of America, **8** Department of Internal Medicine II, University Hospital Regensburg, Regensburg, Germany, **9** Department of Epidemiology and Preventive Medicine, Regensburg University Medical Center, Regensburg, Germany, **10** Department of Neurology, Boston University School of Medicine, Boston, Massachusetts, United States of America, **11** Department of Biostatistics, Boston University School of Public Health, Boston, Massachusetts, United States of America, **12** Division of Statistical Genomics, Washington University School of Medicine, St. Louis, Missouri, United States of America, **13** Department of Epidemiology and Preventive Medicine, University Hospital Regensburg, Regensburg, Germany, **14** Institute of Epidemiology I, Helmholtz Zentrum München, German Research Center for Environmental Health, Neuherberg, Germany, **15** Department of Biostatistics, Boston University School of Public Health, Boston, Massachusetts, United States of America, **16** Renal Division, Freiburg University Clinic, Freiburg, Germany, **17** National Heart, Lung, and Blood Institute's Framingham Heart Study and the Center for Population Studies, Framingham, Massachusetts, United States of America, **18** Division of Nephrology, Brigham and Women's Hospital and Harvard Medical School, Boston, Massachusetts, United States of

America, **19** Section of Preventive Medicine and Epidemiology, Department of Medicine, Boston University School of Medicine, Boston, Massachusetts, United States of America, **20** Genetic Epidemiology Unit, Department of Epidemiology, Erasmus University Medical Center, Rotterdam, The Netherlands, **21** Centre for Medical Systems Biology, Leiden, The Netherlands, **22** Department of Biostatistics, Boston University School of Public Health, Boston, Massachusetts, United States of America, **23** Icelandic Heart Association, Research Institute, Kopavogur, Iceland, **24** University of Iceland, Reykjavik, Iceland, **25** Department of Medicine, University of Maryland Medical School, Baltimore, Maryland, United States of America, **26** Department of Epidemiology and Biostatistics and Department of Forensic Molecular Biology, Erasmus University Medical Centre, Rotterdam, The Netherlands, **27** Clinical Research Branch, National Institute of Aging, Baltimore, Maryland, United States of America, **28** University of Washington, Seattle, Washington, United States of America, **29** Department of Developmental Biology, Stanford University, Stanford, California, United States of America, **30** Division of Biomedical Statistics and Informatics, Mayo Clinic, Rochester, Minnesota, United States of America, **31** Department of Epidemiology and Prevention, Public Health Sciences, Wake Forest School of Medicine, Winston-Salem, North Carolina, United States of America, **32** Department of Nutrition, Harvard School of Public Health, Boston, Massachusetts, United States of America, **33** Genetics and Pathology, Rudbeck Laboratory, Uppsala University, Uppsala, Sweden, **34** Department of Medicine, University of Leipzig, Leipzig, Germany, **35** IFB Adiposity Diseases, University of Leipzig, Leipzig, Germany, **36** Department of Epidemiology, Erasmus University Medical Center, Rotterdam, The Netherlands, **37** Inserm UMR744, Institut Pasteur, Lille, France, **38** Centre for Clinical Epidemiology and Biostatistics, School of Medicine and Public Health, University of Newcastle, Newcastle, Australia, **39** Centre for Information-based Medicine, Hunter Medical Research Institute, Newcastle, Australia, **40** Institute of Genetics and Biophysics ''Adriano-Buzzati Traverso''–CNR, Napoli, Italy, **41** Department of Medical Genetics, University of Lausanne, Lausanne, Switzerland, **42** Swiss Institute of Bioinformatics, Lausanne, Switzerland, **43** Department of Clinical Chemistry, University of Tampere and Tampere University Hospital, Centre for Laboratory Medicine Tampere Finn-Medi 2, Tampere, Finland, **44** Estonian Genome Center of University of Tartu (EGCUT), Tartu, Estonia, **45** Estonian Biocenter and Institute of Molecular and Cell Biology, University of Tartu, Tartu, Estonia, **46** Wellcome Trust Centre for Molecular Medicine, Clinical Research Centre, Ninewells Hospital, University of Dundee, Dundee, United Kingdom, **47** Institute for Maternal and Child Health – IRCCS ''Burlo Garofolo'', Trieste, Italy, **48** Brigham and Women's Hospital, Boston, Massachusetts, United States of America, **49** Institute of Population Genetics – CNR, Sassari, Italy, **50** Department of Cardiology, Leiden University Medical Center, Leiden, The Netherlands, **51** Unit of Chronic Disease Epidemiology, Swiss Tropical and Public Health Institute, Basel, Switzerland, **52** Division of Genetic Epidemiology, Innsbruck Medical University, Innsbruck, Austria, **53** Division of Genetics and Cell Biology, San Raffaele Scientific Institute, Milano, Italy, **54** Laboratory of Epidemiology, Demography, and Biometry, NIA, Bethesda, Maryland, United States of America, **55** Human Genetics Center, University of Texas Health Science Center, Houston, Texas, United States of America, **56** Austrian Stroke Prevention Study, Institute of Molecular Biology and Biochemistry and Department of Neurology, Medical University Graz, Graz, Austria, **57** Austrian Stroke Prevention Study, University Clinic of Neurology, Department of Special Neurology, Medical University Graz, Graz, Austria, **58** Division of Nephrology/ Tufts Evidence Practice Center, Tufts University School of Medicine, Tufts Medical Center, Boston, Massachusetts, United States of America, **59** Department of Internal Medicine, Division of Nephrology and Hypertension, Mayo Clinic, Rochester, Minnesota, United States of America, **60** Department of Internal Medicine/Geriatrics, Wake Forest School of Medicine, Winston-Salem, North Carolina, United States of America, **61** Department of Biostatistical Sciences, Public Health Sciences, Wake Forest School of Medicine, Winston-Salem, North Carolina, United States of America, **62** Department of Internal Medicine, Wake Forest School of Medicine, Winston-Salem, North Carolina, United States of America, **63** Abteilung Innere II, Universitätsklinikum Ulm, Ulm, Germany, **64** Institute of Epidemiology II, Helmholtz Zentrum München, German Research Center for Environmental Health, Neuherberg, Germany, **65** Institute of Medical Informatics, Biometry, and Epidemiology, Ludwig-Maximilians-Universität, Munich, Germany, **66** Klinikum Grosshadern, Neuherberg, Germany, **67** Croatian Centre for Global Health, University of Split Medical School, Split, Croatia, **68** Department of Genetics, Stanford University, Stanford, California, United States of America, **69** Department of Medicine, University of Chicago, Chicago, Illinois, United States of America, **70** Center for Population Health Sciences, University of Edinburgh Medical School, Edinburgh, United Kingdom, **71** MRC Human Genetics Unit, Institute of Genetics and Molecular Medicine, Western General Hospital, Edinburgh, United Kingdom, **72** Institute of Clinical Molecular Biology, Christian-Albrechts University, Kiel, Germany, **73** popgen Biobank, University Hospital Schleswig-Holstein, Kiel, Germany, **74** Clinic for Prosthodontic Dentistry, Gerostomatology, and Material Science, University of Greifswald, Greifswald, Germany, **75** Institute of Anatomy and Cell Biology, University of Greifswald, Greifswald, Germany, **76** Institute of Pharmacology, University of Greifswald, Greifswald, Germany, **77** Institute of Clinical Chemistry and Laboratory Medicine, Ernst-Moritz-Arndt-University Greifswald, Greifswald, Germany, **78** Clinic for Internal Medicine A, University of Greifswald, Greifswald, Germany, **79** Institute for Community Medicine, University of Greifswald, Greifswald, Germany, **80** Department of Medicine, University of Leipzig, Leipzig, Germany, **81** Wellcome Trust Centre for Human Genetics and Oxford Centre for Diabetes, Endocrinology, and Metabolism, University of Oxford, Oxford, United Kingdom, **82** Department of Internal Medicine, Erasmus University Medical Center, Rotterdam, The Netherlands, **83** Croatian Centre for Global Health, Faculty of Medicine, University of Split, Split, Croatia, **84** MRC Human Genetics Unit, Institute of Genetics and Molecular Medicine, Western General Hospital, Edinburgh, United Kingdom, **85** INSERM U897, Université Victor Ségalen Bordeaux 2, ISPED, Bordeaux, France, **86** Université Bordeaux 2 Victor Segalen, Bordeaux, France, **87** Centre for Vision Research, Westmead Millennium Institute, Westmead Hospital, University of Sydney, Sydney, Australia, **88** Centre for Eye Research Australia (CERA), University of Melbourne, Melbourne, Australia, **89** Department of Clinical Physiology, University of Tampere and Tampere University Hospital, Tampere, Finland, **90** Department of Medicine, University of Turku and Turku University Hospital, Turku, Finland, **91** NHS Tayside, Wellcome Trust Centre for Molecular Medicine, Clinical Research Centre, Ninewells Hospital, University of Dundee, Dundee, United Kingdom, **92** Institute for Maternal and Child Health, IRCCS ''Burlo Garofolo,'' University of Trieste, Trieste, Italy, **93** University Medical Centre Mannheim, 5th Department of Medicine, Mannheim, Germany, **94** Robertson Centre for Biostatistics, University of Glasgow, Glasgow, United Kingdom, **95** Department of Pharmacology and Therapeutics, University College Cork, Cork, Ireland, **96** First Department of Internal Medicine, Paracelsus Medical University, Salzburg, Austria, **97** Division of Genetic Epidemiology, Innsbruck Medical University, Innsbruck, Austria, **98** Inserm UMRS 1018, CESP Team 10, Université Paris Sud, Villejuif, France, **99** Department of Internal Medicine, Centre Hospitalier Universitaire Vaudois, Lausanne, Switzerland, **100** Research Centre of Applied and Preventive Cardiovascular Medicine, Department of Clinical Physiology, Turku University Hospital, University of Turku, Turku, Finland, **101** Biomedical Research Institute, Ninewells Hospital and Medical School, University of Dundee, Dundee, United Kingdom, **102** Interuniversity Cardiology Institute of the Netherlands (ICIN), Utrecht, The Netherlands, **103** Einthoven Laboratory for Experimental Vascular Medicine, Leiden, The Netherlands, **104** Durrer Center for Cardiogenetic Research, Amsterdam, The Netherlands, **105** Geriatric Research and Education Clinical Center, Veterans Administration Medical Center, Baltimore, Maryland, United States of America, **106** Welch Center for Prevention, Epidemiology, and Clinical Research, Baltimore, Maryland, United States of America, **107** Department of Epidemiology, School of Public Health, University of Michigan, Ann Arbor, Michigan, United States of America, **108** Brigham and Women's Hospital and Channing Laboratory, Harvard Medical School, Boston, Massachusetts, United States of America, **109** Institute of Physiology, University of Greifswald, Greifswald, Germany, **110** Harvard Medical School, Boston, Massachusetts, United States of America, **111** Division of Nephrology, University of Maryland Medical School, Baltimore, Maryland, United States of America, **112** University Institute of Social and Preventive Medicine, Centre Hospitalier Universitaire Vaudois and University of Lausanne, Epalinges, Switzerland, **113** Department of Epidemiology and Preventive Medicine, University Hospital Regensburg, Regensburg, Germany, **114** Institute of Epidemiology I, Helmholtz Zentrum München, German Research Center for Environmental Health, Neuherberg, Germany, **115** Divisions of Genetics and Gastroenterology, Department of Internal Medicine, Brigham and Women's Hospital, Boston, Massachusetts, United States of America, **116** Harvard Stem Cell Institute, Harvard University, Cambridge, Massachusetts, United States of America, **117** Division of Endocrinology, Brigham and Women's Hospital and Harvard Medical School, Boston, Massachusetts, United States of America

Abstract

Chronic kidney disease (CKD) is an important public health problem with a genetic component. We performed genome-wide association studies in up to 130,600 European ancestry participants overall, and stratified for key CKD risk factors. We uncovered 6 new loci in association with estimated glomerular filtration rate (eGFR), the primary clinical measure of CKD, in or near *MPPED2*, *DDX1*, *SLC47A1*, *CDK12*, *CASP9*, and *INO80*. Morpholino knockdown of *mpped2* and *casp9* in zebrafish embryos revealed podocyte and tubular abnormalities with altered dextran clearance, suggesting a role for these genes in renal function. By providing new insights into genes that regulate renal function, these results could further our understanding of the pathogenesis of CKD.

Citation: Pattaro C, Köttgen A, Teumer A, Garnaas M, Böger CA, et al. (2012) Genome-Wide Association and Functional Follow-Up Reveals New Loci for Kidney Function. PLoS Genet 8(3): e1002584. doi:10.1371/journal.pgen.1002584

Editor: Greg Gibson, Georgia Institute of Technology, United States of America

Received October 1, 2011; **Accepted** January 22, 2012; **Published** March 29, 2012

Funding: The AGES study has been funded by NIH contract N01-AG-1-2100, the NIA Intramural Research Program, Hjartavernd (the Icelandic Heart Association), and the Althingi (the Icelandic Parliament). The Amish study was supported by grants and contracts from the NIH including R01 AG18728 (Amish Longevity Study), R01 HL088119 (Amish Calcification Study), U01 GM074518-04 (PAPI Study), U01 HL072515-06 (HAPI Study), U01 HL084756 and NIH K12RR023250 (University of Maryland MCRDP), the University of Maryland General Clinical Research Center, grant M01 RR 16500, the Baltimore Veterans Administration Medical Center Geriatrics Research and Education Clinical Center, and the Paul Beeson Physician Faculty Scholars in Aging Program. The ASPS research reported in this article was funded by the Austrian Science Fund (FWF) grant number P20545-P05 and P13180. The Medical University of Graz supported the databank of the ASPS. The Atherosclerosis Risk in Communities Study is carried out as a collaborative study supported by National Heart, Lung, and Blood Institute contracts (HHSN268201100005C, HHSN268201100006C, HHSN268201100007C, HHSN268201100008C, HHSN268201100009C, HHSN268201100010C, HHSN268201100011C, and HHSN268201100012C), R01HL087641, R01HL59367, and R01HL086694; National Human Genome Research Institute contract U01HG004402; and National Institutes of Health contract HHSN268200625226C. Infrastructure was partly supported by Grant Number UL1RR025005, a component of the National Institutes of Health and NIH Roadmap for Medical Research. A Köttgen and C Hundertmark were supported by the grant KO3598/2-1 (Emmy Noether Programme) of the German Research Foundation. The BLSA was supported in part by the Intramural Research Program of the NIH (National Institute on Aging). The CHS research reported in this article was supported by contract numbers N01-HC-85079 through N01-HC-85086, N01-HC-35129, N01 HC-15103, N01 HC-55222, N01-HC-75150, N01-HC-45133, and grant numbers U01 HL080295 and R01 HL087652 from the National Heart, Lung, and Blood Institute, with additional contribution from the National Institute of Neurological Disorders and Stroke. A full list of principal CHS investigators and institutions can be found at http://www.chs-nhlbi.org/pi.htm. DNA handling and genotyping was supported in part by National Center for Research Resources grant M01RR00425 to the Cedars-Sinai General Clinical Research Center Genotyping core and National Institute of Diabetes and Digestive and Kidney Diseases grant DK063491 to the Southern California Diabetes Endocrinology Research Center. The ERF study was supported by grants from the Netherlands Organization for Scientific Research (NWO; Pioneergrant), Erasmus Medical Center, the Centre for Medical Systems Biology (CMSB), and the Netherlands Kidney Foundation. The Family Heart Study (FHS) work was supported in part by NIH grants 5R01HL08770003, 5R01HL08821502 (M Province) from the NHLBI and 5R01DK07568102, 5R01DK06833603 from the NIDDK (I Borecki). The Framingham Heart Study research reported in this paper was conducted in part using data and resources from the Framingham Heart Study of the National Heart Lung and Blood Institute of the National Institutes of Health and Boston University School of Medicine. The analyses reflect intellectual input and resource development from the Framingham Heart Study investigators participating in the SNP Health Association Resource (SHARe) project. This work was partially supported by the National Heart, Lung, and Blood Institute's Framingham Heart Study (Contract No. N01-HC-25195) and its contract with Affymetrix for genotyping services (Contract No. N02-HL-6-4278). A portion of this research utilized the Linux Cluster for Genetic Analysis (LinGA-II) funded by the Robert Dawson Evans Endowment of the Department of Medicine at Boston University School of Medicine and Boston Medical Center. The GENOA research was partially supported by the National Heart, Lung, and Blood Institute of the National Institutes of Health R01 HL-87660. The Health Aging and Body Composition Study (Health ABC) was funded by the National Institutes of Aging. This research was supported by NIA contracts N01AG62101, N01AG62103, and N01AG62106. The GWAS was funded by NIA grant 1R01AG032098-01A1 to Wake Forest University Health Sciences and genotyping services were provided by the Center for Inherited Disease Research (CIDR). CIDR is fully funded through a federal contract from the National Institutes of Health to The Johns Hopkins University, contract number HHSN268200782096C. This research was supported in part by the Intramural Research Program of the NIH, National Institute on Aging. For the KORA F3 and F4 studies, the genetic epidemiological work was funded by the NIH subcontract from the Children's Hospital, Boston, US, (HE Wichmann, IM Heid, prime grant 1 R01 DK075787-01A1), the German National Genome Research Net NGFN2 and NGFNplus (H.E.Wichmann 01GS0823; WK project A3, number 01GS0834), the Munich Center of Health Sciences (MC Health) as part of LMUinnovativ, and by the Else Kröner-Fresenius-Stiftung (P48/08//A11/08; CA Böger, BK Krämer). The kidney parameter measurements in F3 were funded by the Else Kröner-Fresenius-Stiftung (CA Böger, BK Krämer) and the Regensburg University Medical Center, Germany; in F4 by the University of Ulm, Germany (W Koenig). Genome-wide genotyping costs in F3 and F4 was in part funded by the Else Kröner-Fresenius-Stiftung (CA Böger, BK Krämer). De novo genotyping in F3 and F4 was funded by the Else Kröner-Fresenius-Stiftung (CA Böger, BK Krämer). The KORA research platform and the MONICA Augsburg studies were initiated and financed by the Helmholtz Zentrum München, German Research Center for Environmental Health, by the German Federal Ministry of Education and Research, and by the State of Bavaria. Genotyping was performed in the Genome Analysis Center (GAC) of the Helmholtz Zentrum München. The LINUX platform for computation was funded by the University of Regensburg for the Department of Epidemiology and Preventive Medicine at the Regensburg University Medical Center. The NHS/HPFS type 2 diabetes GWAS (U01HG004399) is a component of a collaborative project that includes 13 other GWAS (U01HG004738, U01HG004422, U01HG004402, U01HG004729, U01HG004726, U01HG004735, U01HG004415, U01HG004436, U01HG004423, U01HG004728, RFAHG006033; National Institute of Dental and Craniofacial Research: U01DE018993, U01DE018903) funded as part of the Gene Environment-Association Studies (GENEVA) under the NIH Genes, Environment and Health Initiative (GEI). Assistance with phenotype harmonization and genotype cleaning, as well as with general study coordination, was provided by the GENEVA Coordinating Center (U01HG004446). Assistance with data cleaning was provided by the National Center for Biotechnology Information. Genotyping was performed at the Broad Institute of MIT and Harvard, with funding support from the NIH GEI (U01HG04424), and Johns Hopkins University Center for Inherited Disease Research, with support from the NIH GEI (U01HG004438) and the NIH contract "High-throughput genotyping for studying the genetic contributions to human disease" (HHSN268200782096C). Additional funding for the current research was provided by the National Cancer Institute (P01CA087969, P01CA055075) and the National Institute of Diabetes and Digestive and Kidney Diseases (R01DK058845). We thank the staff and participants of the NHS and HPFS for their dedication and commitment. The Korcula study was supported through the grants from the Medical Research Council UK to H Campbell, AF Wright, and I Rudan and by Ministry of Science, Education, and Sport of the Republic of Croatia to I Rudan (number 108-1080315-0302). The MICROS study was supported by the Ministry of Health and Department of Educational Assistance, University and Research of the Autonomous Province of Bolzano, the South Tyrolean Sparkasse Foundation, and the European Union framework program 6 EUROSPAN project (contract no. LSHG-CT-2006-018947). The Northern Swedish Population Health Study was supported by grants from the Swedish Natural Sciences Research Council, the European Union through the EUROSPAN project (contract no. LSHG-CT-2006-018947), the Foundation for Strategic Research (SSF), and the Linneaus Centre for Bioinformatics (LCB). The NHS renal function and albuminuria work was supported by DK66574. Additional funding for the current research was provided by the National Cancer Institute (P01CA087969, P01CA055075) and the National Institute of Diabetes and Digestive and Kidney Diseases (R01DK058845). ORCADES was supported by the Chief Scientist Office of the Scottish Government, the Royal Society and the European Union framework program 6 EUROSPAN project (contract no. LSHG-CT-2006-018947). DNA extractions were performed at the Wellcome Trust Clinical Research Facility in Edinburgh. The popgen study was supported by the German Ministry of Education and Research (BMBF) through the National Genome Research Network (NGFN) and the Ministry of Science, Commerce, and Transportation of the State of Schleswig-Holstein. The project has also received infrastructure support through the DFG excellence cluster "Inflammation at Interfaces." The Sorbs study was funded by grants from the German Research Council KFO-152 (to M Stumvoll) and the IFB (Integrated Research

and Treatment Center) AdiposityDiseases (K7-37 to M Stumvoll and A Tönjes). We also thank Dr. Knut Krohn (Microarray Core Facility of the Interdisciplinary Centre for Clinical Research, University of Leipzig, Germany) for providing the genotyping platform. The research of Inga Prokopenko is funded in part through the European Community's Seventh Framework Programme (FP7/2007–2013), ENGAGE project, grant agreement HEALTH-F4-2007- 201413. R Mägi acknowledges financial support from the European Commission under a Marie Curie Intra-European Fellowship. For the Rotterdam Study-I and Rotterdam Study-II, the GWAS was funded by the Netherlands Organisation of Scientific Research NWO Investments (nr. 175.010.2005.011, 911-03-012), the Research Institute for Diseases in the Elderly (014-93-015; RIDE2), the Netherlands Genomics Initiative (NGI)/Netherlands Consortium for Healthy Aging (NCHA) project nr. 050-060-810. The Rotterdam Study is funded by Erasmus Medical Center and Erasmus University, Rotterdam, The Netherlands Organization for the Health Research and Development (ZonMw), the Research Institute for Diseases in the Elderly (RIDE), the Ministry of Education, Culture, and Science, the Ministry for Health, Welfare, and Sports, the European Commission (DG XII), and the Municipality of Rotterdam. The Erasmus Computing Grid, Rotterdam (The Netherlands) and the national German MediGRID and Services@MediGRID part of the German D-Grid were both funded by the German Bundesministerium fuer Forschung und Technology under grants #01 AK 803 A-H and # 01 IG 07015 G, for access to their grid resources. A Dehghan is supported by NWO grant (vici, 918-76-619). The Study of Health in Pomerania (SHIP) is part of the Community Medicine Research net of the University of Greifswald, Germany, funded by the Federal Ministry of Education and Research (grants no. 01ZZ9603, 01ZZ0103, and 01ZZ0403), the Ministry of Cultural Affairs as well as the Social Ministry of the Federal State of Mecklenburg-West Pomerania. Genome-wide data have been supported by the Federal Ministry of Education and Research (grant no. 03ZIK012) and a joint grant from Siemens Healthcare, Erlangen, Germany, and the Federal State of Mecklenburg-West Pomerania. The University of Greifswald is a member of the 'Center of Knowledge Interchange' program of the Siemens AG. The Vis study was supported through the grants from the Medical Research Council UK to H Campbell, AF Wright, and I Rudan; and Ministry of Science, Education, and Sport of the Republic of Croatia to I Rudan (number 108-1080315-0302) and the European Union framework program 6 EUROSPAN project (contract no. LSHG-CT-2006-018947). The WGHS is supported by HL 043851 and HL69757 from the National Heart, Lung, and Blood Institute and CA 047988 from the National Cancer Institute, the Donald W. Reynolds Foundation and the Fondation Leducq, with collaborative scientific support and funding for genotyping provided by Amgen. The 3 City Study was supported by the National Foundation for Alzheimer's disease and related disorders, the Institut Pasteur de Lille and the Centre National de Génotypage. The 3 City Study was performed as part of a collaboration between the Institut National de la Santé et de la Recherche Médicale (Inserm), the Victor Segalen Bordeaux II University and Sanofi-Synthélabo. The Fondation pour la Recherche Médicale funded the preparation and initiation of the study. The 3C Study was also funded by the Caisse Nationale Maladie des Travailleurs Salariés, Direction Générale de la Santé, MGEN, Institut de la Longévité, Agence Française de Sécurité Sanitaire des Produits de Santé, the Aquitaine and Bourgogne Regional Councils, Fondation de France and the joint French Ministry of Research/INSERM "Cohortes et collections de données biologiques" programme. Lille Génopôle received an unconditional grant from Eisai. The Blue Mountains Eye Study (BMES) has been supported by the Australian RADGAC grant (1992–94) and Australian National Health and Medical Research Council, Canberra Australia (Grant Nos: 974159, 211069, 991407, 457349). The GWAS studies of BMES population are supported by the Australian National Health and Medical Research Council (Grant Nos: 512423, 475604, 529912) and the Wellcome Trust, UK (2008), as part of Wellcome Trust Case Control Consortium 2 (A Viswanathan, P McGuffin, P Mitchell, F Topouzis, P Foster, grant numbers 085475/B/08/Z and 085475/08/Z). EG Holliday and JJ Wang are funded by the Australian National Health and Medical Research Council Fellowship Schemes. The CoLaus study received financial contributions from GlaxoSmithKline, the Faculty of Biology and Medicine of Lausanne, and the Swiss National Science Foundation (33CSCO-122661). M Bochud is supported by the Swiss School of Public Health Plus (SSPH+). The Cardiovascular Risk in Young Finns study (YFS) is supported by the Academy of Finland (grant no. 117797, 121584, and 126925), the Social Insurance Institution of Finland, University Hospital Medical funds to Tampere and Turku University Hospitals, and the Finnish Foundation of Cardiovascular Research. The Emil Aaltonen Foundation (T Lehtimäki). EGCUT received support from FP7 grants ((201413 ENGAGE, 212111 BBMRI, 205419 ECOGENE, 245536 OPENGENE) and also received targeted financing from Estonian Government SF0180142s08 and from the European Union through the European Regional Development Fund, in the frame of Centre of Excellence in Genomics. The research of the FamHS-II was conducted in part using data and resources from the NHLBI Family Heart Study supported in part by NIH grant 5R01HL08770002. For the GoDARTs study, the Wellcome Trust provides support for Wellcome Trust United Kingdom Type 2 Diabetes Case Control Collection and the informatics support is provided by the Chief Scientist Office, and the Wellcome Trust funded Scottish Health Informatics Programme (SHIP). The INGI-Carlantino and INGI-FVG studies were supported by grants from Telethon, FVG region, and Fondo Trieste. The INGI-Cilento study was supported by grants from the EU (Vasoplus-037254), the Italian Ministry of Universities (FIRB -RBIN064YAT), the Assessorato Ricerca Regione Campania, the Ente Parco Nazionale del Cilento e Vallo di Diano, and the Fondazione Banco di Napoli to M Ciullo. The INGI – Val Borbera Study was supported from Compagnia di San Paolo, Torino, Italy, the Cariplo Fundation, Milano, Italy, and Italian Ministry of Health Progetto Finalizzato 2007 and 2009. The JUPITER trial and the genotyping were supported by AstraZeneca. The Ogliastra Genetic Park (OGP) - Replication Study and OGP - Talana study were supported by grants from the Italian Ministry of Education, University, and Research (MIUR) no. 5571/DSPAR/2002 and (FIRB) D. M. no. 718/Ric/2005. The Prospective Study of Pravastatin in the Elderly at Risk (PROSPER) trial was supported by an investigator initiated grant from Bristol-Myers Squibb, USA. The study was conducted, analyzed, and reported independently of the company. The SAPALDIA study was supported by the Swiss National Science Foundation (grants no 33CSCO-108796, 3247BO-104283, 3247BO-104288, 3247BO-104284, 3247-065896, 3100-059302, 3200-052720, 3200-042532, 4026-028099), the Federal Office for Forest, Environment, and Landscape, the Federal Office of Public Health, the Federal Office of Roads and Transport, the canton's government of Aargau, Basel-Stadt, Basel-Land, Geneva, Luzern, Ticino, Zurich, the Swiss Lung League, the canton's Lung League of Basel Stadt/Basel Landschaft, Geneva, Ticino, and Zurich. The SAPHIR-study was partially supported by a grant from the Kamillo Eisner Stiftung to B Paulweber and by grants from the "Genomics of Lipid-associated Disorders – GOLD" of the "Austrian Genome Research Programme GEN-AU" to F Kronenberg. eQTL analysis: HJ Gierman received support from the AFAR/EMF postdoctoral fellowship and the Stanford Dean's postdoctoral fellowship. HE Wheeler and SK Kim were supported by grants from the NIA, NHGRI and NIGMS.

Competing Interests: The authors have declared that no competing interests exist.

* E-mail: foxca@nhlbi.nih.gov (CS Fox); wkao@jhsph.edu (WHL Kao)

❧ These authors contributed equally to this work.

¶ These authors were joint senior authors on this work.

Introduction

Chronic kidney disease (CKD) affects nearly 10% of the global population [1,2], and its prevalence continues to increase [3]. Reduced estimated glomerular filtration rate (eGFR), the primary measure used to define CKD (eGFR<60 ml/min/1.73 m^2) [4], is associated with an increased risk of cardiovascular morbidity and mortality [5], acute kidney injury [6], and end stage renal disease (ESRD) [6,7].

Using genome-wide association studies (GWAS) in predominantly population-based cohorts, we and others have previously identified more than 20 genetic loci associated with eGFR and CKD [8–11]. Although most of these genetic effects seem largely robust across strata of diabetes or hypertension status [9], evidence suggests that some of the loci such as the *UMOD* locus may have heterogeneous effects across these strata [11]. We thus hypothesized that GWAS in study populations stratified by four key CKD risk factors - age, sex, diabetes or hypertension status - may permit the identification of novel eGFR and CKD loci. We carried this out by extending our previous work [9] to a larger discovery sample of 74,354 individuals with independent replication in additional 56,246 individuals, resulting in a total of 130,600 individuals of European ancestry. To assess for potential heterogeneity, we performed separate genome-wide association analyses across strata of CKD risk factors, as well as in a more extreme CKD phenotype.

Results

Meta-analyses of GWAS on the 22 autosomes were performed for: 1) eGFR based on serum creatinine (eGFRcrea) and CKD (6,271 cases) in the overall sample, 2) eGFRcrea and CKD stratified by the four risk factors, and 3) CKD45, a more severe CKD phenotype defined as eGFRcrea <45 ml/min/1.73 m^2 in

Author Summary

Chronic kidney disease (CKD) is an important public health problem with a hereditary component. We performed a new genome-wide association study in up to 130,600 European ancestry individuals to identify genes that may influence kidney function, specifically genes that may influence kidney function differently depending on sex, age, hypertension, and diabetes status of individuals. We uncovered 6 new loci associated with estimated glomerular filtration rate (eGFR), the primary measure of renal function, in or near *MPPED2*, *DDX1*, *SLC47A1*, *CDK12*, *CASP9*, and *INO80*. *CDK12* effect was stronger in younger and absent in older individuals. *MPPED2*, *DDX1*, *SLC47A1*, and *CDK12* loci were associated with eGFR in African ancestry samples as well, highlighting the cross-ethnicity validity of our findings. Using the zebrafish model, we performed morpholino knockdown of *mpped2* and *casp9* in zebrafish embryos and revealed podocyte and tubular abnormalities with altered dextran clearance, suggesting a role for these genes in renal function. These results further our understanding of the pathogenesis of CKD and provide insights into potential novel mechanisms of disease.

the overall sample (2,181 cases). For the stratified analyses, in addition to identifying loci that were significant within each stratum, we performed a genome-wide comparison of the effect estimates between strata of the four risk factors. A complete overview of the analysis workflow is given in Figure S1. All studies participating in the stage 1 discovery and stage 2 replication phases are listed in Tables S1 and S2. The characteristics of all stage 1 discovery samples by study are reported in Table S3, and information on study design and genotyping are reported in Table S4. Results of the eGFRcrea analyses are summarized in the Manhattan and quantile-quantile plots reported in Figures S2 and S3. A total of 21 SNPs from the discovery stage were carried forward for replication in an independent set of 56,246 individuals (Tables S5 and S6). These SNPs were selected for replication for the following (Figure S1): 5 reached genome-wide significance in either eGFRcrea overall or stratified analyses, 1 based on a test of direction-consistency of SNP-eGFR associations across the discovery cohorts for eGFRcrea overall, 4 demonstrated a P value$\leq 10^{-6}$ and high between-study homogeneity ($I^2<25\%$) in the CKD45 analysis (Table S7), and 11 demonstrated between-strata P value$\leq 5\times10^{-5}$ along with a P value$\leq 5\times10^{-5}$ for association with eGFRcrea in at least one of the two strata (Table S8).

While none of the loci identified for CKD45 or the test for between-strata difference analyses replicated, all 6 loci identified from the eGFRcrea overall analysis, stratified analyses, and the direction test did (Table 1). These 6 loci were identified and replicated in the overall analysis (rs3925584, located upstream of the *MPPED2* gene; rs6431731 near the *DDX1* gene), in the diabetes-free sub-group (rs2453580 in an intron of the *SLC47A1* gene), in the younger age stratum (rs11078903 in an intron of the *CDK12* gene; rs12124078 located near the *CASP9* gene), and the direction test (rs2928148, located in the *INO80* gene, see Methods for details). In the combined meta-analysis of all 45 studies used in the discovery and replication stages, all six SNPs met the genome-wide significance threshold of 5×10^{-8}, with individual P values ranging from 4.3×10^{-8} to 8.4×10^{-18} (Table 1). The imputation quality of these SNPs is reported in Table S9, and Figure S4 shows the regional association plots for each of the 6 loci. We also confirmed all previously identified renal function loci in the current data (Table S10). Brief descriptions of the genes included within the 6 new loci uncovered can be found in Table S11. Forest plots for the associations between the index SNP at each of the 6 novel loci and eGFR across all discovery studies and all strata are presented in Figures S5 and S6. Most of the 6 new loci had similar associations across strata of CKD risk factors except for the *CDK12* locus, which revealed stronger association in the younger ($\leq$65 years of age) as compared to the older age group ($>$65 years of age).

We further examined our findings in 8,110 African ancestry participants from the CARe consortium [12] (Table 2). Not surprisingly, given linkage disequilibrium (LD) differences between Europeans and African Americans, none of the 6 lead SNPs uncovered in CKDGen achieved significance in the African American samples. Next, we interrogated the 250 kb flanking regions from the lead SNP at each locus, and showed that 4 of the 6 regions (*MPPED2*, *DDX1*, *SLC47A1*, and *CDK12*) harbored SNPs that achieved statistical significance after correcting for multiple comparisons based on the genetic structure of each region (see Methods for details). Figure 1 presents the regional association plots for *MPPED2*, and Figure S7 presents the plots of the remaining loci in the African American sample. Imputation scores for the lead SNPs can be found in Table S12. We observed that rs12278026, upstream of *MPPED2*, was associated with eGFRcrea in African Americans (P value $= 5\times10^{-5}$, threshold for statistical significance: P value $= 0.001$). While rs12278026 is monomorphic in the CEU population in HapMap, rs3925584 and rs12278026 have a D′ of 1 ($r^2 = 0.005$) in the YRI population, suggesting that these SNPs may have arisen from the same ancestral haplotype.

We also performed eQTL analyses of our 6 newly identified loci using known databases and a newly created renal eSNP database (see Methods) and found that rs12124078 was associated with *cis* expression of the nearby *CASP9* gene in myocytes, which encodes caspase-9, the third apoptotic activation factor involved in the activation of cell apoptosis, necrosis and inflammation (P value for the monocyte eSNP of interest $= 3.7\times10^{-13}$). In the kidney, caspase-9 may play an important role in the medulla response to hyperosmotic stress [13] and in cadmium-induced toxicity [14]. The other 5 SNPs were not associated with any investigated eQTL. Additional eQTL analyses of 81 kidney biopsies (Table S13) did not reveal further evidence of association with eQTLs (Table S14).

Of the 6 novel loci identified, 2 (*MPPED2* and *DDX1*) were in regions containing only a single gene, and 1 (*CASP9*) had its expression associated with the locus lead SNP. Thus, to determine the potential involvement of these three genes during zebrafish kidney development, we independently assessed the expression of 4 well-characterized renal markers following morpholino knockdown: *pax2a* (global kidney) [15], *nephrin* (podocyte) [16], *slc20a1a* (proximal tubule) [17], and *slc12a3* (distal tubule) [17]. While we observed no abnormalities in *ddx1* morphants (Figure S8), *mpped2* and *casp9* knockdown resulted in expanded *pax2a* expression in the glomerular region in 90% and 75% of morphant embryos, respectively, compared to 0% in controls (P value<0.0001 for both genes; Figure 2A versus 2F and 2K; 2B versus 2G and 2L; and 2P). Significant differences were also observed in expression of the podocyte marker *nephrin* (Figure 2C versus 2H and 2M; 80% and 74% abnormalities for *mpped2* and *casp9*, respectively, versus 0% in controls, P value<0.0001 for both genes). For *mpped2*, no differences were observed in expression of the proximal or distal tubular markers *slc20a1a* and *slc12a3* (P value $= 1.0$; Figure 2D versus 2I and 2E versus 2J). *Casp9* morphants and controls showed no differences in proximal tubular marker expression (Figure 2D versus 2N), but abnormalities were observed in distal tubular marker expression in *casp9* knockdown embryos (30% versus 0%; Figure 2E versus 2O; P value $= 0.0064$).

Table 1. Novel loci associated with eGFRcrea.

Locus description						Discovery analysis		Replication analysis			Combined analysis†		
Analysis subgroup	**SNP ID**	**Chr**	**Position (bp)‡**	**Genes nearby‡**	**Ref./Non-Ref. alleles (RAF)**	**Effect(SE)§**	***P* value§**	**Effect(SE)**	**1-sided *P* value**	**Q value**	**Effect(SE)**	***P* value**	**I^2**
Overall	rs3925584	11	30,716,911	*MPPED2*	T/C(0.54)	−0.0077(0.0013)	1.0×10^{-09}	−0.0073(0.0013)	4.0×10^{-9}	1.1×10^{-08}	−0.0075(0.0009)	8.4×10^{-18}	21%
Overall	rs6431731	2	15,780,453	*DDX1*	T/C(0.94)	−0.0181(0.0033)	4.6×10^{-08}	−0.0065(0.0034)	0.0277	0.0195	−0.0127(0.0023)	4.3×10^{-08}	11%
No Diabetes	rs2453580	17	19,378,913	***SLC47A1***	T/C(0.59)	0.0076(0.0014)	4.6×10^{-08}	0.0038(0.0014)	0.0037	0.0039	0.0059(0.0010)	2.1×10^{-09}	21%
Age≤65 yrs*	rs12124078	1	15,742,486	***DNAJC16***, *CASP9*, *AGMAT*	A/G(0.70)	0.0096(0.0015)	9.8×10^{-10}	0.0098(0.0017)	5.0×10^{-9}	1.1×10^{-08}	0.0097(0.0011)	1.5×10^{-17}	20%
Age≤65 yrs	rs11078903	17	34,885,450	***CDK12***, *MED1*, *FBXL20*	A/G(0.76)	−0.0103(0.0017)	2.4×10^{-09}	−0.0083(0.0023)	1.4×10^{-4}	2.0×10^{-04}	−0.0096(0.0013)	9.0×10^{-13}	0%
Direction Test (Overall)**	rs2928148	15	39,188,842	***INO80***, *EXD1*, *CHAC1*	A/G(0.52)	0.0064(0.0012)	1.2×10^{-07}	0.0033(0.0015)	0.0145	0.0122	0.0051(0.0009)	4.0×10^{-08}	0%

SNPs are listed in the stratum where the smallest *P* value in the discovery analysis was observed. Sample size/number of studies in the discovery phase: 74,354/26 (overall, direction test), 66,931/24 (No Diabetes), 46,435/23 (age ≤65 years); replication phase: 56,246/19 (overall, direction test), 41,218/17 (No Diabetes), 28,631/16 (age ≤65 years); combined analysis: 130,600/45 (overall, direction test), 108,149/41 (No Diabetes), 75,066/39 (age ≤65 years). Chr.: chromosome; bp: base-pairs; Ref./Non-Ref. All.: reference/non-reference alleles; RAF: reference allele frequency; SE: standard error.

‡Genes nearby were based on RefSeq genes (build 36). The gene closest to the SNP is listed first and is in boldface if the SNP is located within the gene.

§Effects on log(eGFRcrea); post GWAS meta-analysis genomic control correction applied to *P* values and SEs.

*While being uncovered in the younger samples, this locus showed consistent results in the non-diabetic group (combined-analysis *P* value 5.7×10^{-16}) and in the overall population (*P* value 9.5×10^{-22}) - see Tables S16 and S10 for additional details.

**The direction test was performed in the overall dataset; the genomic control corrected *P* value from the direction test for the SNP rs2928148 was 4.0×10^{-7}. In the combined analysis, the largest effect size (0.0054 on log eGFR in ml/min/1.73 m^2) and the smallest *P* value (3.7×10^{-8}) were observed in the non-diabetic group.

†All results were confirmed by random-effect meta-analysis.

doi:10.1371/journal.pgen.1002584.t001

Table 2. Interrogation of the six novel loci uncovered in the European ancestry (EA) individuals (CKDGen consortium) in individuals of African ancestry (AA) from the CARe consortium for the trait eGFRcrea.

Results for the lead SNPs in the CARe AA individuals					Best SNP in region in the CARe AA individuals							
SNP ID*	Nearby genes§	Ref./Non-Ref. alleles (RAF)	Effect(SE)	*P* value	SNP ID	Position (build 36)	LD (R^2) with lead SNP	RAF (Ref./Non-Ref. alleles)	Effect(SE)	*P* value	S**	Bonferroni *P* value threshold (0.05/S)
rs3925584	*MPPED2*	T/C (0.88)	−0.0005(0.0066)	0.9349	rs12278026	30,744,460	0.005	0.89 (A/G)	0.0342(0.0084)	4.6×10^{-5}	46	0.0011
rs6431731	*DDX1*	T/C (0.99)	−0.0181(0.0213)	0.3948	rs4669002	15,874,859	NA†	0.56 (T/C)	−0.0196(0.0047)	2.6×10^{-5}	78	6.4×10^{-4}
rs12124078	***SLC47A1***	A/G (0.69)	−0.0024(0.0045)	0.5956	rs1472554	15,987,920	0.004	0.50 (C/G)	−0.0120(0.0041)	0.0035	44	0.0011
rs2453580	***DNAJC16***, *CASP9*, *AGMAT*	T/C (0.59)	0.0056(0.0049)	0.2524	rs1800869	19,505,226	0.011	0.93 (C/G)	−0.0294(0.0082)	3.6×10^{-4}	33	0.0015
rs11078903‡	***CDK12***, *MED1*, *FBXL20*	A/G (NA‡)	NA‡	NA‡	rs1874226	34,982,557	0.112	0.34 (T/C)	0.0157(0.0045)	4.2×10^{-4}	15	0.0033
rs2928148	***INO80***, *EXD1*, *CHAC1*	A/G (0.22)	−0.0003(0.0053)	0.9497	rs8039934	39,284,719	0.105	0.50 (T/C)	−0.0086(0.0042)	0.0412	22	0.0023

Ref./Non-Ref. All.: reference/non-reference alleles; RAF: reference allele frequency; SE: standard error.
*Characteristics of the six lead SNPs in the EA individuals from the CKDGen consortium can be found in Table 1.
§The gene closest to the SNP is listed first and is in boldface if the SNP is located within the gene.
**S = number of independent, typed SNPs interrogated.
†No LD information available in the HapMap database between the target SNP and the best SNP in the DDX1 region.
‡The SNP rs11078903 was not present in the CARe consortium database.
doi:10.1371/journal.pgen.1002584.t002

Casp9 morphants displayed diminished clearance of 70,000 MW fluorescent dextran 48 hours after injection into the sinus venosus compared to controls, revealing significant functional consequences of *casp9* knockdown (Figure 2Q–2V). No clearance abnormalities were observed in *mpped2* morphants. The occurrence of abdominal edema is a non-specific finding that is frequently observed in zebrafish embryos with kidney defects. We examined the occurrence of edema in *mpped2* and *casp9* knockdown embryos at 4 and 6 days post fertilization (dpf), both in the absence and presence of dextran, and observed a significant increase in edema prevalence in *casp9* with (P value<0.0001) and without (P value $= 0.0234$) dextran challenge but not in *mpped2* morphants (Figure 2W).

In order to further demonstrate differences in kidney function in response to knockdown of *mpped2* and *casp9*, we injected the nephrotoxin gentamicin which predictably causes edema in a subset of embryos. Casp9 morphants were more susceptible to developing edema compared to both controls and mpped2 morphants (Figure 2X). In addition, edema developed earlier and was more severe, encompassing a greater area of the entire embryo (Figure S9). Together, these findings suggest that *casp9* and *mpped2* knockdowns result in altered kidney gene expression and function. Specifically, abnormal expression of *pax2a* and *nephrin* in casp9 morphants in addition to dextran retention and edema formation suggest loss of *casp9* impacts glomerular development and function.

The lead SNP at the *MPPED2* locus is located approximately 100 kb upstream of the gene metallophosphoesterase domain containing 2 (*MPPED2*), which is highly evolutionary conserved and encodes a protein with metallophosphoesterase activity [18]. It has been recognized for a role in brain development and tumorigenesis [19] but thus far not for kidney function.

To determine whether the association at our newly identified eGFRcrea loci was primarily due to creatinine metabolism or renal function, we compared the relative associations between eGFRcrea and eGFR estimated using cystatin C (eGFRcys) (Figure S10, File S1). The new loci showed similar effect sizes and consistent effect directions for eGFRcrea and eGFRcys, suggesting a relation to renal function rather than to creatinine metabolism. Placing the results of these 6 loci in context with our previously identified loci [8,9] (23 known and 6 novel), 18 were associated with CKD at a 0.05 significance level (odds ratio, OR, from 1.05 to 1.26; P values from 3.7×10^{-16} to 0.01) and 11 with CKD45 (OR from 1.08 to 1.34; P values from 1.1×10^{-5} to 0.047; Figure S11 and Table S15).

When we examined these 29 renal function loci by age group, sex, diabetes and hypertension status (Tables S16, S17, S18, and S19), we observed consistent associations with eGFRcrea for most loci across all strata, with only two exceptions: *UMOD* had a stronger association in older individuals (P value for difference 8.4×10^{-13}) and in those with hypertension (P value for difference 0.002), and *CDK12* was stronger in younger subjects (P value for difference 0.0008). We tested the interaction between age and rs11078903 in one of our largest studies, the ARIC study. The interaction was significant (P value $= 0.0047$) and direction consistent with the observed between-strata difference.

Finally, we tested for associations between our 6 new loci and CKD related traits. The new loci were not associated with urinary albumin-to-creatinine ratio (UACR) or microalbuminuria [20] (Tables S20 and S21), with blood pressure from the ICBP Consortium [21] (Table S22) or with myocardial infarction from the CARDIoGRAM Consortium [22] (Table S23).

Discussion

We have extended prior knowledge of common genetic variants for kidney function [8–11,23] by performing genome-wide

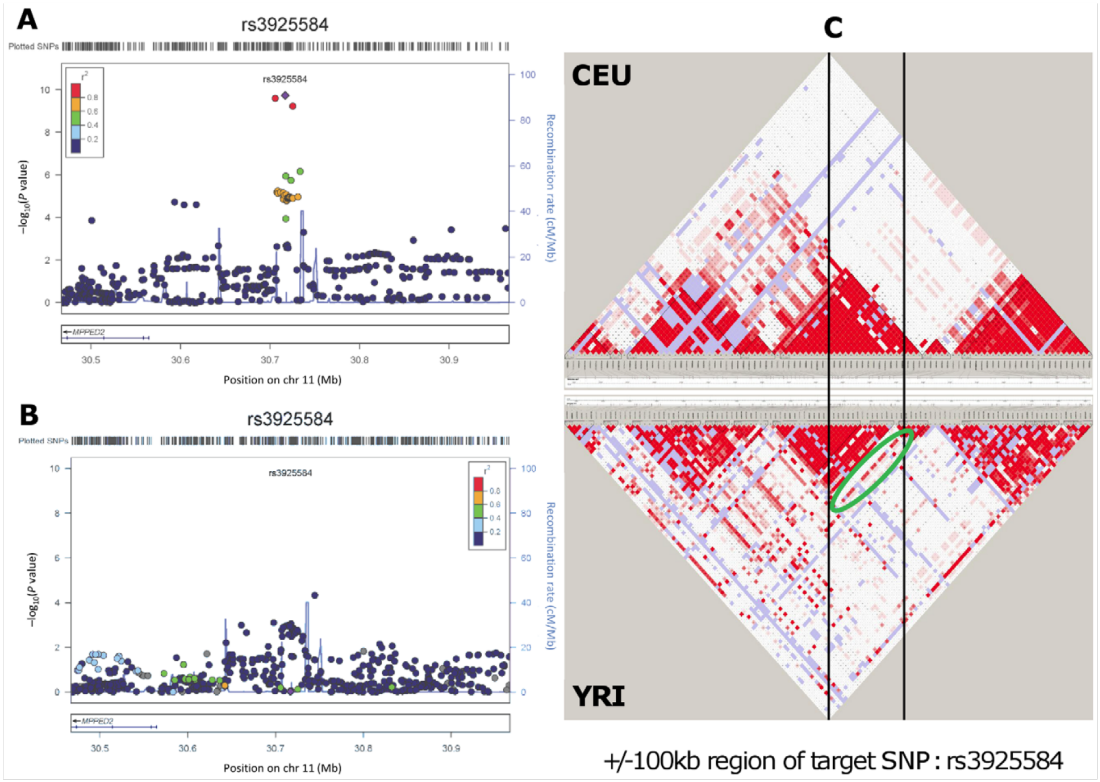

Figure 1. Genetic association and LD distribution of the *MPPED2* gene locus in European and African ancestry populations. Regional association plots in the CKDGen European ancestry discovery analysis (N = 74,354) (A) and in the CARe African ancestry discovery analysis (N = 8,110) (B). LD structure: comparison between the HapMap release II – CEU and YRI samples in the region included within +/−100 kb from the target SNP rs3925584 identified in the CKDGen GWAS. The green circle highlights a stream of high LD connecting the two blocks, indicating the presence of common haplotypes (C).
doi:10.1371/journal.pgen.1002584.g001

association tests within strata of key CKD risk factors, including age, sex, diabetes, and hypertension, thus uncovering 6 loci not previously known to be associated with renal function in population-based studies (*MPPED2*, *DDX1*, *CASP9*, *SLC47A1*, *CDK12*, *INO80*). In contrast to our prior genome-wide analysis [8,9], the majority of the new loci uncovered in the present analysis have little known prior associations with renal function. This highlights a continued benefit of the GWAS approach by using large sample sizes to infer new biology.

Despite our hypothesis that genetic effects are modified by CKD risk factors, most of the identified variants did not exhibit strong cross-strata differences. This highlights that many genetic associations with kidney function may be shared across risk factor strata. The association of several of these loci with kidney function in African Americans underscores the generalizability of identified renal loci across ethnicities. Zebrafish knockdown of *mpped2* resulted in abnormal podocyte anatomy as assessed by expression of glomerular markers, and loss of *casp9* led to altered podocyte and distal tubular marker expression, decreased dextran clearance, edema, and enhanced susceptibility to gentamicin-induced kidney damage. These findings demonstrate the potential importance of these genes with respect to renal function and illustrate that zebrafish are a useful *in vivo* model to explore the functional consequences of GWAS-identified genes.

Despite these strengths, there are some limitations of our study that warrant discussion. Although we used cystatin C to separate creatinine metabolism from true filtration loci, SNPs within the cystatin C gene cluster have been shown to be associated with cystatin C levels [8], which might result in some degree of misclassification in absolute levels. While we used standard definitions of diabetes and hypertension in the setting of population-based studies, these may differ from those definitions used in clinical practice. In addition, we were unable to differentiate the use of anti-hypertension medications from other clinical indications of these agents or type 1 from type 2 diabetes. The absence of association between our six newly discovered SNPs and the urinary albumin to creatinine ratio, blood pressure, and cardiovascular disease may have resulted from disparate genetic underpinnings of these traits, the overall small effect sizes, or the cross-sectional nature of our explorations; and we were unable to differentiate between these potential issues. Finally, power was modest to detect between-strata heterogeneity.

With increased sample size and stratified analyses, we have identified additional loci for kidney function that continue to have novel biological implications. Our primary findings suggest that there is substantial generalizability of SNPs associations across strata of important CKD risk factors, specifically with hypertension and diabetes.

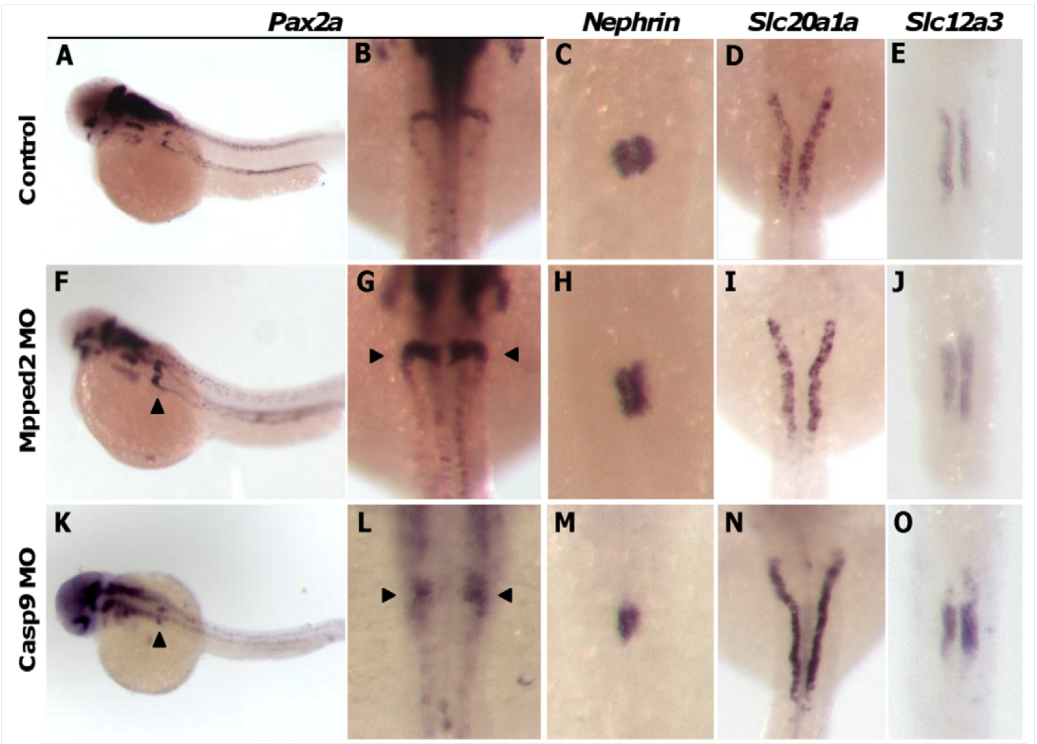

P

Number of observed abnormalities /number of embryos examined				
	Global Renal Marker *pax2a*	Podocyte Marker *nephrin*	Proximal Tubular Marker *slc20a1a*	Distal Tubular Marker *slc12a3*
Control MO	2/59 (3%)	0/38 (0%)	0/30 (0%)	0/23 (0%)
Mpped2 MO (400 uM)	66/73 (90%)	53/66 (80%)	1/46 (2%)	0/30 (0%)
P value	<0.0001	<0.0001	1.0	1.0
Casp9 MO (100 uM)	15/20 (75%)	17/23 (74%)	0/20 (0%)	6/20 (30%)
P value	<0.0001	<0.0001	1.0	0.0064

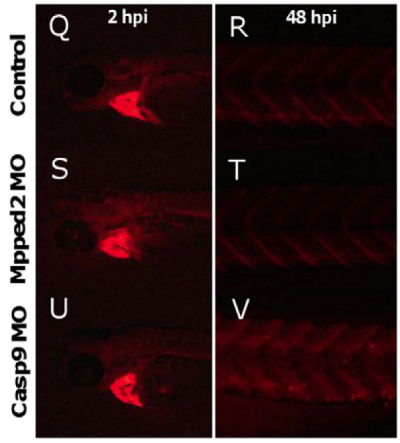

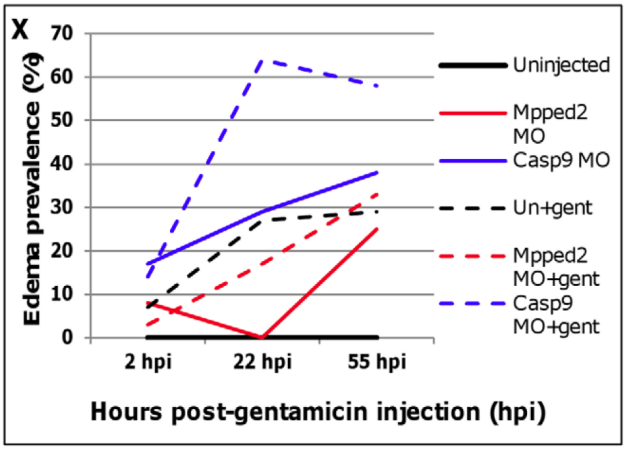

W

Edema prevalence (70 kDa dextran injection)			
	Control MO	Mpped2 MO	Casp9 MO
-dex (4 dpf)	0/21 (0%)	0/47 (0%)	0/43 (0%)
-dex (6 dpf)	0/21 (0%)	0/47 (0%)	10/43 (23%)
+dex (4 dpf)	0/16 (0%)	1/16 (6%)	21/29 (72%)
+dex (6 dpf)	N/A	N/A	N/A

Figure 2. *Mpped2* and *casp9* knockdowns result in defective kidney development. (A–E) Whole mount *in situ* hybridization in control embryos demonstrates normal expression of the global kidney marker *pax2a* (A: lateral view; B: dorsal view), the glomerular marker *nephrin* (C), and the tubular markers *slc20a1a* (proximal tubule, D), and *slc12a3* (distal tubule, E) at 48 hours post fertilization (hpf). (F–J) *Mpped2* morpholino (MO) knockdown embryos develop glomerular gene expression defects (F–H, arrowheads), but tubular marker expression is normal (I, J). (K–O) *Casp9* MO knockdown embryos demonstrate reduced glomerular gene expression (K–M, arrowheads) and shortened distal tubules (O). (P) Quantification of observed abnormalities per number of embryos reveal significant differences in expression of *pax2a* and *nephrin* in response to knockdown of both *mpped2* and *casp9* (Fisher's exact test). (Q–V) Embryos were injected with control, *mpped2*, *or casp9* MO at the one-cell stage and subsequently injected with 70,000 MW fluorescent rhodamine dextran at 80 hpf. Dextran fluorescence was monitored over the next 48 hours. All dextran-injected embryos show equal loading into the cardiac sinus venosus at 2 hours post-injection (2 hpi/82 hpf; Q, S, U). Compared to control MO-injected embryos (R) and *mpped2* knockdown embryos (T), knockdown of *casp9* resulted in reduced dextran clearance at 48 hpi as shown by increased trunk fluorescence (V). (W) *Casp9* knockdown results in increased susceptibility to edema formation both spontaneously (−dex) (*P* value = 0.0234, Fisher's exact test) and after dextran challenge (+dex) (*P* value<0.0001). Embryos injected with both MO and dextran did not survive to 6 dpf (N/A). (X) Edema develops earlier and with higher frequency in *casp9* morphants following injection of the nephrotoxin gentamicin.
doi:10.1371/journal.pgen.1002584.g002

Materials and Methods

Phenotype definition

Serum creatinine and cystatin C were measured as detailed in Tables S1 and S2. To account for between-laboratory variation, serum creatinine was calibrated to the US nationally representative National Health and Nutrition Examination Study (NHANES) standards in all discovery and replication studies as described previously [8,24,25]. GFR based on serum creatinine (eGFRcrea) was estimated using the four-variable MDRD Study equation [26]. GFR based on cystatin C (eGFRcys) was estimated as eGFRcys = 76.7×(serum cystatin C)$^{-1.19}$ [27]. eGFRcrea and eGFRcys values<15 ml/min/1.73 m^2 were set to 15, and those >200 were set to 200 ml/min/1.73 m^2. CKD was defined as eGFRcrea <60 ml/min/1.73 m^2 according to the National Kidney Foundation guidelines [28]. A more severe CKD phenotype, CKD45, was defined as eGFRcrea <45 ml/min/1.73 m^2. Control individuals for both CKD and CKD45 analyses were defined as those with eGFRcrea >60 ml/min/1.73 m^2.

Covariate definitions

In discovery and replication cohorts, diabetes was defined as fasting glucose ≥126 mg/dl, pharmacologic treatment for diabetes, or by self-report. Hypertension was defined as systolic blood pressure ≥140 mmHg or diastolic blood pressure ≥90 mmHg or pharmacologic treatment for hypertension.

Discovery analyses

Genotyping was conducted as specified in Table S4. After applying quality-control filters to exclude low-quality SNPs or samples, each study imputed up to ~2.5 million HapMap-II SNPs, based on the CEU reference samples. Imputed genotypes were coded as the estimated number of copies of a specified allele (allelic dosage). Additional, study-specific details can be found in Table S1.

Primary association analysis

A schematic view of our complete analysis workflow is presented in Figure S1. Using data from 26 population-based studies of individuals of European ancestry, we performed GWA analyses of the following phenotypes: 1) $\log_e$(eGFRcrea), $\log_e$(eGFRcys), CKD, and CKD45 overall and 2) $\log_e$(eGFRcrea) and CKD stratified by diabetes status, hypertension status, age group (≤/>65 years), and sex. GWAS of $\log_e$(eGFRcrea) and $\log_e$(eGFRcys) were based on linear regression. GWAS of CKD and CKD45 were performed in studies with at least 25 cases (i.e. all 26 studies for CKD and 11 studies for CKD45) and were based on logistic regression. Additive genetic effects were assumed and models were adjusted for age and, where applicable, for sex, study site and principal components. Imputation uncertainty was accounted for by including allelic dosages in the model. Where necessary, relatedness was modeled with appropriate methods (see Table S1 for study-specific details). Before including in the meta-analysis, all GWA data files underwent to a careful quality control, performed using the GWAtoolbox package in R (www.eurac.edu/GWAtoolbox.html) [29].

Meta-analyses of study-specific SNP-association results, assuming fixed effects and using inverse-variance weighting, i.e.: the pooled effect $\hat{\beta}_{pooled}$ is estimated as $\sum_{i=1}^{K} w_i\hat{\beta}_i \Big/ \sum_{i=1}^{K} w_i$, where $\hat{\beta}_i$ is the effect of the SNP on the outcome in the i^{th} study, K is the number of studies, and $w_i = 1 \Big/ SE(\hat{\beta}_i)$ is the weight given to the i^{th} study. The meta-analyses were performed using METAL [30], with genomic control correction applied across all imputed SNPs [31] if the inflation factor λ>1 at both the individual study level and after the meta-analysis. SNPs with minor allele frequency (MAF)<1% were excluded. All SNPs with a meta-analysis *P* value≤5×10^{-8} for any trait or any stratum were deemed genome-wide significant [32].

In the eGFRcrea analyses, after excluding loci that were previously reported [8,9], we selected for replication all SNPs with *P* value<5×10^{-8} in any trait or stratum that were independent (defined by pairwise r^2<0.2), in the primary association analysis. This yielded five SNPs in five independent loci. The same criterion was applied to the CKD analysis, where no SNPs passed the selection threshold. Given the smaller number of cases with severe CKD resulting in less statistical power, a different selection strategy was adopted for the CKD45 analysis: selected for replication were SNPs with discovery *P* value≤5×10^{-6}, MAF≥5%, and homogeneous effect size across studies (I^2≤25%). Four additional SNPs were thereby selected for replication from the CKD45 analysis.

Direction test to identify SNPs for replication

In addition to identifying SNPs for replication based on the genome-wide significance threshold from a fixed effect model meta-analysis, we performed a "direction test" to identify additional SNPs for which between-study heterogeneity in effect size might have obscured the overall association that was nevertheless highly consistent in the direction of allelic effects. Under the null hypothesis of no association, the *a priori* probability that a given effect allele of a SNP has either a positive or negative association with eGFRcrea is 0.5. Because the meta-analysis includes independent studies, the number of concordant effect directions follows a binomial distribution. Therefore, we tested whether the number of discovery cohorts with the same sign of association (i.e. direction of effect) was greater than expected by chance given the binomial distribution and a null expectation of equal numbers of associations with positive and negative sign. The test was only applied for eGFRcrea in the overall analysis. Multiple testing was controlled by applying the same *P* value

threshold of 5×10^{-8} as in the overall GWAS. Given that no SNP met this criterion, we selected for replication one novel SNP with the lowest *P* value of 4.0×10^{-7}.

Genome-wide between-strata difference test to identify SNPs for replication

Based on the results of the stratified GWAS of eGFRcrea and CKD, for each SNP we tested the hypothesis whether the effect of a SNP on eGFRcrea or CKD was the same between strata (null hypothesis), i.e. diabetes versus non-diabetes subjects, hypertensive versus normotensive, younger versus older, females versus males. We used a two-sample test defined as $Z=(b_1-b_2)/(SE(b_1)^2+SE(b_2)^2)^{0.5}$, with b_1 and b_2 indicating the effect estimates in the two strata and $SE(b_1)$ and $SE(b_2)$ their standard errors [33]. For large samples, the test statistic follows a standard normal distribution. SNPs were selected for replication if they had a between-stratum difference *P* value$\leq5\times10^{-5}$, an association *P* value$\leq5\times10^{-5}$ in one of the two strata, and MAF$\geq$10%. Independent loci were defined using the same criteria as described above. Eleven further SNPs, one per locus, were selected for replication from the between-strata difference test.

Replication analysis

Replication was performed for a total of 21 SNPs including 5 from the overall and stratified eGFRcrea analyses, 1 from the direction test on eGFRcrea, 4 from the overall CKD45 analysis, and 11 from the between-strata difference test. Replication studies used the same phenotype definition, and had available genotypes from imputed *in silico* genome-wide SNP data or *de novo* genotyping. The same association analyses including the identical stratifications were performed as in discovery studies. Details can be found in the Tables S2, S5 and S6. Study-specific replication results for the selected SNPs were combined using the same meta-analysis approach and software as in the discovery stage. One-sided *P* values were derived with regard to the effect direction found in the discovery stage. Based on the *P* value distribution of all SNPs submitted for replication (the 10 from eGFRcrea and CKD45 and the 11 from the between strata difference test), we estimated the False Discovery Rate as a q-value using the QVALUE [34] package in R. SNPs with q-value$<$0.05 were called significantly replicating, thus specifying a list of associations expected to include not more than 5% false positives.

Finally, study-specific results from both the discovery and replication stage were combined in a joint inverse-variance weighted fixed-effect meta-analysis and the two-sided *P* values were compared to the genome-wide significance threshold of 5×10^{-8} to test whether a SNP was genome-wide significant. Between-study heterogeneity of replicated SNPs was quantified by the I^2 statistic [35].

Replication genotyping

For *de novo* genotyping in 10,446 samples from KORA F3, KORA F4, SAPHIR and SAPALDIA, the MassARRAY system at the Helmholtz Zentrum (München, Germany) was used, using Assay Design v3.1.2 and the iPLEX chemistry (Sequenom, San Diego, USA). Assay design failed for rs1322199 and genotyping was not performed. Ten percent of the spectra were checked by two independent, trained persons, and 100% concordance between investigators was obtained. SNPs with a *P* value$<$0.001 when testing for Hardy-Weinberg equilibrium (rs10490130, rs10068737, rs11078903), SNPs with call rate $<$90% (rs500456 in KORA F4 only) or monomorphic SNPs (rs2928148) were excluded from analyses without attempting further genotyping. The call rates of rs4149333 and rs752805 were near 0% on the MassARRAY system. These SNPs were thus genotyped on a 7900HT Fast Real-Time PCR System (Applied Biosystems, Foster City, USA). Mean call rate across all studies and SNPs ranged from 96.8% (KORA F4) to 99% (SAPHIR). Duplicate genotyping was performed in at least 14% of the subjects in each study with a concordance of 95–100% (median 100%). In the Ogliastra Genetic Park Replication Study (n = 3000) *de novo* genotyping was conducted on a 7900HT Fast Real-Time PCR System (Applied Biosystems, Foster City, USA), with a mean call rate of 99.4% and 100% concordance of SNPs genotyped in duplicate.

Between-strata analyses for candidate SNPs in replication samples

Twenty-nine SNPs, including the 6 novel loci reported in the current manuscript along with 23 previously confirmed to be associated with renal function [9], were tested for differential effects between the strata. The same Z statistics as described for discovery (above) was used and the Bonferroni-adjusted significance level was set to 0.10/29 = 0.003.

SNP-by-age interaction, for the one SNP showing significantly different effects between strata of age, was tested in the ARIC study by fitting a linear model on log(eGFRcrea) adjusted for sex, recruitment site, the first and the seventh genetic principal components (only these two were associated with the outcome at *P* value$<$0.05). Both the interaction term and the terms for the main effects of age and the SNP were included in the model.

Power to assess between-strata effect difference

To assess genome-wide between-strata differences, with alpha = 5×10^{-8} and power = 80%, the maximum detectable difference was 0.025 when comparing nonDM versus DM and 0.015 when comparing nonHTN versus HTN. Similarly, when testing for between-strata differences the 29 known and new loci (Bonferroni-corrected alpha = 0.003) in the combined sample (n = $\sim$125,000 in nonDM and n = $\sim$13,000 in DM) we had 80% power to detect differences as large as 0.035.

Look-up in African Americans (CARe)

For each of the 6 lead SNPs identified in our European ancestry samples, we extracted eGFR association statistics from a genome-wide study in the CARe African ancestry consortium [12]. We further investigated potential allelic heterogeneity across ethnicities by examining the 250 kb flanking region surrounding each lead SNP to determine whether other SNPs with stronger associations exist in each region. A SNP with the smallest association *P* value with MAF$>$0.03 was considered the top SNP in the African ancestry sample. We defined statistical significance of the identified lead SNP in African ancestry individuals based on a region-specific Bonferroni correction. The number of independent SNPs was determined based on the variance inflation factor (VIF) with a recursive calculation within a sliding window of 50 SNPs and pairwise r^2 of 0.2. These analyses were performed using PLINK.

Analyses of related phenotypes

For each replicating SNP, we obtained association results for urinary albumin-to-creatinine ratio and microalbuminuria from our previous genome-wide association analysis [20], and for blood pressure and myocardial infarction from genome-wide association analysis from the ICBP [21] and CARDIoGRAM [22] consortia, respectively.

eSNP analysis

Significant renal SNPs were searched against a database of expression SNPs (eSNP) including the following tissues: fresh lymphocytes [36], fresh leukocytes [37], leukocyte samples in individuals with Celiac disease [38], lymphoblastoid cell lines (LCL) derived from asthmatic children [39], HapMap LCL from 3 populations [40], a separate study on HapMap CEU LCL [41], peripheral blood monocytes [42,43], adipose [44,45] and blood samples [44], 2 studies on brain cortex [42,46], 3 large studies of brain regions including prefrontal cortex, visual cortex and cerebellum (Emilsson, personal communication), liver [45,47], osteoblasts [48], skin [49] and additional fibroblast, T cell and LCL samples [50]. The collected eSNP results met criteria for statistical significance for association with gene transcript levels as described in the original papers.

A second expression analysis of 81 biopsies from normal kidney cortex samples was performed as described previously [51,52]. Genotyping was performed using Affymetrix 6.0 Genome-wide chip and called with GTC Software (Affymetrix). For eQTL analyses, expression probes (Affymetrix U133set) were linked to SNP probes with >90% call-rate using RefSeq annotation (Affymetrix build a30). *P* values for eQTLs were calculated using linear multivariable regression in both cohorts and then combined using Fisher's combined probability test (see also [52]). Pairwise LD was calculated using SNAP [53] on the CEU HapMap release 22.

Zebrafish functional experiments

Zebrafish were maintained according to established IACUC protocols. Briefly, we injected zebrafish embryos with newly designed (mpped2, ddx1) or previously validated (casp9 [54]) morpholino antisense oligonucleotides (MO, GeneTools, Philomath OR) at the one-cell stage at various doses. We fixed embryos in 4% PFA at the appropriate stages for in situ hybridization (http://zfin.org/ZFIN/Methods/ThisseProtocol.html). Different anatomic regions of the kidney were visualized using a panel of 4 established markers: *pax2a* (global kidney marker) [15], *nephrin* (podocyte marker) [16], *slc20a1a* (proximal tubule) [17], and *slc12a3* (distal tubule marker) [17]. Abnormalities in gene expression were independently scored by two investigators. We compared the number of abnormal morphant embryos to control embryos, injected with a standard control MO designed by GeneTools, with the Fisher's exact test, at the Bonferroni-corrected significance level of 0.0125, i.e.: 0.05/4 markers. We documented the development of gross edema at 4 and 6 days post-fertilization in live embryos.

We performed dextran clearance experiments following previously described protocols [55]. Briefly, 80 hours after MO injection, we anesthetized embryos in 4 mg/ml Tricaine in embryo water (1:20 dilution), then positioned embryos on their back in a 1% agarose injection mold. We injected an equal volume of tetramethylrhodamine dextran (70,000 MW; Invitrogen) into the cardiac sinus venosus of each embryo. We then returned the embryos to fresh embryo water. Using fluorescence microscopy, we imaged the embryos at 2 hours post-injection (82 hpf) to demonstrate equal loading, then at 48 hours post-injection (128 hpf) to evaluate dextran clearance.

Embryos were injected with control, mpped2, or casp9 MOs at the one-cell stage. At 48 hpf, embryos were manually dechorionated, anesthetized in a 1:20 dilution of 4 mg/ml Tricaine in embryo water, and oriented on a 1% agarose injection mold. As previously described [56], embryos were injected with equal volumes of 10 mg/ml gentamicin (Sigma) in the cardiac sinus venosus, returned to fresh embryo water, and subsequently scored for edema (prevalence, time of onset) over the next 3 days.

Supporting Information

Figure S1 Flowchart of the project.
(TIF)

Figure S2 Genome-wide $-\log_{10}$ *P* values plot from stage 1 discovery meta-analysis. Plots show the discovery analysis of eGFRcrea in the overall group, with known loci [8,9] highlighted in orange and novel loci highlighted in blue (A), and in strata of the main CKD risk factors (B, C, D, and E), with complementary groups being contrasted each other. The dotted line indicates the genome-wide significance threshold at *P* value = 5×10^{-8}. The unmarked locus is *RNASEH2*C on chromosome 11, colored in gray despite genome-wide significance. The P value for the current stage 1 discovery for rs4014195 was 2.7×10^{-9}. This locus previously did not replicate [9]; when we additionally considered our prior non-overlapping in silico and de novo replication data, the current stage 2 *P* value was 0.8832, yielding a combined stage 1+stage 2 *P* value of 2.6×10^{-7}. Therefore, we did not submit this SNP for further replication.
(PDF)

Figure S3 Quantile-quantile plots of observed versus expected $-\log_{10}$ *P* values from the discovery analysis of eGFRcrea overall (A) and by strata of the main CKD risk factors (B). The orange line and its 95% confidence interval (shaded area) represent the null hypothesis of no association. In panel (A), results are compared when considering all SNPs (black dots) and when removing SNPs from loci that were already reported in previous GWAS [8,9] (orange dots). The meta-analysis inflation factor λ is reported along with the discovery sample size. Individual-study minimum, maximum and median λs are also reported for comparison. Genomic-control correction was applied twice: on individual study results, before the meta-analysis, and on the meta-analysis results.
(PDF)

Figure S4 Regional association plots for the six new loci in the European ancestry discovery samples: (A) *MPPED2*; (B) *DDX1*; (C) *SLC47A1*; (D) *CASP9*; (E) *CDK12*; (F) *INO80*. $-\log_{10}$ *P* values are plotted versus genomic position(build 36). The lead SNP in each region is labeled. Other SNPs in each region are color-coded based on their LD to the lead SNP(LD based on the HapMap CEU, see color legend). Gene annotations are based on UCSC Genome Browser(RefSeq Genes, build 36) and arrows indicate direction of transcription. Graphs were generated using the stand-alone version of LocusZoom [57], version 1.1.
(PDF)

Figure S5 Forest plots of the six novel loci in the discovery phase.
(TIF)

Figure S6 Results from discovery meta-analysis of eGFRcrea for the six new loci: overall sample and all strata are considered. Reported is the effect size on log(eGFRcrea) and its 95% confidence interval. The stratum where the SNP was discovered is marked with a triangle for discovery based on meta-analysis *P* value or with a circle for discovery based on direction test.
(TIF)

Figure S7 Regional association plots for the six new loci in the African ancestry CARe samples: (A) *MPPED2*; (B) *DDX1*; (C) *SLC47A1*; (D) *CASP9*; (E) *CDK12*; (F) *INO80*. $-\log_{10}$ *P* values are plotted versus genomic position (build 36). The lead SNP in each region is labeled and identified by a blue arrow and blue *P* value. The SNP with the smallest *P* value in the region is indicated by a red arrow. Other SNPs in each region are color-coded based on their LD to the lead SNP (based on the HapMap YRI, see color

legend). Gene annotation is based on UCSC Genome Browser (RefSeq Genes, build 36) and arrows indicate direction of transcription. Graphs were generated using the stand-alone version of LocusZoom [57], version 1.1.
(PDF)

Figure S8 Ddx1 knockdown does not affect kidney gene expression. (A–E) Uninjected control embryos show normal kidney development as demonstrated by in situ hybridization for the renal markers *pax2a* (A, B), *nephrin* (C), *slc20a1a* (D) and *slc12a3* (E). (F–J) *Ddx1* morpholino(MO)-injected embryos do not show significant changes in renal marker expression. (K) Number of observed abnormalities per number of embryos examined at 400 uM MO injection for renal gene expression analysis.
(TIF)

Figure S9 Casp9 and mpped2 knockdown embryos are more susceptible to gentamicin-induced kidney injury. Compared to control embryos (A), casp9 and mpped2 knockdown embryos develop edema at 103 hpf (C, E), suggestive of a renal defect. When injected with gentamicin, a nephrotoxin that reproducibly induces edema in control embryos (B), mpped2 and casp9 knockdown embryos develop edema earlier, more frequently, and in a more severe fashion (D, F). Whereas control embryos primarily develop cardiac edema, mpped2 and casp9 knockdown embryos display cardiac (arrowhead), ocular (black arrow), and visceral (white arrow) edema, demonstrating that mpped2 and casp9 knockdown predisposes embryos to kidney injury. (G) Quantification of edema prevalence in control, mpped2, and casp9 knockdown embryos 2, 22, and 55 hours post-injection (hpi) of gentamicin. These numbers are presented graphically in Figure 2X.
(TIF)

Figure S10 Comparison of the effect size on eGFRcrea and on eGFRcys for the lead SNPs of known and new loci. Results are based on the largest sample size available for each locus, i.e. the combined discovery and replication sample for the novel loci (N = 130,600), the discovery sample only for the known loci (N = 74,354). Sign of effect estimates has been changed to reflect the effects of the eGFRcrea lowering alleles. Original beta coefficients and their standard errors for the two traits can be downloaded from the File S1.
(TIF)

Figure S11 Odds ratios (ORs) and 95% confidence intervals of CKD and CKD45 for the lead SNPs of all known and new loci, sorted by decreasing OR of CKD.
(TIF)

File S1 Effect size on eGFRcrea and on eGFRcys for the lead SNPs of known and new loci.
(XLSX)

Table S1 Study-specific methods and full acknowledgments—discovery studies.
(DOC)

Table S2 Study-specific methods and full acknowledgments—replication studies and functional follow-up studies.
(DOC)

Table S3 Characteristics of stage 1 discovery studies.
(DOC)

Table S4 Study-specific genotyping information for stage 1 discovery studies.
(DOC)

Table S5 Characteristics of stage 2 replication studies.
(DOC)

Table S6 Study-specific genotyping information for stage 2 *in silico* replication studies.
(DOC)

Table S7 Top four SNPs from the CKD45 analysis.
(DOC)

Table S8 Loci identified by the test for differential effects between strata in the GWAS. Results are sorted by trait, group and chromosome. For each SNP, the *P* value of the test for difference between strata is reported.
(DOC)

Table S9 Imputation quality of replicated SNPs in all discovery and replication studies: median MACH-Rsq and interquartile range (IQR) are reported.
(DOC)

Table S10 Effects of novel and known loci on log(eGFRcrea) in the overall population.
(DOC)

Table S11 Genes nearest to loci associated with renal traits.
(DOC)

Table S12 Imputation Quality (MACH-Rsq) for the best SNPs in the African ancestry samples of the CARe consortium (1.00 refers to genotyped data).
(DOC)

Table S13 Baseline characteristics of the kidney biopsies for the eQTL analysis.
(DOC)

Table S14 Analysis of the new loci for eQTL status in meta-analysis of two cohorts of kidney biopsies.
(DOC)

Table S15 Association of novel and known loci with CKD and CKD45: Odds Ratios (OR), 95% confidence intervals (95%CI) and *P* values.
(DOC)

Table S16 Association between novel and known loci and log(eGFRcrea) in individuals without and with diabetes and test for difference between strata.
(DOC)

Table S17 Association between novel and known loci and log(eGFRcrea) in individuals without and with hypertension and test for difference between strata.
(DOC)

Table S18 Association between novel and known loci and log(eGFRcrea) in individuals younger and older than 65 years and test for difference between strata.
(DOC)

Table S19 Association between novel and known loci and log(eGFRcrea) in females and in males and test for difference between strata.
(DOC)

Table S20 Effects of novel loci on the logarithm of urinary albumin-to-creatinine ratio (log(UACR)) in the overall sample and by diabetes and hypertension status.
(DOC)

Table S21 Effects (log odds ratios) of novel loci on microalbuminuria (MA) in the overall sample and by diabetes and hypertension status.
(DOC)

Table S22 Association of novel loci with diastolic and systolic blood pressure in the ICBP consortium.
(DOC)

Table S23 Association of novel loci with myocardial infarction in the CARDIoGRAM consortium.
(DOC)

Author Contributions

Study design: V Gudnason, TB Harris, LJ Launer, G Eiriksdottir, A Parsa, A Köttgen, WHL Kao, R Schmidt, L Ferrucci, DS Siscovick, BA Oostra, CM van Duijn, I Borecki, CS Fox, FB Hu, CA Böger, M Gorski, T Illig, A Döring, HE Wichmann, IM Heid, I Rudan, PP Pramstaller, GC Curhan, U Gyllensten, JF Wilson, SH Wild, AF Wright, H Campbell, A Hofman, AG Uitterlinden, JCM Witteman, R Biffar, K Endlich, R Rettig, S Stracke, H Völzke, P Kovacs, A Tönjes, O Polasek, N Hastie, C Hayward, V Vitart, DI Chasman, P Ridker, C Helmer, A Metspalu, JJ Wang, P Mitchell, M Province, X Gao, M Ciullo, P Vollenweider, M Pirastu, B Paulweber, D Toniolo, T Lehtimäki, O Raitakari, M Kähönen, J Viikari, P Gasparini, H Colhoun, A Doney, C Palmer, H Deshmukh, S Trompet, I Ford, BM Buckley, JW Jukema, NM Probst-Hensch. Study management: V Gudnason, TB Harris, LJ Launer, G Eiriksdottir, A Parsa, WHL Kao, R Schmidt, H Schmidt, M Cavalieri, L Ferrucci, DS Siscovick, A Isaacs, BA Oostra, CM van Duijn, I Borecki, CS Fox, J Ding, Y Liu, MC Cornelis, FB Hu, W Koenig, T Illig, A Döring, HE Wichmann, I Rudan, I Kolcic, T Zemunik, M Boban, C Pattaro, PP Pramstaller, GC Curhan, A Johansson, G Zaboli, U Gyllensten, JF Wilson, SH Wild, U Nöthlings, A Hofman, AG Uitterlinden, JCM Witteman, R Biffar, K Endlich, R Rettig, U Völker, H Völkze, M Stumvoll, A Tönjes, O Polasek, N Hastie, C Hayward, V Vitart, DI Chasman, P Ridker, C Helmer, A Metspalu, JJ Wang, P Mitchell, M Province, X Gao, M Ciullo, M Bochud, P Vollenweider, M Pirastu, B Kollerits, M Haun, B Paulweber, F Kronenberg, D Toniolo, T Lehtimäki, O Raitakari, M Kähönen, J Viikari, P Gasparini, F Giulianini, H Colhoun, A Doney, C Palmer, H Deshmukh, S Trompet, I Ford, BM Buckley, JW Jukema, BK Krämer, NM Probst-Hensch, M Imboden. Subject recruitment: G Eiriksdottir, AR Shuldiner, BD Mitchell, J Coresh, R Schmidt, M Cavalieri, DS Siscovick, BA Oostra, CM van Duijn, TB Harris, T Illig, A Döring, HE Wichmann, I Rudan, I Kolcic, PP Pramstaller, A Johansson, JF Wilson, SH Wild, A Hofman, AG Uitterlinden, JCM Witteman, R Biffar, R Rettig, S Stracke, H Völkze, A Tönjes, O Polasek, C Helmer, P Mitchell, M Ciullo, P Vollenweider, M Pirastu, B Paulweber, D Toniolo, O Raitakari, M Kähönen, J Viikari, S Ulivi, A Robino, P Ridker, H Colhoun, A Doney, C Palmer, I Ford, BM Buckley, JW Jukema, NM Probst-Hensch. Genotyping: AR Shuldiner, BD Mitchell, E Boerwinkle, H Schmidt, A Isaacs, A Demirkan, BA Oostra, CM van Duijn, M de Andrade, EJ Atkinson, ST Turner, SLR Kardia, Y Liu, CA Böger, M Gorski, T Illig, HE Wichmann, IM Heid, JF Wilson, H Campbell, A Franke, AG Uitterlinden, F Rivadeneira, F Ernst, G Homuth, HK Kroemer, M Nauck, U Völker, M Stumvoll, O Polasek, C Hayward, DI Chasman, T Esko, M Haun, F Kronenberg, T Lehtimäki, F Giulianini, S Trompet, JW Jukema. Statistical methods and analysis: T Aspelund, AV Smith, A Parsa, JR O'Connell, A Köttgen, WHL Kao, A Tin, C Hundertmark, M Struchalin, T Tanaka, G Li, A Isaacs, A Demirkan, M Feitosa, CS Fox, MH Chen, MC Foster, SJ Hwang, Q Yang, K Lohman, JS Andrews, Y Liu, MC Cornelis, CA Böger, M Gorski, IM Heid, C Pattaro, D Taliun, C Fuchsberger, C Minelli, A Johansson, W Igl, D Ellinghaus, A Franke, A Dehghan, F Rivadeneira, YS Aulchenko, A Teumer, I Prokopenko, R Mägi, C Hayward, V Vitart, DI Chasman, T Esko, EG Holliday, X Gao, S Ketkar, D Ruggiero, R Sorice, Z Kutalik, S Bergmann, F Murgia, L Portas, B Kollerits, F Kronenberg, G Pistis, S Ulivi, A Robino, AY Chu, H Colhoun, A Doney, C Palmer, H Deshmukh, I Ford, NM Probst-Hensch, M Adam, GA Thun, M Olden, M Li, N Glazer, HJ Gierman, V Chouraki, HE Wheeler, G Jacobs, T Nikopensius, M Metzger. Bioinformatics: AV Smith, JR O'Connell, C Hundertmark, M Struchalin, G Li, MH Chen, Q Yang, K Lohman, JS Andrews, Y Liu, MC Cornelis, CA Böger, M Gorski, IM Heid, C Pattaro, D Taliun, C Fuchsberger, A Johansson, W Igl, D Ellinghaus, A Dehghan, F Rivadeneira, YS Aulchenko, HK Kroemer, A Teumer, I Prokopenko, R Mägi, DI Chasman, T Esko, D Ruggiero, R Sorice, S Bergmann, F Murgia, L Portas, G Pistis, C Sala, T Lehtimäki, O Raitakari, S Ulivi, F Giulianini, S Trompet, I Ford, M Imboden, C-T Liu, AD Johnson, SK Kim. Zebrafish studies: M Garnaas, W Goessling. Interpretation of results: V Gudnason, TB Harris, LJ Launer, AV Smith, A Parsa, A Köttgen, WHL Kao, A Tin, DS Siscovick, G Li, M Rao, A Isaacs, MH Chen, MC Foster, SJ Hwang, Q Yang, J Ding, K Lohman, Y Liu, CA Böger, M Gorski, IM Heid, I Rudan, T Zemunik, M Boban, C Pattaro, D Taliun, A Johansson, W Igl, G Zaboli, U Gyllensten, JF Wilson, SH Wild, R Biffar, K Endlich, HK Kroemer, M Nauck, R Rettig, S Stracke, A Teumer, U Völker, H Völkze, O Polasek, N Hastie, C Hayward, V Vitart, DI Chasman, BI Freedman, T Esko, A Metspalu, EG Holliday, I Borecki, M Province, X Gao, M Ciullo, M Bochud, B Kollerits, M Haun, B Paulweber, F Kronenberg, D Toniolo, G Pistis, C Sala, AY Chu, S Trompet, JW Jukema, M Garnaas, W Goessling, CS Fox. Wrote the manuscript: C Pattaro, A Köttgen, A Teumer, M Garnaas, CA Böger, C Fuchsberger, A Tin, CM O'Seaghdha, A Parsa, M Bochud, IM Heid, W Goessling, DI Chasman, WHL Kao, CS Fox.

References

1. Meguid El Nahas A, Bello AK (2005) Chronic kidney disease: The global challenge. Lancet 365(9456): 331–340.
2. Imai E, Matsuo S (2008) Chronic kidney disease in asia. Lancet 371(9631): 2147–2148.
3. Coresh J, Selvin E, Stevens LA, Manzi J, Kusek JW, et al. (2007) Prevalence of chronic kidney disease in the united states. JAMA 298(17): 2038–2047.
4. Levey AS, de Jong PE, Coresh J, El Nahas M, Astor BC, et al. (2011) The definition, classification, and prognosis of chronic kidney disease: A KDIGO controversies conference report. Kidney Int 80(1): 17–28.
5. van der Velde M, Matsushita K, Coresh J, Astor BC, Woodward M, et al. (2011) Lower estimated glomerular filtration rate and higher albuminuria are associated with all-cause and cardiovascular mortality. A collaborative meta-analysis of high-risk population cohorts. Kidney Int 79(12): 1341–1352.
6. Gansevoort RT, Matsushita K, van der Velde M, Astor BC, Woodward M, et al. (2011) Lower estimated GFR and higher albuminuria are associated with adverse kidney outcomes. A collaborative meta-analysis of general and high-risk population cohorts. Kidney Int 80(1): 93–104.
7. Astor BC, Matsushita K, Gansevoort RT, van der Velde M, Woodward M, et al. (2011) Lower estimated glomerular filtration rate and higher albuminuria are associated with mortality and end-stage renal disease. A collaborative meta-analysis of kidney disease population cohorts. Kidney Int 79(12): 1331–1340.
8. Kottgen A, Glazer NL, Dehghan A, Hwang SJ, Katz R, et al. (2009) Multiple loci associated with indices of renal function and chronic kidney disease. Nat Genet 41(6): 712–717.
9. Kottgen A, Pattaro C, Boger CA, Fuchsberger C, Olden M, et al. (2010) New loci associated with kidney function and chronic kidney disease. Nat Genet 42(5): 376–384.
10. Chambers JC, Zhang W, Lord GM, van der Harst P, Lawlor DA, et al. (2010) Genetic loci influencing kidney function and chronic kidney disease. Nat Genet 42(5): 373–375.
11. Gudbjartsson DF, Holm H, Indridason OS, Thorleifsson G, Edvardsson V, et al. (2010) Association of variants at UMOD with chronic kidney disease and kidney stones-role of age and comorbid diseases. PLoS Genet 6: e1001039. doi:10.1371/journal.pgen.1001039.
12. Liu CT, Garnaas MK, Tin A, Kottgen A, Franceschini N, et al. (2011) Genetic association for renal traits among participants of african ancestry reveals new loci for renal function. PLoS Genet 7: e1002264. doi:10.1371/journal.pgen.1002264.
13. Allan LA, Clarke PR (2009) Apoptosis and autophagy: Regulation of caspase-9 by phosphorylation. FEBS J 276(21): 6063–6073.
14. Gobe G, Crane D (2010) Mitochondria, reactive oxygen species and cadmium toxicity in the kidney. Toxicol Lett 198(1): 49–55.
15. Drummond IA, Majumdar A, Hentschel H, Elger M, Solnica-Krezel L, et al. (1998) Early development of the zebrafish pronephros and analysis of mutations affecting pronephric function. Development 125(23): 4655–4667.
16. Kramer-Zucker AG, Wiessner S, Jensen AM, Drummond IA (2005) Organization of the pronephric filtration apparatus in zebrafish requires nephrin, podocin and the FERM domain protein mosaic eyes. Dev Biol 285(2): 316–329.
17. Wingert RA, Selleck R, Yu J, Song HD, Chen Z, et al. (2007) The cdx genes and retinoic acid control the positioning and segmentation of the zebrafish pronephros. PLoS Genet 3: e189. doi:10.1371/journal.pgen.0030189.
18. Tyagi R, Shenoy AR, Visweswariah SS (2009) Characterization of an evolutionarily conserved metallophosphoesterase that is expressed in the fetal brain and associated with the WAGR syndrome. J Biol Chem 284(8): 5217–5228.

19. Schwartz F, Eisenman R, Knoll J, Gessler M, Bruns G (1995) cDNA sequence, genomic organization, and evolutionary conservation of a novel gene from the WAGR region. Genomics 29(2): 526–532.
20. Boger CA, Chen MH, Tin A, Olden M, Kottgen A, et al. (2011) CUBN is a gene locus for albuminuria. J Am Soc Nephrol 22(3): 555–570.
21. The International Consortium for Blood Pressure Genome-Wide Association Studies, Ehret GB, Munroe PB, Rice KM, Bochud M, et al. (2011) Genetic variants in novel pathways influence blood pressure and cardiovascular disease risk. Nature 478(7367): 103–109.
22. Schunkert H, Konig IR, Kathiresan S, Reilly MP, Assimes TL, et al. (2011) Large-scale association analysis identifies 13 new susceptibility loci for coronary artery disease. Nat Genet 43(4): 333–338.
23. Pattaro C, De Grandi A, Vitart V, Hayward C, Franke A, et al. (2010) A meta-analysis of genome-wide data from five european isolates reveals an association of COL22A1, SYT1, and GABRR2 with serum creatinine level. BMC Med Genet 11: 41.
24. Fox CS, Larson MG, Leip EP, Culleton B, Wilson PW, et al. (2004) Predictors of new-onset kidney disease in a community-based population. JAMA 291(7): 844–850.
25. Coresh J, Astor BC, McQuillan G, Kusek J, Greene T, et al. (2002) Calibration and random variation of the serum creatinine assay as critical elements of using equations to estimate glomerular filtration rate. Am J Kidney Dis 39(5): 920–929.
26. Levey AS, Bosch JP, Lewis JB, Greene T, Rogers N, et al. (1999) A more accurate method to estimate glomerular filtration rate from serum creatinine: A new prediction equation. modification of diet in renal disease study group. Ann Intern Med 130(6): 461–470.
27. Stevens LA, Coresh J, Schmid CH, Feldman HI, Froissart M, et al. (2008) Estimating GFR using serum cystatin C alone and in combination with serum creatinine: A pooled analysis of 3,418 individuals with CKD. Am J Kidney Dis 51(3): 395–406.
28. National Kidney Foundation. (2002) K/DOQI clinical practice guidelines for chronic kidney disease: Evaluation, classification, and stratification. Am J Kidney Dis 39(2 Suppl 1): S1–266.
29. Fuchsberger C, Taliun D, Pramstaller PP, Pattaro C, on behalf of the CKDGen consortium (2011) GWAtoolbox: An R package for fast quality control and handling of GWAS meta-analysis data. Bioinformatics10.1093/bioinformatics/btr679.
30. Willer CJ, Li Y, Abecasis GR (2010) METAL: Fast and efficient meta-analysis of genomewide association scans. Bioinformatics 26(17): 2190–2191.
31. Devlin B, Roeder K (1999) Genomic control for association studies. Biometrics 55(4): 997–1004.
32. Pe'er I, Yelensky R, Altshuler D, Daly MJ (2008) Estimation of the multiple testing burden for genomewide association studies of nearly all common variants. Genet Epidemiol 32(4): 381–385.
33. Cohen A (1983) Comparing regression coefficients across subsamples. Sociol Methods Res 12: 77–94.
34. Storey JD, Tibshirani R (2003) Statistical significance for genomewide studies. Proc Natl Acad Sci U S A 100(16): 9440–9445.
35. Higgins JP, Thompson SG, Deeks JJ, Altman DG (2003) Measuring inconsistency in meta-analyses. BMJ 327(7414): 557–560.
36. Goring HH, Curran JE, Johnson MP, Dyer TD, Charlesworth J, et al. (2007) Discovery of expression QTLs using large-scale transcriptional profiling in human lymphocytes. Nat Genet 39(10): 1208–1216.
37. Idaghdour Y, Czika W, Shianna KV, Lee SH, Visscher PM, et al. (2010) Geographical genomics of human leukocyte gene expression variation in southern morocco. Nat Genet 42(1): 62–67.
38. Heap GA, Trynka G, Jansen RC, Bruinenberg M, Swertz MA, et al. (2009) Complex nature of SNP genotype effects on gene expression in primary human leucocytes. BMC Med Genomics 2: 1.
39. Dixon AL, Liang L, Moffatt MF, Chen W, Heath S, et al. (2007) A genome-wide association study of global gene expression. Nat Genet 39(10): 1202–1207.
40. Stranger BE, Nica AC, Forrest MS, Dimas A, Bird CP, et al. (2007) Population genomics of human gene expression. Nat Genet 39(10): 1217–1224.
41. Kwan T, Benovoy D, Dias C, Gurd S, Provencher C, et al. (2008) Genome-wide analysis of transcript isoform variation in humans. Nat Genet 40(2): 225–231.
42. Heinzen EL, Ge D, Cronin KD, Maia JM, Shianna KV, et al. (2008) Tissue-specific genetic control of splicing: Implications for the study of complex traits. PLoS Biol 6: e1. doi:10.1371/journal.pbio.1000001.
43. Zeller T, Wild P, Szymczak S, Rotival M, Schillert A, et al. (2010) Genetics and beyond—the transcriptome of human monocytes and disease susceptibility. PLoS ONE 5: e10693. doi:10.1371/journal.pone.0010693.
44. Emilsson V, Thorleifsson G, Zhang B, Leonardson AS, Zink F, et al. (2008) Genetics of gene expression and its effect on disease. Nature 452(7186): 423–428.
45. Greenawalt DM, Dobrin R, Chudin E, Hatoum IJ, Suver C, et al. (2011) A survey of the genetics of stomach, liver, and adipose gene expression from a morbidly obese cohort. Genome Res 21(7): 1008–1016.
46. Webster JA, Gibbs JR, Clarke J, Ray M, Zhang W, et al. (2009) Genetic control of human brain transcript expression in alzheimer disease. Am J Hum Genet 84(4): 445–458.
47. Schadt EE, Molony C, Chudin E, Hao K, Yang X, et al. (2008) Mapping the genetic architecture of gene expression in human liver. PLoS Biol 6: e107. doi:10.1371/journal.pbio.0060107.
48. Grundberg E, Kwan T, Ge B, Lam KC, Koka V, et al. (2009) Population genomics in a disease targeted primary cell model. Genome Res 19(11): 1942–1952.
49. Ding J, Gudjonsson JE, Liang L, Stuart PE, Li Y, et al. (2010) Gene expression in skin and lymphoblastoid cells: Refined statistical method reveals extensive overlap in cis-eQTL signals. Am J Hum Genet 87(6): 779–789.
50. Dimas AS, Deutsch S, Stranger BE, Montgomery SB, Borel C, et al. (2009) Common regulatory variation impacts gene expression in a cell type-dependent manner. Science 325(5945): 1246–1250.
51. Rodwell GE, Sonu R, Zahn JM, Lund J, Wilhelmy J, et al. (2004) A transcriptional profile of aging in the human kidney. PLoS Biol 2: e427. doi:10.1371/journal.pbio.0020427.
52. Wheeler HE, Metter EJ, Tanaka T, Absher D, Higgins J, et al. (2009) Sequential use of transcriptional profiling, expression quantitative trait mapping, and gene association implicates MMP20 in human kidney aging. PLoS Genet 5: e1000685. doi:10.1371/journal.pgen.1000685.
53. Johnson AD, Handsaker RE, Pulit SL, Nizzari MM, O'Donnell CJ, et al. (2008) SNAP: A web-based tool for identification and annotation of proxy SNPs using HapMap. Bioinformatics 24(24): 2938–2939.
54. Sidi S, Sanda T, Kennedy RD, Hagen AT, Jette CA, et al. (2008) Chk1 suppresses a caspase-2 apoptotic response to DNA damage that bypasses p53, bcl-2, and caspase-3. Cell 133(5): 864–877.
55. Hentschel DM, Mengel M, Boehme L, Liebsch F, Albertin C, et al. (2007) Rapid screening of glomerular slit diaphragm integrity in larval zebrafish. Am J Physiol Renal Physiol 293(5): F1746–50.
56. Hentschel DM, Park KM, Cilenti L, Zervos AS, Drummond I, et al. (2005) Acute renal failure in zebrafish: A novel system to study a complex disease. Am J Physiol Renal Physiol 288(5): F923–9.
57. Pruim RJ, Welch RP, Sanna S, Teslovich TM, Chines PS, et al. (2010) LocusZoom: Regional visualization of genome-wide association scan results. Bioinformatics 26(18): 2336–2337.

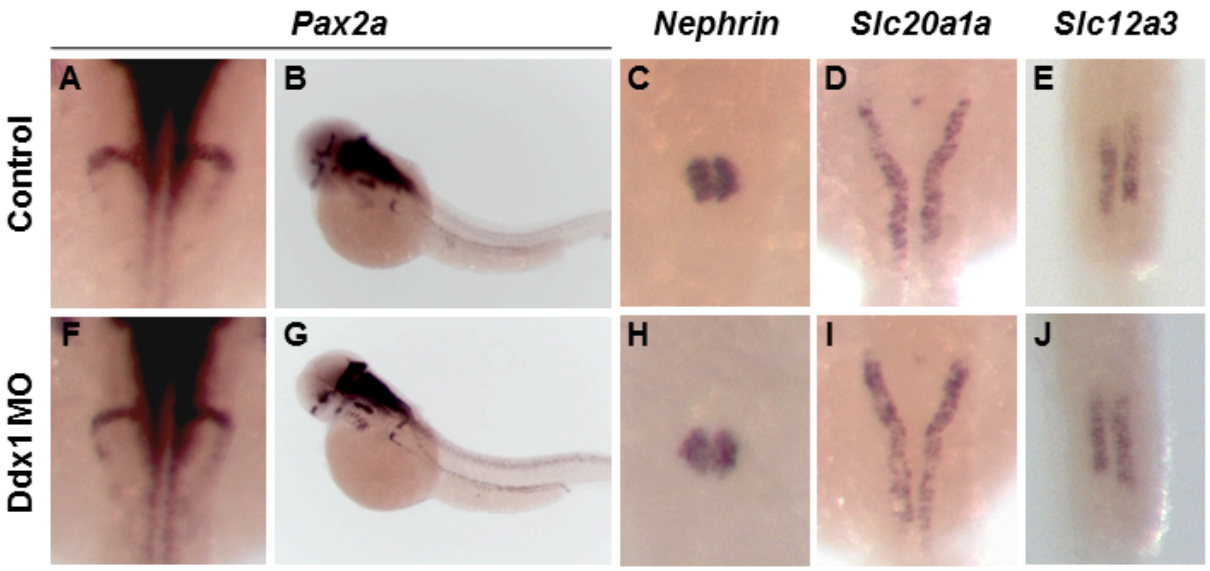

K

Number of observed abnormalities/number of embryos examined at 400 uM injection				
	Global Renal Marker *pax2a*	Podocyte Marker *nephrin*	Proximal Tubular Marker *slc20a1a*	Distal Tubular Marker *slc12a3*
Uninjected Ddx1 MO	0/17 (0%) 0/22 (0%)	0/17 (0%) 1/26 (4%)	0/30 (0%) 0/40 (0%)	0/23 (0%) 0/32 (0%)
Fisher's exact test P value	1.0	1.0	1.0	1.0

Figure S8. ***Ddx1*** **knockdown does not affect kidney gene expression.**

(A–E) Uninjected control embryos show normal kidney development as demonstrated by *in situ* hybridization for the renal markers *pax2a* (A, B), *nephrin* (C), *slc20a1a* (D) and *slc12a3* (E). (F–J) *Ddx1* morpholino (MO)-injected embryos do not show significant changes in renal marker expression. (K) Number of observed abnormalities per number of embryos examined at 400 uM MO injection for renal gene expression analysis.

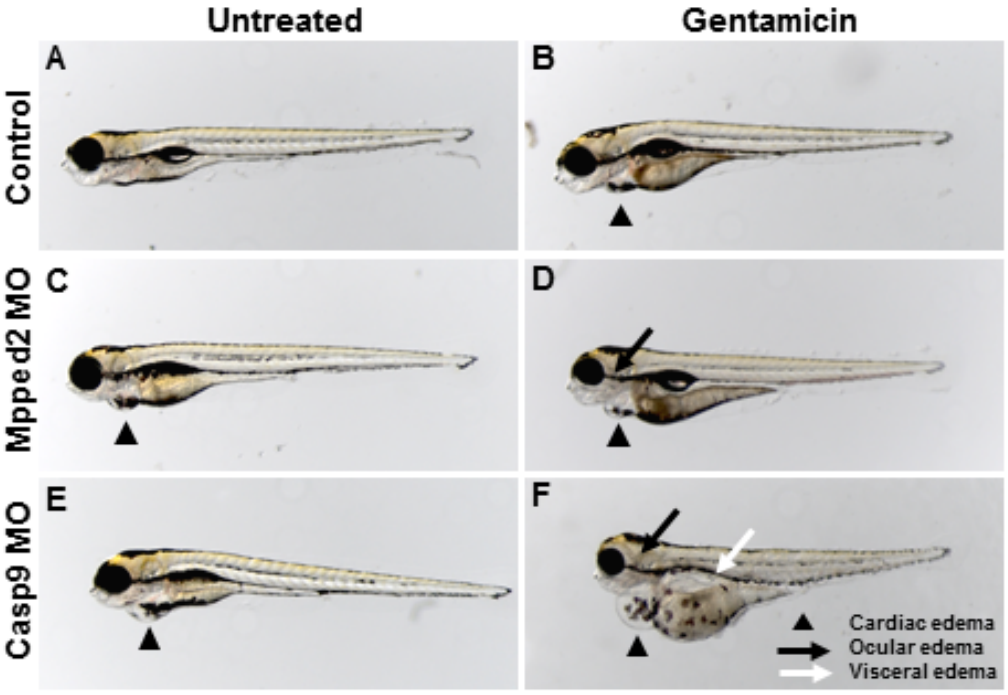

G

Group	% Edema			n
	2 hpi	22 hpi	55 hpi	
Uninjected	0	0	0	28
Mpped2 MO	8	0	25	24
Casp9 MO	17	29	38	24
Uninjected + Gentamicin	7	27	29	41
Mpped2 MO + Gentamicin	3	17	33	36
Casp9 MO + Gentamicin	14	64	58	36

Figure S9. *Casp9* and *mpped2* knockdown embryos are more susceptible to gentamicin-induced kidney injury.

Compared to control embryos (A), *casp9* and *mpped2* knockdown embryos develop edema at 103 hpf (C, E), suggestive of a renal defect. When injected with gentamicin, a nephrotoxin that reproducibly induces edema in control embryos (B), *mpped2* and *casp9* knockdown embryos develop edema earlier, more frequently, and in a more severe fashion (D, F). Whereas control embryos primarily develop cardiac edema, *mpped2* and *casp9* knockdown embryos display cardiac (arrowhead), ocular (black arrow), and visceral (white arrow) edema, demonstrating that *mpped2* and *casp9* knockdown predisposes embryos to kidney injury. (G) Quantification of edema prevalence in control, *mpped2*, and *casp9* knockdown embryos 2, 22, and 55 hours post-gentamicin injection (hpi). These numbers are presented graphically in Figure 2X.